

Ana Mafalda Santos Castro

***In vitro* screening assay using the murine pre-adipocyte cell line 3T3-L1 to study anti-obesogenic activities of cyanobacterial compounds**

Dissertation for the master degree in Environmental Toxicology and Contamination submitted to the Abel Salazar Biomedical Sciences' Institute from the University of Porto.

Supervisor – Doctor Ralph Urbatzka

Category – Assistant Researcher

Affiliation – Interdisciplinary Centre of Marine and Environmental Research (CIIMAR/CIMAR)

Co-supervisor – Professor Vitor Vasconcelos

Category – University Professor

Affiliation – Interdisciplinary Centre of Marine and Environmental Research (CIIMAR/CIMAR) / Faculty of Sciences of University of Porto

Acknowledgements

I would like to thank Dr. Ralph Urbatzka, my supervisor, for the impeccable guidance, for his demanding of me which allowed me to grow so much during this year. His relaxed personality during troubled times helped me keep my focus during each step.

Next I would like to thank Dr. Marco Preto, my second co-supervisor, who helped me greatly in the chemical procedures and throughout my master thesis. I want to thank him for all the knowledge he shared and all the support in the laboratory.

I also would like to thank Professor Doctor Vitor Vasconcelos for accepting me in the laboratory to perform my master's thesis and to all the people at BBE for the help, knowledge and laughs. Here I met some brilliant people with awesome personalities, who made everything easier.

To the Department of Biochemistry from the Faculty of Medicine of the University of Porto for helping me troubleshooting some problems with the cell-line used in this project. Cláudia Marques, Diogo Pestana, Diana Teixeira and Dr. Conceição Calhau were very helpful - a huge thank you.

To the Interdisciplinary Centre of Marine and Environmental Research (CIIMAR), Institute of Biomedical Sciences of Abel Salazar from the University of Porto (ICBAS) and Faculty of Sciences from the University of Porto (FCUP).

To the project MARBIOTECH (reference NORTE-07-0124- FEDER-000047) within the SR&TD Integrated Program MARVALOR - Building research and innovation capacity for improved management and valorization of marine resources, supported by the Programa Operacional Regional do Norte (ON.2 – O Novo Norte) and also by NOVOMAR (reference 0687-NOVOMAR-1-P), supported by the European Regional Development Fund.

This research was also partially supported by the Strategic Funding UID/Multi/04423/2013 through national funds provided by FCT – Foundation for Science and Technology and European Regional Development Fund (ERDF), in the framework of the program PT2020.

Last but not least, I would like to thank to my family and friends who inspire and support me and to my master colleagues, especially Carolina, Sofia, Nelson and Bruno, who were essential throughout these two years. To you all, my biggest thank you.



Abstract

Obesity has been gradually increasing over the last three decades. The only drugs for the long-term obesity treatment currently on the market, approved by both the Food and Drug Administration (FDA) and the European Medicines Agency (EMA), are Orlistat, a powerful inhibitor of pancreatic lipase derived from a natural compound, Phentermine/Topiramate extended release, Exenatide and Dapaglifozin. Recent research has focused on natural product discovery for obesity treatment. Compounds isolated from animals, plants, fungi and marine phytoplankton have shown promising anti-obesity properties. Cyanobacteria, known as blue-green algae and producers of cyanotoxins, have shown high production of secondary metabolites with relevant and beneficial activity.

In this work, we explored the chemical richness of these prokaryotes by testing cyanobacterial strains regarding their anti-obesogenic activity in (pre)adipocyte cells, aiming to isolate and characterize novel cyanobacterial compounds using a bioassay-guided fractionation and isolation approach. Two cell-based screening assays were used, 1) the proliferation of pre-adipocytes, and 2) the adipogenesis from pre-adipocytes to mature adipocytes.

The Blue Biotechnology and Ecotoxicology (BBE) group at CIIMAR, offers a unique collection of cyanobacteria isolated from water samples and solid materials from the Portuguese coast. Six cyanobacterial strains were grown and their extracts were produced. These extracts were then fractionated through vacuum liquid chromatography (VLC) and 60 fractions were obtained. The bioactivity of the resulting fractions was tested in *in vitro* cultures of the murine preadipocyte cell line 3T3-L1 for proliferative and adipogenic activity. Proliferation was assessed by the Sulforhodamine B (SRB) staining and the incorporation of Bromodeoxyuridine (BrdU) into the DNA. Furthermore, the 3-(4,5-dimethylthiazol-2-yl)-2,5-diphenyltetrazolium bromide assay (MTT bioassay) delivers information about the cellular viability and metabolic activity, through the reduction of MTT to formazan. Effects on adipogenesis were assessed using imaging techniques and Oil Red O lipid staining.

The strongest effects on proliferation rate were obtained after the exposure to fractions of *Planktothrix planctonica* LEGEXX280 (E14028 I) and *Aphanizomenon* sp. LEGE03283 (E14035 B); the strongest effects on adipogenesis were obtained from fractions of *Synechocystis* sp. LEGE07211 (E14031 D) and *Oscillatoria limnetica* LEGE00237 (E14032 H). The most promising fractions were selected for further sub-fractionation using wet chemistry extraction techniques as solid phase extraction (SPE) and high pressure liquid chromatography (HPLC). Sub-fraction E14028 I7 8A+9 E7 J1 is the result of seven fractionations, showing

promising pro-proliferative and metabolic activity. The compound is now isolated with few impurities. Sub-fraction E14031 D7 exerted strong pro-adipogenic effects and a further sub-fractionation is being processed. Compound isolation will take place in the following steps.

The combined *in vitro* 3T3-L1 screening with the production of cyanobacterial compounds allows us advance in the isolation of natural compounds with pro-proliferative and pro-adipogenic activities that in the future may be beneficial for the treatment of obesity-related comorbidities.

Furthermore, during this work, a review was submitted to Current Topics in Medicinal Chemistry (Appendix II) with the title "Obesity: the metabolic disease, advances on drug discovery and natural product research", which gives a summary of the state of the art of natural compound discovery related to obesity treatment.

Resumo

A obesidade tem vindo a aumentar gradualmente ao longo das últimas três décadas. Os únicos fármacos actualmente no mercado para o tratamento da obesidade a longo prazo, aprovados pela *Food and Drug Administration* (FDA) e a Agência Europeia de Medicamentos (EMA) são Orlistat, um potente inibidor das lipase pancreática derivado de um composto natural, a Associação Fentermina / Topiramato, Exenatida e Dapaglifozina. A pesquisa mais recente foca-se na descoberta de produtos de origem natural para o tratamento da obesidade. Compostos isolados a partir de animais, plantas, fungos e algas marinhas têm mostrado promissoras actividade anti-obesidade. Cianobactérias, conhecidas como algas verde-azuladas e produtoras de toxinas, têm demonstrado elevada produção de metabolitos secundários de alto valor biotecnológico, farmacêutico e industrial.

Neste trabalho exploramos a riqueza química destes procariontes, testando frações de determinadas estirpes de cianobactérias por actividade anti-obesogénica em pré-adipócitos. O objectivo é isolar e caracterizar novos compostos de cianobactérias, utilizando um sistema de fraccionamento guiado por bioactividade. Foram utilizados dois ensaios celulares para determinação de bioactividade: 1) a proliferação de pré-adipócitos, e 2) a adipogénese de pré-adipócitos em adipócitos maduros.

O grupo Blue Biotechnology and Ecotoxicology (BBE) no CIIMAR oferece uma coleção única de cianobactérias isoladas de amostras de água e materiais sólidos da costa Portuguesa. Várias estirpes de cianobactérias foram cultivadas e os seus extractos foram produzidos. Estes extractos foram então fracionados utilizando cromatografia líquida sob-vácuo de fase normal. A bioactividade das frações preparadas foi testada em cultura *in vitro* da linha de pré-adipócitos 3T3-L1 por actividade pro-proliferativa e pro-adipogénica. A proliferação foi avaliada com o uso da coloração por Sulforrodamina B (SRB) e a incorporação de Bromodeoxiuridina (BrdU) no ADN. Além disso, o bioensaio da redução do brometo 3-(4,5-dimetiltiazol-2-il)-2,5-difeniltetrazolio (MTT) forneceu informação sobre a viabilidade celular e actividade metabólica. A adipogénese foi avaliada usando o *Oil Red O*.

De seis estirpes cianobacterianas, 60 fracções foram obtidas. Os efeitos mais fortes na actividade proliferativa foram obtidos após a exposição a uma fração de *Planktothrix planctonica* LEGE XX280 (E14028 I) e a uma fração de *Aphanizomenon sp.* LEGE03283 (E14035 B); enquanto que os efeitos mais fortes na adipogénese foram obtidos na exposição às fracções das estirpes *Synechocystis sp.* LEGE07211 (E14031 D) e *Oscillatoria limnetica* LEGE00237 (E14032 H).

As frações mais promissoras foram selecionadas para posterior sub-fraccionamento. A sub-fração E14028 I7 8A+9 E7 J1 é o resultado de sete fracionamentos, com actividade proliferativa e metabólica promissora. Este composto encontra-se agora isolado com algumas impurezas. A sub-fração E14031 D7 exerceu também fortes efeitos adipogénicos e está a ser processada.

Os testes *in vitro* utilizando a linha celular 3T3-L1 permitem a triagem de vários compostos de cianobactérias, para além de permitirem testar variados parâmetros essenciais para o estudo da obesidade.

Durante este trabalho, uma revisão foi submetida à revista *Current Topics in Medicinal Chemistry* (Apêndice II) intitulada “Obesity: the metabolic disease, advances on drug discovery and natural product research”, uma revisão que sumariza o estado da arte da descoberta de compostos naturais de interesse ao tratamento da obesidade.

Publications and work dissemination

Review article: Castro, M., Preto, M., Vasconcelos, V. and Urbatzka, R. (submitted) "Obesity: the metabolic disease, advances on drug discovery and natural product research", *Current Topics in Medicinal Chemistry* (Appendix II).

Oral communication "*In vitro* screening assay using the murine pre-adipocyte cell line 3T3-L1 to study anti-obesogenic activities of chemical compounds" at the *IJUP - Encontro de Investigação Jovem da Universidade do Porto*, 13-15th of May, 2015, Oporto, Portugal (Appendix III).

Poster communication "*In vitro* screening assay using the murine pre-adipocyte cell line 3T3-L1 to study anti-obesogenic activities of chemical compounds" at the *ICAAE - International Conference on Alternatives to Animal Experimentation*, 8 and 9th of May, 2015, Lisbon, Portugal (Appendix IV).

Index

1. Introduction	1
1.1. Obesity.....	1
1.1.1. Dynamics of the Adipose Tissue	1
1.1.2. The Metabolic Disease.....	3
1.1.3. Model systems for obesity studies	6
1.1.3.1. Pre-adipocyte Proliferation	6
1.1.3.2. Pre-adipocyte Differentiation	6
1.2. Natural Compound Discovery	7
1.2.1. Anti-obesity Natural Compounds	8
1.2.2. Cyanobacteria as a source of natural compounds.....	11
1.2.2.1. Cyanobacteria	11
1.2.2.2. Bioactive compounds from Cyanobacteria.....	12
1.2.2.3. Leads on bioactive compounds from cyanobacteria with anti-obesity activity	15
2. Objectives	18
3. Materials and Methods.....	19
3.1. Cyanobacterial strains and culture.....	19
3.2. Extraction and bioassay-guided fractionation	19
3.2.1. Normal phase vacuum liquid chromatography of E14028 I.....	21
3.2.2. Flash chromatography of E14028 I7	22
3.2.3. Reverse phase solid phase extraction of E14028 I7 8A+9.....	23
3.2.4. Semi-preparative reverse-phase HPLC for E14028 I7 8A+9 E	25
3.2.5. Semi-preparative reverse-phase HPLC for E14028 I7 8A+9 E7	25
3.2.6. Semi-preparative reverse-phase HPLC for E14028 I7 8A+9 E7J	26
3.2.7. Normal phase solid phase extraction of E14031 D.....	26
3.3. Cell culture and bioassays	26
3.3.1. Cell proliferation assays	27

3.3.1.1. Sulforhodamine B assay	27
3.3.2.2. BrdU ELISA assay	28
3.3.2. Cell viability assay / metabolic activity of pre-adipocytes	28
3.3.3. Cell differentiation assay (adipogenesis)	29
4. Results	31
4.1. Screening of cyanobacterial strains for bioactivity	31
4.1.1. Screening for proliferative activity	33
4.1.2. Bioassay-guided fractionation of E14028 I	40
4.1.3. Screening for adipogenic activity	52
4.1.4. . Bioassay-guided fractionation of E14031 D	59
5. Discussion.....	61
5.1. Pro-proliferative and pro-adipogenic activity as targets for obesity treatment	61
5.2. Cyanobacterial assessment for bioactivity	63
5.2.1. E14028 I pro-proliferative activity.....	64
5.2.2. Cyanobacterial adipogenic bioactivity.....	66
5.3. Methodology for the analysis of cell proliferation	70
5.4. Bioactivity-guided fractionation for compound discovery.....	72
6. Conclusion	74
7. References.....	75
8. Appendixes	93

Figure Index

Figure 1 – Factors intervening in 3T3-L1 preadipocyte differentiation. (Insulin (INS), 3-isobutyl-1-methylxanthine (IBMX), dexamethasone (DEX), cyclic adenosine monophosphate (cAMP), cAMP-responsive element binding protein (CREB), sterol regulatory element-binding protein-1 (SREBP-1), CCAAT-enhancer-binding proteins (C/EBPs) and peroxisome proliferator-activated receptor- γ (PPAR- γ)).	7
Figure 2 – Pie chart for the distribution of reported cyanobacterial secondary metabolites through the five major botanical sub-classes (adapted from Gerwick et al. 2008).	12
Figure 3 – 2D structure of the secondary metabolites Barbamide (on the left) and Apratoxin A (on the right) (from chemspider.com).	14
Figure 4 - Apparatus assembly for the extraction of the crude extract, from the lyophilized cyanobacterial biomass.	20
Figure 5 - A) Setup of the fractionation during Fraction B obtainment; B) Close-up of the silica gel column used in the vacuum liquid chromatography; C) Apparatus assembly for the vacuum liquid chromatography.	21
Figure 6 - Elucidatory scheme of flash chromatography procedure.	23
Figure 7 - Elucidatory scheme of thin layer chromatography procedure.	23
Figure 8 - Visible spectrum (300-700 nm) scanning of the E14026 fractions (A-K) produced after VLC fractionation ($100 \mu\text{g mL}^{-1}$ in DMSO).	32
Figure 9 - Cell proliferation (SRB assay, first and second graph, using cell proliferation rate and cell proliferation rate compared to the solvent control, respectively) and activity of mitochondrial enzymes (MTT assay, third graph), in % of solvent control, for the E14026 (<i>Phormidium sp.</i> LEGE06363) VLC fractions (A – K) with the concentration of $100 \mu\text{g mL}^{-1}$, after 24 and 48 hours of exposure. Solvent control corresponded to 1% DMSO and positive control to 20% DMSO, using 3 replicate wells per treatment and 6 for control, solvent control and positive control.	33
Figure 10 - Cell proliferation (SRB assay, top) and activity of mitochondrial enzymes (MTT assay, bottom), in % of solvent control, for the E14028 (<i>Planktothrix planctonica</i> LEGEXX280) VLC fractions (A – I) with the concentration of $100 \mu\text{g mL}^{-1}$, after 24 and 48 hours of exposure. Solvent control corresponded to 1% DMSO and positive control to 20% DMSO, using 3 replicate wells per treatment and 6 for control, solvent control and positive control.	34
Figure 11 - Cell proliferation (SRB assay, top) and activity of mitochondrial enzymes (MTT assay, bottom), in % of solvent control, for the E14031 (<i>Synechocystis sp.</i> LEGE07211)	

VLC fractions (A – L) with the concentration of 100 µg mL⁻¹, after 24 and 48 hours of exposure. Solvent control corresponded to 1% DMSO and positive control to 20% DMSO, using 3 replicate wells per treatment and 6 for control, solvent control and positive control.35

Figure 12 - Cell proliferation (SRB assay, top) and activity of mitochondrial enzymes (MTT assay, bottom), in % of solvent control, for the E14032 (*Oscillatoria limnetica* LEGE00237) VLC fractions (A – I) with the concentration of 100 µg mL⁻¹, after 24 and 48 hours of exposure. Solvent control corresponded to 1% DMSO and positive control to 20% DMSO, using 3 replicate wells per treatment and 6 for control, solvent control and positive control.36

Figure 13 - Cell proliferation (SRB assay, top) and activity of mitochondrial enzymes (MTT assay, bottom), in % of solvent control, for the E14035 (*Aphanizomenon* sp. LEGE03283) VLC fractions (A – I) with the concentration of 100 µg mL⁻¹, after 24 and 48 hours of exposure. Solvent control corresponded to 1% DMSO and positive control to 20% DMSO, using 3 replicate wells per treatment and 6 for control, solvent control and positive control.37

Figure 14 - Cell proliferation (SRB assay, top) and activity of mitochondrial enzymes (MTT assay, bottom), in % of solvent control, for the E14067 (*Limnothrix* sp. LEGE07212) VLC fractions (A – J) with the concentration of 100 µg mL⁻¹, after 24 and 48 hours of exposure. Solvent control corresponded to 1% DMSO and positive control to 20% DMSO, using 3 replicate wells per treatment and 6 for control, solvent control and positive control.38

Figure 15 - Measurement of color development from 0 to 30 minutes for cell proliferation assessment through BrdU ELISA assay for VLC fractions E14035B, E14032H, E14028A, E14067D and E14067F with the concentration of 100 µg mL⁻¹, control and solvent control (1% DMSO) with 2 hour BrdU pulse, after 48 hours of exposure, using 3 replicate wells per treatment and 6 for control, solvent control and positive control.39

Figure 16 - BrdU incorporation percentage compared to the solvent control for VLC fractions E14035B, E14032H, E14028A, E14067D and E14067F with the concentration of 100 µg mL⁻¹, control and solvent control (1% DMSO) with 2 hour BrdU pulse, after 48 hours of exposure, using 3 replicate wells per treatment and 6 for control, solvent control and positive control.39

Figure 17 - Cell proliferation (SRB assay, top) and activity of mitochondrial enzymes (MTT assay, bottom), in % of solvent control, for the E14028I sub-fractions (1-7) with the concentration of 50 µg mL⁻¹, after 24 and 48 hours of exposure. Solvent control

corresponded to 1% DMSO and positive control to 20% DMSO, using 3 replicate wells per treatment and 6 for control, solvent control and positive control.	41
Figure 18 - BrdU incorporation percentage compared to the solvent control for VLC fraction E14028I7 with the concentration of 50 $\mu\text{g mL}^{-1}$, control and solvent control (1% DMSO) with 2 hour BrdU pulse, after 48 hours of exposure, using 3 replicate wells per treatment and 6 for control, solvent control and positive control.....	41
Figure 19 - Cell proliferation (SRB assay, top) and activity of mitochondrial enzymes (MTT assay, bottom), in % of solvent control, for the E14028 I7 sub-fractions (1-14) with the concentration of 50 $\mu\text{g mL}^{-1}$, after 24 and 48 hours of exposure. Solvent control corresponded to 1% DMSO and positive control to 20% DMSO, using 3 replicate wells per treatment and 6 for control, solvent control and positive control.	43
Figure 20 - $^1\text{H-NMR}$ spectra for sub-fractions 9 (top) and 8A (bottom) in CD_3OD (recorded at 400 MHz).	44
Figure 21 - Cell proliferation (SRB assay, top) and activity of mitochondrial enzymes (MTT assay bottom), in % of solvent control, for the E14028 I7 8A+9 sub-fractions (A-H) with the concentration of 25 $\mu\text{g mL}^{-1}$, after 24 and 48 hours of exposure. Solvent control corresponded to 1% DMSO and positive control to 20% DMSO, using 3 replicate wells per treatment and 6 for control, solvent control and positive control.	46
Figure 22 - Chromatogram of E14028 I7 8A+9 E showing highlighted sub-fractions that were collected. Conditions of the injection were 200 μL at a concentration of approximately 43.5 mg mL^{-1}	47
Figure 23 - Cell proliferation (SRB assay, top) and activity of mitochondrial enzymes (MTT assay, bottom), in % of solvent control, for the E14028 I7 8A+9 E sub-fractions (1-10) with the concentration of 25 $\mu\text{g mL}^{-1}$, after 24 and 48 hours of exposure. Solvent control corresponded to 1% DMSO and positive control to 20% DMSO, using 3 replicate wells per treatment and 6 for control, solvent control and positive control..	48
Figure 24 - BrdU incorporation percentage compared to the solvent control for HPLC fractions E14028I7 8A+9 E 1,6,7 and 9 with the concentration of 25 $\mu\text{g mL}^{-1}$, control and solvent control (1% DMSO) with 2 hour BrdU pulse, after 48 hours of exposure, using 3 replicate wells per treatment and 6 for control, solvent control and positive control..	49
Figure 25 - Chromatogram of E14028 I7 8A+9 E7 showing highlighted sub-fractions that were collected. Conditions of the injection were 35 μL at a concentration of approximately 3.8 mg mL^{-1}	49

Figure 26 - Cell proliferation (SRB assay, top) and activity of mitochondrial enzymes (MTT assay, bottom), in % of solvent control, for the E14028 I7 8A+9 E7 sub-factions (A-J) with the concentration of 10 $\mu\text{g mL}^{-1}$, after 24 and 48 hours of exposure. Solvent control corresponded to 1% DMSO and positive control to 20% DMSO, using 3 replicate wells per treatment and 6 for control, solvent control and positive control.50

Figure 27 - Chromatogram of E14028 I7 8A+9 E7J showing highlighted sub-fractions that were collected. Conditions of the injection were 50 μL at a concentration of approximately 2.65 mg mL^{-1}51

Figure 28 - Cell proliferation (SRB assay, top) and activity of mitochondrial enzymes (MTT assay, bottom), in % of solvent control, for the E14028 I7 8A+9 E7J sub-factions (1-7) with the concentration of 25 $\mu\text{g mL}^{-1}$, after 24 and 48 hours of exposure. Solvent control corresponded to 1% DMSO and positive control to 20% DMSO, using 3 replicate wells per treatment and 6 for control, solvent control and positive control.52

Figure 29 - Results for the adipogenesis assay (Oil Red O staining), in % of control in 3T3-L1 cell line using DMSO (0.2%), resveratrol (100 μM), rosiglitazone (0.2 μM) and troglitazone (0.2 μM), after exposure from day 0 to day 12 of the differentiation process, using 2 replicate wells per treatment and 4 for solvent control.53

Figure 30 - Results for the adipogenesis assay (Oil Red O staining), in % of solvent control, for the E14026 (*Phormidium sp.* LEGE06363) VLC fractions (A – I) with the concentration of 20 $\mu\text{g mL}^{-1}$, after exposure from day 0 to day 12 of the differentiation process. Solvent control corresponded to 0.2% DMSO and 2 replicate wells per treatment and 4 for solvent control were used.53

Figure 31 - Results for the adipogenesis assay (Oil Red O staining), in % of solvent control, for the E14028 (*Planktothrix planctonica* LEGEXX280) VLC fractions (A – I) with the concentration of 20 $\mu\text{g mL}^{-1}$, after exposure from day 0 to day 12 of the differentiation process. Solvent control corresponded to 0.2% DMSO and 2 replicate wells per treatment and 4 for solvent control were used.54

Figure 32 - Results for the adipogenesis assay (Oil Red O staining), in % of solvent control, for the E14031 (*Synechocystis sp.* LEGE07211) VLC fractions (A – I) with the concentration of 20 $\mu\text{g mL}^{-1}$, after exposure from day 0 to day 12 of the differentiation process. Solvent control corresponded to 0.2% DMSO and 2 replicate wells per treatment and 4 for solvent control were used.55

Figure 33 - Results for the adipogenesis assay (Oil Red O staining), in % of solvent control, for the E14032 (*Oscillatoria limnetica* LEGE00237) VLC fractions (A – J) with the concentration

of 20 µg mL ⁻¹ , after exposure from day 0 to day 12 of the differentiation process. Solvent control corresponded to 0.2% DMSO and 2 replicate wells per treatment and 4 for solvent control were used.	55
Figure 34 - Results for the adipogenesis assay (Oil Red O staining), in % of solvent control, for the E14035 (<i>Aphanizomenon</i> sp. LEGE03283) VLC fractions (A – J) with the concentration of 20 µg mL ⁻¹ , after exposure from day 0 to day 12 of the differentiation process. Solvent control corresponded to 1% DMSO and 2 replicate wells per treatment and 4 for solvent control were used.	56
Figure 35 - Results for the adipogenesis assay (Oil Red O staining), in % of solvent control, for the E14067 (<i>Limnothrix</i> sp. LEGE07212) VLC fractions (A – J) with the concentration of 20 µg mL ⁻¹ , after exposure from day 0 to day 12 of the differentiation process. Solvent control corresponded to 0.2% DMSO and 2 replicate wells per treatment and 4 for solvent control were used.	56
Figure 36 - Results for the adipogenesis assay (Oil Red O staining), in % of solvent control, for the E14028 I7 sub-factions (1-11) with the concentration of 10 µg mL ⁻¹ , after exposure from day 0 to day 12 of the differentiation process. Solvent control corresponded to 0.2% DMSO and 2 replicate wells per treatment and 4 for solvent control were used.	57
Figure 37 - Mature adipocytes after Oil Red O Staining under the optical microscope (40x). (1) Example of abnormal mature adipocyte; (2) Mature adipocytes exposed to 0.2% DMSO; (3) Mature adipocytes obtained after 12 day exposure to E14032 H; (4) Mature adipocytes after 12 days exposure to E14028 I7 7; (5) Mature adipocytes obtained after exposure to E14031D; (6) Pre-adipocytes after 12 day exposure to resveratrol.	58
Figure 38 - Results for the adipogenesis assay (Oil Red O staining), in % of solvent control, for the E14031 D sub-factions (1-10) with the concentration of 10 µg mL ⁻¹ , after exposure from day 0 to day 12 of the differentiation process. Solvent control corresponded to 0.2% DMSO and 3 replicate wells per treatment and 4 for solvent control were used.	59
Figure 39 - Mature adipocytes after Oil Red O Staining under the optical microscope after 12 day exposure to cyanobacterial subfractions E1431 D 7 (1) and 3 (2), at a concentration of 10 µg mL ⁻¹ (40x).	59

Table Index

Table 1 - Gradients used in the vacuum liquid chromatography (VLC).	20
Table 2 - Gradients used in the vacuum liquid chromatography (VLC).	22
Table 3 - Gradients used in the flash chromatography, for E14028I7 rendering.	23
Table 4 - Fraction pooling after thin layer chromatography for E14028I7.	23
Table 5 - Gradients used in the flash chromatography, for E14028I7 8A+9 rendering.	24
Table 6 - Fraction pooling after TLC for E14028I7 8A+9.	24
Table 7 - Mobile phase gradient used for the semi-preparative HPLC on sub-fraction E14028I7 8A+9 E.	25
Table 8 - Gradients used in the SPE of E14031 D.	26
Table 9 - Data of the extracts obtained of the cultured and collected cyanobacterial strains. .	31
Table 10 - Data of the VLC fractionations and fractions obtained for the extracts produced. .	31
Table 11 - Summary of the activities obtained in the screening for proliferative activity: comparison between SRB, MTT and BrdU ELISA assay for selected cyanobacterial fractions.	40
Table 12 – Average effect of exposure to DMSO after 48 hours, in % of control, through SRB, MTT and BrdU ELISA assay.	40
Table 13 - Fraction pooling for E14028I7 with the respective Rf values from TLC after observation under UV light (254 nm).	42
Table 14 - Fraction pooling for E14028 I7 8A+9 with the respective Rf values obtained from TLC after observation under UV light (254 nm) and PMA staining for the samples collected in SPE (left) and after sample assembly in 50% MeOH (EtOAc) (right).	45

Equation Index

Equation 1 - Formula used in the calculation of the values for the SRB assay.....	28
Equation 2 - Formula used in the calculation of the values of each time point for the BrdU assay.	28
Equation 3 - Formula used in the calculation of the values for the MTT assay.....	29
Equation 4 - Formula used in the calculation of the values for the Oil Red O assay.	30

List of abbreviations

BAT - Brown adipose tissue
BBE - Blue Biotechnology and Ecotoxicology Group
BrdU - Bromodeoxyuridine
C/EBP - CCAAT-enhancer-binding proteins
CREB - CAMP-responsive element binding
DEX – Dexamethasone
DMEM - Dulbecco's modified Eagle Medium
DMSO – Dimethyl sulfoxide
DNA - Deoxyribonucleic acid
EMA - European Medicines Agency
ELISA - Enzyme-linked immunosorbent assay
FBS - Fetal bovine serum
FDA - Food and Drug Administration (USA)
GRK-2 - G protein-coupled receptor kinase-2
GLUT4 - Glucose transporter type 4
HDL - High-density lipoprotein
HPLC - High pressure liquid chromatography
HMG-CoA reductase - 3-hydroxy-3-methyl-glutaryl-CoA reductase
IMBX - 3-isobutyl-1-methylxanthine
IGF-1 - Insulin-like growth factor-1
IRS-1 - Insulin receptor substrate 1
IFN - Interferon
IL - Interleukin
LDL - Low-density lipoprotein
MeCN - Acetonitrile
MeOH – Methanol
PKS - Mixed polyketide enzymatic systems
MTT - 3-(4,5-dimethylthiazol-2-yl)-2,5-diphenyl tetrazolium bromide
NRPS - Multimodular nonribosomal polypeptide system
NMR - Nuclear magnetic resonance
NF- κ B - Nuclear factor kappa-light-chain-enhancer
OECD - Organization for Economic Co-operation and Development
PCNA - Proliferating cell nuclear antigen

PKB - Protein kinase B
PMA - Phosphomolybdic acid
PRDM16 - Positive regulatory domain containing 16
PPAR- γ - Peroxisome proliferator-activated receptor gamma
R_f - Retention factor
RB - Round bottom
RGZ - Rosiglitazone
SGLT - Sodium/glucose co-transporter
SPE - Solid phase extraction
SREBP-1 - Sterol regulatory element-binding protein-1 (SREBP-1)
SRB - Sulforhodamine B
T2DM - Type 2 diabetes mellitus
TGZ – Troglitazone
TMB - Tetramethyl-benzidine
TLC - Thin layer chromatography
TNF- α - Tumor necrosis factor alpha
UV – Ultraviolet
UCP1 - Uncoupling protein-1 (UCP1)
VLC - Vacuum liquid chromatography

Appendixes

Appendix I – ¹ H NMR data for sub-fractions resulting from E14028I successive fractionings.....	92
Figure 1 – ¹ H NMR spectral data for E14028I in CD ₃ OD (recorded at 400 MHz).	
Figure 2 – ¹ H NMR spectral data for E14028 I7 in CDCl ₃ (recorded at 400 MHz).	
Figure 3 – ¹ H NMR spectral data for E14028I7 8A in CD ₃ OD (recorded at 400 MHz).	
Figure 4 – ¹ H NMR spectral data for E14028I7 9 in CD ₃ OD (recorded at 400 MHz).	
Figure 5 – ¹ H NMR spectral data for E14028I7 8A+9 E in CD ₃ OD (recorded at 400 MHz).	
Figure 6 – ¹ H NMR spectral data for E14028I7 8A+9 E6 in CD ₃ OD (recorded at 400 MHz).	
Figure 7 – ¹ H NMR spectral data for E14028I7 8A+9 E7 in CD ₃ OD (recorded at 400 MHz).	
Figure 8 – ¹ H NMR spectral data for E14028I7 8A+9 E7 J1 in CD ₃ OD (recorded at 600 MHz).	
Figure 9 – ¹ H NMR spectral data for E14031D in CDCl ₃ (recorded at 400 MHz).	
Figure 10 – ¹ H NMR spectral data for E14031D7 in CDCl ₃ (recorded at 400 MHz).	
Appendix II – Abstract for the review paper “Obesity: the metabolic disease, advances on drug discovery and natural product research”.....	97
Appendix III – Abstract for the oral communication " <i>In vitro</i> screening assay using the murine pre-adipocyte cell line 3T3-L1 to study anti-obesogenic activities of chemical compounds" at the IJUP - Encontro de Investigação Jovem da Universidade do Porto, 13-15th of May, 2015, Oporto, Portugal.....	98
Appendix IV – Poster for the communication " <i>In vitro</i> screening assay using the murine pre-adipocyte cell line 3T3-L1 to study anti-obesogenic activities of chemical compounds" at the ICAAE - International Conference on Alternatives to Animal Experimentation, 8 and 9th of May, 2015, Lisbon, Portugal.....	99

1. Introduction

Obesity is a global hazard associated with health problems such as hypertension, high cholesterol, diabetes, cardiovascular diseases, respiratory problems (asthma), musculoskeletal diseases (arthritis) and some forms of cancer (Fox et al. 2007). In the last 20 years, the percentage of obesity has nearly doubled in many European countries. The highest rates of obese adults are found in Mexico, followed by New Zealand and the United States, representing more than one third of the population, whereas in Asian countries the rates are between 2 and 4% (OECD, 2014). The promotion of a healthy lifestyle and lifestyle changes are preventive and straightforward. However, a large percentage of the world's population may not be able to depend on this methodology alone, when treating obesity. Throughout history, pharmaceutical companies have been unable to develop safe and effective anti-obesity drugs. Despite the increasing need, the only drugs for the long-term obesity treatment currently on the market, approved by both the Food and Drug Administration (FDA) and the European Medicines Agency (EMA), are Orlistat, a powerful inhibitor of pancreatic and intestinal lipases derived from a natural compound, Phentermine/Topiramate extended release, Exenatide and Dapagliflozin. A demand is present for new anti-obesogenic drugs without major toxicological side-effects.

Natural products are recognized as an extremely rich source of new beneficial compounds with high impact on drug development for infectious, neurological, cardiovascular, immunological, inflammatory and oncological human diseases (Butler et al. 2014). Natural products are produced by a wide array of living organisms as vertebrate and invertebrate animals, plants, marine phytoplankton, fungi and bacteria. The marine and freshwater environment, recognized as the richest ecosystems, are currently the main sources of natural compounds, wherein cyanobacteria represent a promising and fruitful source (Nagarajan et al. 2012). Cyanobacteria are being studied in high-scale due to their capability of producing many secondary metabolites with unusual structures and powerful activities against cancer and other diseases; cyanobacteria are thus an exciting source for leads in drug discovery.

1.1. Obesity

1.1.1. Dynamics of the Adipose Tissue

The perception of the adipose tissue changed markedly from simple fat storing cells to hormone-secreting cells with impact on the whole-body metabolism, energy metabolism in distant tissues, and sensitivity regulation towards insulin signaling. Today, adipocytes are

recognized as critical regulators of the whole-body metabolism (Stephens 2012). The tissue is composed of many cell types, as endothelial cells, hematocytes, pericytes, preadipocytes, macrophages and other immune cells (Geloën et al. 1989). However, in mammals, the adipose tissue is mainly constituted by two morphologically and physiologically very different types of cells: white adipocytes are cells with a single cytoplasmic lipid droplet and a squeezed nucleus, whereas brown adipocytes are polygonal cells with a round nucleus, several cytoplasmic lipid droplets and numerous large mitochondria. These two types of cells also differ in their distribution in the human body: white adipocytes are mostly found in subcutaneous (under the skin) and visceral depots (near internal organs), while brown adipocytes are found in visceral depots and near the aorta (Barbatelli et al. 2010). Brown adipose tissue (BAT) is exclusive to mammals and recognized as an evolutionary advantage, since it is specialized in body temperature maintenance, allowing mammals to survive during cold stress. This function is mediated by uncoupling protein-1 (UCP1) in the mitochondria (Farmer 2008), an exclusive protein of the BAT. Scientists also consider a third type of adipose tissue which is under intense investigation, but its origin and function remain unclear. Beige adipocytes (Ishibashi & Seale 2010) are regions in the white adipose tissue containing brown or brown-like adipocytes. Since the adipose tissue responds to physiological and environmental stimuli, due to its high density in nerve fibers in contact with adipocytes (Bartness et al. 2010), beige adipocytes were seen to arise after environmental and hormonal stimuli. Beige adipocytes within the white adipose tissue were found to be originated from white adipocytes with the expression of positive regulatory domain containing 16 (PRDM16), a transcriptional modulator required for thermogenesis (Ishibashi & Seale 2010), when under β 3-adrenergic stimulation, chronic activation of peroxisome proliferator-activated receptor gamma (PPAR- γ) or adaptation to cold response (Petrovic et al. 2010); this process is also known as white-to-brown transdifferentiation (Himms-Hagen et al. 2000).

Adipocytes have also been known to play a role in endocrine functions, and secrete important hormones and peptides for energy homeostasis, vascular diseases and appetite regulation. Hormones produced specifically from adipocytes are considered to be important regulators of whole-body metabolism. Leptin was the first characterized hormone to be secreted by the adipose tissue (Zhang et al. 1994). Leptin is responsible for appetite and food uptake, directed by anorexigenic (appetite suppressing) or orexigenic (appetite stimulating) neuropeptides. When the adipose tissue decreases in mass, leptin levels decline and neuropeptide Y levels rise, leading to higher food intake. Weight gain increases the adipokine levels, resulting in decreased food intake. Through this feedback mechanism, leptin is able to

regulate body fat mass and adipose tissue mass. Pivotal roles of this hormone have been described as regulation of the reproductive, cognitive, immune system, and related autoimmune disorders, as well as bone metabolism and hematopoiesis. Other hormones produced by adipocytes are for example adiponectin or resistin. Adiponectin acts on the regulation of many physiological processes as glucose and lipid metabolism (Kadowaki & Yamauchi 2005). Resistin, mainly produced by monocytes and macrophages within the adipose tissue, is involved in the pathogenesis of insulin resistance (McTernan et al. 2006). The adipose tissue is crucial for a well-functioning metabolism and characterized as a complex organ due to its inherent plasticity, its ability to increase or decrease the number of constituent cells, and its transdifferentiation potential.

1.1.2. The Metabolic Disease

Obesity is a complex metabolic disorder, characterized by the accumulation of fat in different body regions, which is caused by a positive energy balance. Obesity, at the cellular level, is manifested as the increase in cell size (hypertrophy) and cell number (hyperplasia) and both of these processes are largely dependent on the regulation of adipocyte differentiation (Rosen & MacDougald 2006). Metabolic complications of obesity are type 2 diabetes mellitus (T2DM), non-alcoholic fatty liver disease, cardiovascular disease or cancer.

Interaction between genetic, behavioral and environmental factors has been proven to lead to obesity. Excessive nutrient intake, lack of exercise and genetic susceptibility are established as the main causes of obesity (Ogden et al. 2012). However, well-known endocrine disrupting chemicals, such as phthalates, bisphenol A and alkylphenols, interfere with the individual hormonal levels, hence leading to high prevalence of obesity or developing obesity (vom Saal et al. 2012; Tang-Péronard et al. 2011). Interestingly, associations exist between gut microbiota composition and obesity. The mechanisms through which these microbes exert their anti-obesity effects are still unclear. However, links have been made between two distinct phyla of bacteria: the phylum *Firmicutes* is associated with obesity, whereas the phylum *Bacteroidetes* is associated with weight loss. Furthermore, the transplant of microbiota from obese or western diet-fed mice to lean mice resulted in weight gain (Ley et al. 2006).

Adipocyte plasticity is critical for insulin sensitivity and overall metabolic health. Consequently, disturbances of adipocyte regulation are the origin of some metabolic diseases such as T2DM. However, T2DM and obesity are not exclusively correlated. Some obese people are diabetic but a huge percentage of the population is non-diabetic obese people, identified as metabolically healthy obese (Blüher 2014). Metabolically healthy obese people have well-

functioning adipocytes and thus a lower mortality risk. The correlation commonly seen between obesity and T2DM is insulin resistance, characterized by cells becoming resistant to the effects of insulin and therefore glucose uptake. Physiological transformations in the adipose tissue, in particular adipocyte hypertrophy, adipocyte death and adipocyte stress result in increasing adipocyte remnants that need absorption by specialized cells as macrophages. Chronic deposition of these remnants causes therefore the chronic deposition of macrophages in the adipose tissue, which finally causes inflammation (Yao et al. 2014). The higher presence of macrophages lead to higher content in cytokines in the obese adipose tissue; furthermore, circulation of free fatty acids (FFAs) and FFAs depots in non-adipose tissues, as muscles, can also contribute to insulin resistance through the release of chemoattractant proteins (Guilherme et al. 2008). Cytokines as tumor necrosis factor- α (TNF- α), interleukin-6 (IL-6), interleukin-1 α (IL-1 α) and interferon gamma (IFN γ) inhibit cellular proliferation and differentiation and lead to insulin resistant-mature adipocytes (Finucane et al. 2012). Cytokines, and in particular TNF α , are potent inhibitors of adipocyte differentiation via the PPAR γ receptor, and lead to decreased triglyceride deposition and higher serum fatty acid levels. Resulting consequences are ectopic lipid deposition and impaired glucose transport, which ultimately cause insulin resistance in mature adipocytes or muscle cells. Significantly reduced insulin receptor substrate 1 (IRS-1) and protein kinase B (PKB) phosphorylation levels were observed in adipocytes from patients with T2DM. Concomitantly, high levels of pro-inflammatory cytokines (IL-6 and nuclear factor kappa-light-chain-enhancer (NF- κ B) of activated B cells) were detected (Wang et al. 2011). Nitric oxide released by macrophages may as well be responsible for increasing the susceptibility of adipocytes to become resistant to insulin (Kraus et al. 2012).

The metabolic complications of obesity may also be a result of other stimuli, which are present in the expanding adipose tissue microenvironment. Hypoxia, due to the rapid tissue expansion, results in higher levels of fatty acids and products of cell death, and causes migration of innate and adaptive immunity system cells, which in turn lead to inflammation of the adipose tissue (Surmi & Hasty 2008). Hence, inflammatory conditions due to adipose tissue expansion is another underlying cause of T2DM development (Phieler et al. 2013; Chatzigeorgiou et al. 2014).

Obesity has further been linked with a series of cancers. Hormone dependent cancers as postmenopausal breast and ovarian cancers can be of higher incidence in individuals with high body mass and fat index, since adipokines as leptin are increased in obesity and have pro-inflammatory activities. Leptin exerts its activity through leptin receptor and Fusco et al. (2010) showed that inactivation of this receptor inhibits proliferation and viability of human breast

cancer cell lines. The association between obesity and cancer was also demonstrated *in vitro* by the fact that glucose and fatty acids modulated the growth factor and cytokine secretion of adipocytes, which in turn induced the proliferation of cancer cells (D'Esposito et al. 2012).

Even though there is little information about behavioral and obesity profiles, certain neurotransmitters are linked with this disease. Neurotransmitters as dopamine and norepinephrine have been found to modulate the food intake. The relationship between the stimuli to higher or lowered food intake is thought to be the underlying mechanism. Dopamine has been described to modulate food reward through the meso-limbic circuitry of the brain (Martel & Fantino 1996). Blockers of dopamine D2 receptors result in increases of appetite and weight gain (Baptista 1999); while drugs that increase brain dopamine concentration present anorexigenic (appetite suppressing) properties (Towell et al. 1988; Foltin et al. 1990). Food intake can be mediated as well by the endogenous levels of norepinephrine. Decreases in norepinephrine will lead to lowered food intake, (Bays & Dujovne 2002) and serotonin and norepinephrine reuptake inhibitors induce satiety and effectively reduce the accumulation of abdominal fat (Hainer et al. 2006). The availability of norepinephrine transporter is decreased in the thalamus of obese individuals, supporting a link between noradrenergic dysfunction and norepinephrine levels in obesity (Li et al. 2014).

Moreover, physical activity is also an important regulator of obesity via alteration of neurotransmitter level or inflammatory cytokines. Decreases in bodily activity (e.g. sedentary lifestyle) can lead to lowered noradrenergic levels, causing weight gain. Cardiorespiratory fitness was demonstrated to help preventing by decreasing inflammation and by protecting against adrenergic desensitization. Inflammatory cytokines were described to desensitize β -adrenergic receptors to their ligands by elevating G protein-coupled receptor kinase-2 (GRK-2) (Eisenhut 2012). Several studies that reported weight loss, either through hypocaloric diet, exercise or liposuction, observed the reduction of the levels of circulating cytokines, as IL-6 and TNF- α , due to the decrease in adipose tissue mass (Polak et al. 2006; Esposito et al. 2002). Also, neurohormones as catecholamines, adenosine and dopamine, which are higher during exercise, have the ability to inhibit pro-inflammatory functions of macrophages (Bush et al. 1999; Van Der Horst et al. 1999).

1.1.3. Model systems for obesity studies

Model cell culture systems have been vital in obesity studies. Preadipocyte cell lines, as 3T3-F442A and 3T3-L1, were first established as a valid model system in the laboratory of Green (Green & Meuth 1974). Both were originally developed by clonal expansion from murine Swiss 3T3 embryo cells and became a standard for studying preadipocyte differentiation, due to its efficiency to differentiate from fibroblasts to adipocytes.

1.1.3.1. Pre-adipocyte Proliferation

Preadipocyte differentiation and proliferation are the main factors determining the mass of the white adipose tissue. The adipose tissue derives from pluripotent mesenchymal stem cells. These cells have the ability to undergo differentiation into adipocytes, myocytes, chondrocytes and osteocytes (Pereira-Fernandes et al. 2014) depending on the stimuli received. Differentiation into adipocytes requires passage through a preadipocyte stage, which, under appropriate conditions, will originate mature adipocytes. Pre-adipocyte proliferation occurs through clonal expansion and represents the initial steps towards adipogenesis, determining the number of mature adipocytes throughout adulthood. During proliferation, some genes are significantly up-regulated as cyclin B2, cyclin D1 and cyclin E1, proliferating cell nuclear antigen (PCNA) and the insulin-like growth factor-1 (IGF-1) that is a potent activator of the protein kinase B (Akt) pathway leading to cell growth and proliferation.

1.1.3.2. Pre-adipocyte Differentiation

During adipogenesis, pre-adipocytes lose their fibroblastic morphology, start to accumulate triglycerides into their characteristic fat droplets, and acquire the appearance and metabolic features of mature adipocytes (Green & Meuth 1974). To trigger the cascade of cell differentiation, protocols have been developed for effective differentiation. At the point of growth arrest, cells can be exposed to a differentiation cocktail composed of agents such as insulin or adrenergic agents (epinephrine, cellular cyclic adenosine monophosphate (cAMP)). For the complete differentiation of the cell line 3T3-L1, an appropriate and effective cocktail has been established containing insulin, dexamethasone (DEX), and 3-isobutyl-1-methylxanthine (IBMX) (Mendes et al. 2008). Insulin acts through the activation of the IGF-R signaling pathway, altering the expression of the sterol regulatory element-binding protein-1 (SREBP-1), resulting in the stimulation of glucose transporter type 4 (GLUT4) - mediated glucose uptake and lipid synthesis; dexamethasone acts through the glucocorticoid signaling pathway, with an opposite action as of cortisol, ultimately activating the CCAAT-enhancer-binding proteins β and γ

(C/EBPs) and inhibiting fat breakdown; IBMX is an agent used to elevate cAMP, leading to phosphorylation of the cAMP response element-binding protein (CREB) that activates the expression of endogenous C/EBP- α , a transcription factor crucial for adipocyte differentiation and lipid synthesis and accumulation. PPAR- γ is a nuclear receptor with an active role in the regulation of adipogenesis, stimulating the expression of target genes involved in adipocyte differentiation and increased lipid storage (Sarjeant & Stephens 2012) (Figure 1).

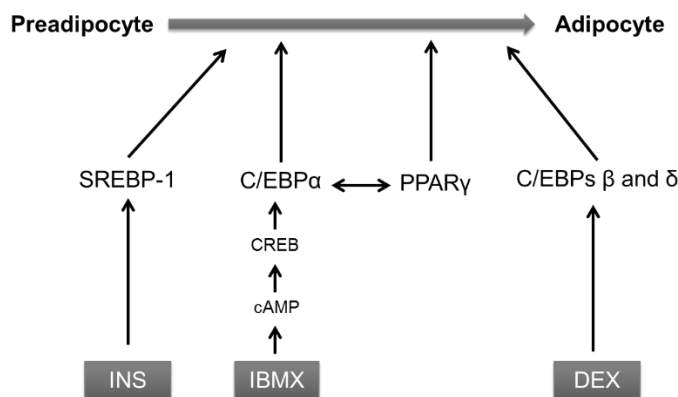


Figure 1 – Factors intervening in 3T3-L1 preadipocyte differentiation. (Insulin (INS), 3-isobutyl-1-methylxanthine (IBMX), dexamethasone (DEX), cyclic adenosine monophosphate (cAMP), cAMP-responsive element binding protein (CREB), sterol regulatory element-binding protein-1 (SREBP-1), CCAAT-enhancer-binding proteins (C/EBPs) and peroxisome proliferator-activated receptor- γ (PPAR- γ)).

1.2. Natural Compound Discovery

Drug discovery is an active research area, with a broad selection of drug candidates and increasing investment. Natural compounds from organisms as primary metabolites (steroids, nucleosides, etc.), vitamins, hormones, protein fragments, herbal mixtures and polyamines fall into the category of natural product drugs, even if they are synthetically produced, whereas compounds inspired from a natural product template, but synthetically derived are considered natural product derived drugs. Semi-synthetic drugs of natural origin had a natural compound as a template, and currently marketed with some modifications and synthetically produced. Synthetic drugs don't share similarities with known natural compounds and are therefore synthetically derived. In the pipeline of drug discovery are now thousands of drug-like chemicals in the various phases of clinical trials. In 2010, around 10% of the drugs on the market were unaltered natural products, 29% derived from natural products, known as semi-synthetic, and the rest (61%) was composed with compounds of synthetic origin (Bate et al., 2010). Between 2000 and 2013, 25% (14 out of the 56) approved drugs with natural origin were unaltered natural products, while the majority were semi-synthetic natural products (Butler, et

al. 2014). These numbers underline the importance of natural product discovery. Important therapeutic areas for new natural products and semi-synthetic natural compounds are oncology and infectious diseases, which make up to 64% of the natural drug targets (Butler et al. 2014).

The first two marine-derived natural products used to treat human disease were Cytarabine (Cytosar-U®, Depocyt®), a synthetic pyrimidine nucleoside last approved by the EMA in 2001 for the treatment of cancer, and Vidarabine, a synthetic purine nucleoside with antiviral properties, both developed from natural compounds from the Caribbean sponge *Tethya crypta* (Newman et al. 2009). About 6 years later, Ziconotide (Prialt®), was approved for the treatment of moderate to severe pain. Ziconotide is the synthetic formula of a 25-amino acid peptide, originally isolated from the venom of the marine snail *Conus magus* (Olivera 2000). Trabectedin (Yondelis®) is another marine-derived product with EMA's approval in 2003 for the treatment of soft tissue sarcoma and ovarian carcinoma, isolated from the tunicate *Ecteinascidia turbinata* found in the Caribbean and Mediterranean seas (Wright et al. 1990). In 2010, the FDA and EMA approved Halichondrin B, a polyether isolated from the marine sponge *Halichondria okadaic*, for the treatment of metastatic breast cancer: (Hirata & Uemura, 1986).

Brentuximab vedotin (Adcetris™) was approved by the FDA in 2011 for patients with classical Hodgkin's lymphoma, peripheral T-cell lymphoma, diffuse large B-cell lymphoma or systemic anaplastic large cell lymphoma (Stathis & Younes 2015). This compound is a novel anti-body drug conjugate composed by a chimeric monoclonal anti-CD30 antibody, cAC10, directing this compound specifically into CD30-positive malignancies, and a cathepsin-cleavable linker as a backbone to carry monomethyl auristatin E (MMAE) (Ansell 2014). MMAE is a synthetic compound derived from dolastatin 10 that was first isolated from the sea hare *Dolabella auricularia* with potent antineoplastic activity (Pettit et al. 1987). The compound was later found to be produced by the cyanobacteria *Symploca hydroides* and *Lyngbya majuscula*, which are part of the sea hare's diet (Niedermeyer & Brönstrup 2012).

1.2.1. Anti-obesity Natural Compounds

The potential of natural compounds on drug development has been widely explored and proven to be a reliable and fruitful source. Therefore, isolation and characterization of novel functional compounds from biological organisms has gained much attention.

Many natural compounds have been studied that demonstrated interesting activities for the prevention and treatment of obesity and related metabolic complications as diabetes and cardiovascular disease. Most of the research employed *in vitro* methodologies (e.g. modulation

of the differentiation of 3T3-L1 cell line), *in vivo* techniques (e.g. adipose mass tissue decreases in mice or rats), or direct enzymatic assays (e.g. lipase activity screening).

As of December 2013, four drugs have been approved by both the FDA and the EMA for chronic weight management and obesity complications: Orlistat (Alli®, GlaxoSmithKline; Xenical®, Roche), Phentermine/topiramate extended release (Qsymia®, Vivus), Exenatide (Byetta®, Bydureon®) and Dapagliflozin (Forxiga®). The FDA has also approved Lorcaserin (Belviq®, Arena Pharmaceuticals), Pramlintide (Symlin®, Amylin Pharmaceuticals) and Phentermine (Qnexa®, Vivus), for the long-term treatment of obesity in 2012. Phentermine and Lorcaserin are two appetite suppressants used for the treatment of obesity through noradrenergic activation. Pramlintide is the synthetic analogue of amylin that promotes satiety and inhibits the secretion of glucagon. However, EMA has rejected these drugs due to limited efficacy, carcinogenic and teratogenic potential, cardiovascular events and cognitive impairment, considering that their side-effects would not outweigh their benefits. Many natural compounds have been studied and shown interesting activities for the prevention and treatment of diabetes, obesity and cardiovascular diseases. The drugs usually applied in obesity treatment can be mainly divided in four groups: drugs suppressing appetite, drugs increasing insulin sensitivity, drugs targeting sodium/glucose co-transporters and drugs decreasing lipid absorption. Natural compound discovery on obesity treatment has, however, focused mainly on compounds that act on lipid absorption and insulin resistance.

Most of the research focused on *in vitro*, using appropriate cell lines, and *in vivo* techniques, using model systems as mice or rats, while others focused on direct enzymatic assays for lipase activity screening. Some of the latest articles describing anti-obesity natural products have shown promising activities, through direct pancreatic lipase inhibition as for the methyl xestospongic ester from the marine sponge *Xestospongia testudinaria* (Liang et al. 2014), the methanol extract of the brown algae *Eisenia bicyclis*, composed mainly of phlorotannins (Eom et al. 2013), flower buds of *Splilanthus acmella* (Ekanem et al. 2007), and galangin, a flavonol glycoside isolated from *Alpinia galanga* Wild, a plant from the ginger family (Kumar & Alagawadi 2013).

The identified compounds found to have anti-obesity properties also have various and numerous chemical identities. Many phenols had a direct activity on 3T3-L1 pre-adipocyte differentiation. Phenols are naturally present in a wide variety of organisms. Catechins from green tea leaves (Ahmad et al. 2015), licochalcone A from the root of *Glycyrrhiza glabra* (Quan et al. 2012), tyrosol from *Rhodiola crenulata* (Lee et al. 2011) and dehydrodiconiferyl alcohol from *Cucurbita moschata* (Lee et al. 2012) are phenols and polyphenols with described anti-

obesity activities. Terpenes are also a representative group of identified natural compounds, with either neurohormonal activity, as the xylarenals A and B from *Xylaria persicaria* (Smith et al. 2002), or adipose tissue mass regulation properties, as for the ursolic acid from *Sambucus australis* Cham. (Rao et al. 2011). Polysaccharides from marine brown algae also showed interesting activity, namely the main active compounds L-fucose (sugar) and sulphate ester groups that stimulated lipolysis through hormone sensitive lipase activation (Kim et al. 2009). Two polyketides, moccasin and ankaflavin from the mold *Monascus* sp., also inhibited adipose tissue differentiation and lipogenesis *in vitro* (Jou et al. 2010).

Natural compounds acting on the regulation of neurohormone levels and UCP modulation, an important protein involved in thermogenesis and a possible therapeutic target for obesity, have been described as well. Xylarenals A and B, two sesquiterpenoids, isolated from the ascomycete *Xylaria persicaria*, were found to be selective antagonists for the Neuropeptide Y5 (Smith et al. 2002), which is a receptor found in peripheral and central nervous system, involved in mediating food intake and body weight (Schaffhauser et al. 1997). Fucoxanthin, a carotenoid from *Undaria pinnatifida* (Miyashita et al. 2011) and evodiamine, an alkaloid traditionally used in China as a “fat burner” (Kobayashi et al. 2001) induced UCP-1 expression; phytochemicals from the leaves of *Peucedanum japonicum* Thunb increased the expression of the UCP-3 gene in muscle (Nukitragan et al. 2012).

A new group of compounds currently being studied are the sodium/glucose co-transporter (SGLT) inhibitors, derived from the natural product phlorizin, a polyphenol. Phlorizin blocks the absorption of glucose in the SGLT-2 present in the nephrons, resulting in decreases of glucose reabsorption. This represents a novel therapeutic approach to diabetes that is independent of insulin secretion or action. Preclinical and clinical studies of SGLT2 inhibitors in subjects with T2DM, as well as genetic mutations in kidney-specific SGLT2 that result in no adverse sequelae, appear to support this strategy (Ehrenkranz et al. 2005). Synthetic compounds derived from phlorizin were actually seen to be more effective and selective, mainly due to the reduced degradation by glucosidase enzymes and increased intestinal absorption (Ehrenkranz et al. 2005). Many natural product derived drugs acting on SGLT have been developed. Dapagliflozin (Farxiga®, Forxiga®) and canagliflozin (Invokana®) were approved by the EMA and many other analogues are currently in phase III and phase II clinical trials.

1.2.2. Cyanobacteria as a source of natural compounds

1.2.2.1. Cyanobacteria

Phytoplankton has been found in almost every ecological niche of aquatic systems, recognized for its crucial contribution to ecosystems in atmospheric oxygen renewal and sink for carbon dioxide. Even though they represent less than 1% of Earth's biomass, phytoplankton organisms are primary producers, highly important to every food chain.

Cyanobacteria have fossil records from over 2 billion years ago and are widely distributed through terrestrial, marine and freshwater ecosystems. They are the only bacteria capable of oxygenic photosynthesis and their high adaptability to each ecosystem could be the reason why they are so prolific in secondary metabolites. The need for UV protection, feeding avoidance (Cruz-Rivera & Paul 2007) or for microbial communication as quorum sensors (Sharif et al. 2008) led them to produce ecologically significant compounds. Cyanobacteria are gram-negative photosynthetic prokaryotes, believed to be at the origin of the rise of atmospheric oxygen, an event known as the Great Oxidation Event. Cyanobacteria lack flagella, however, they are able to move in the water column using atmospheric nitrogen as a buoyancy regulation mechanism. Other environmental adaptations include the ability to reproduce through differentiated cells (hormogonia) and to, when in stress (periods of lowered light, nutrients or water) thrive through resting cells, known as akinets, a survival cell used for storing nutrients, or heterocysts, used for nitrogen fixation when nitrogen sources are depleted (Madigan et al. 2010).

Cyanobacteria are a Phylum that belongs to the Bacteria Domain. Morphologically, they are 2 to 40 µm diameter organisms with a complex cell wall constituted by a thick peptidoglycan layer and periplasmic space between the inner cytoplasmic membrane and the outer cell membrane. The outer cell membrane is composed by lipopolysaccharides, phospholipids and proteins, while the intracellular space is composed of proteins, enzymes and metabolites (Madigan et al. 2010).

Cyanobacteria taxa was determined according to the Botanical Code of Nomenclature and includes five major groups as was proposed by Rippka et al. (1979): I (*Chroococcales*) — unicellular cyanobacteria that reproduce by binary fission or budding, II (*Pleurocapsales*) — unicellular cyanobacteria that reproduce by multiple fission, III (*Oscillatoriales*) — filamentous non-heterocystous cyanobacteria that divide in only one plane, IV (*Nostocales*) — filamentous heterocystous cyanobacteria that divide in only one plane, V (Stigonematales) — filamentous heterocystous cyanobacteria that divide in more than one plane (Boone & Castenholz 2001).

1.2.2.2. Bioactive compounds from Cyanobacteria

Cyanobacteria can have negative impacts on ecosystems. They are known to produce toxins, causing the death of animals and harmful algal blooms in eutrophicated aquatic systems, detrimental to water quality and biological variability. However, recent research enlightened the ability of cyanobacteria to synthesize other compounds highly relevant for economical, industrial, medicinal and biological fields. 24% of the commercially available natural products for biomedical research are of cyanobacterial origin (Gerwick & Moore 2012).

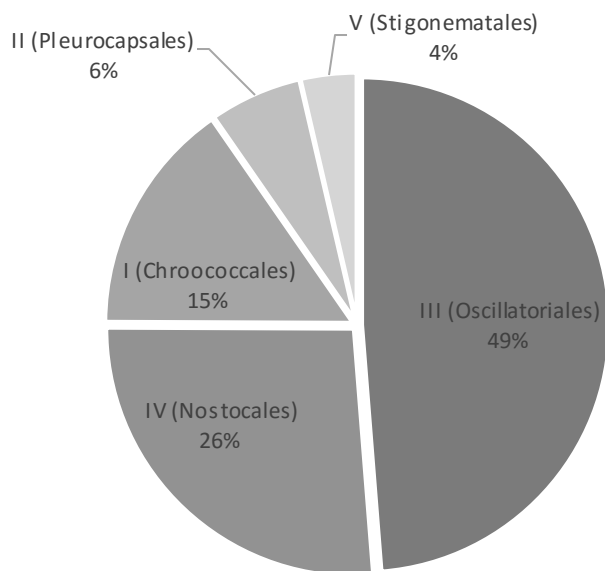


Figure 2 – Pie chart for the distribution of reported cyanobacterial secondary metabolites through the five major botanical sub-classes (adapted from Gerwick et al. 2008).

Compounds from cyanobacteria have been seen to interact with specific cellular targets such as actin filaments, microtubules and proteasome, explaining why they are so prolific in compounds for disease treatment. The main focus has, however, been in drug discovery for cancer treatment and some of the described molecules have been in preclinical and/or clinical trials as potential anticancer drugs (Gerwick et al., 2001).

Up to now, more than 800 metabolites have been described from various taxa and beyond that, one single strain of cyanobacteria is able to produce a wide array of structurally different secondary metabolites. Filamentous marine cyanobacteria from subclass III (*Oscillatoriales*) represent nearly half of the 800 compounds reported so far (Gerwick et al. 2008). From a single

genus, there are almost 300 compounds described, 236 compounds are ascribed to *Lyngbya majuscula* and a further 11 to *L. bouillonii* (Gerwick et al. 2008).

Certain genera of marine cyanobacteria as *Lyngbya*, *Oscillatoria*, *Nostocales*, *Symploca*, *Calothrix*, *Leptolyngbya*, *Dichothrix*, among others, have been shown to produce many secondary metabolites with several chemical identities. Even though the majority of studies report beneficial biological compounds from filamentous and colonial cyanobacteria, probably biased due to the easy collection and large density of these strains (Gerwick et al. 2008), further studies have shown that both free-living unicellular (*Synechocystis*, *Synechococcus*) and more complex cyanobacterial strains (*Nodosilinea*, *Leptolyngbya*, *Pseudoanabaena* and *Romeria*) have promising activities towards numerous cancer cell lines (Costa et al. 2014).

Most of the cyanobacterial metabolites are partially composed of amino acids with lipopeptide backbones and the unique structural and functional composition is mainly due to modification through oxidation, methylation or various halogenations. Metabolites are mainly biosynthesized in large multifunctional megaproteins called multimodular nonribosomal polypeptide (NRPS) and mixed polyketide enzymatic systems (PKS). Peptide-based natural products produced by this machinery have a tremendous chemical diversity, including not only the 20 established L-amino acids, but also other non-proteic amino acids, heterocyclic rings, sugars and fatty acids. These peptides can have therefore a wide array of biological activities, from antibacterial (Gutiérrez et al. 2010), antimalarial (Tripathi et al. 2011) and anti-inflammatory (Malloy et al. 2011) activities, amongst others.

The non-ribosomal peptide system produces cyanobacterial compounds through the specific condensation of amino acids and target carboxyl groups, without the need for nucleic acids. The NRPS peptide synthesis is mediated by peptidyl carrier protein, a protein composed of approximately 80 amino acids, that acts as a scaffold, tethering the amino acid building blocks and peptidyl intermediates as they are modified and condensed by other domains of the NRPS (Lai et al. 2006). The NRPS genes encoding for the catalytic domains that compose the multi-module proteins are some of the largest known genes (Finking & Marahiel 2004). The other catalytic domains activate amino acids through other protein domains responsible for adenylation, thiolation and condensation of active intermediates (Finking & Marahiel 2004). In addition to the core domains are the tailoring domains, responsible for diversity in structure and function of NRPs, as the epimerase, cyclization, methyltransferase, and oxidation domains (Schneider & Marahiel 1998). Polyketide enzymatic systems produce polyketides, through the polymerization of acetyl and propionyl subunits onto a growing carbon chain, a process functionally similar to the fatty acid synthesis in the lipid metabolism (John et al. 2008). Both

pathways also share similar functional domains, as ketoacyl synthase, acyl transferase, ketoacyl reductase, dehydratase, enoyl reductase, acyl carrier protein and thioesterase (John et al. 2008), even though the minimal structure of PKS requires only the domains acyl carrier protein, ketoacyl synthase and acyl transferase.

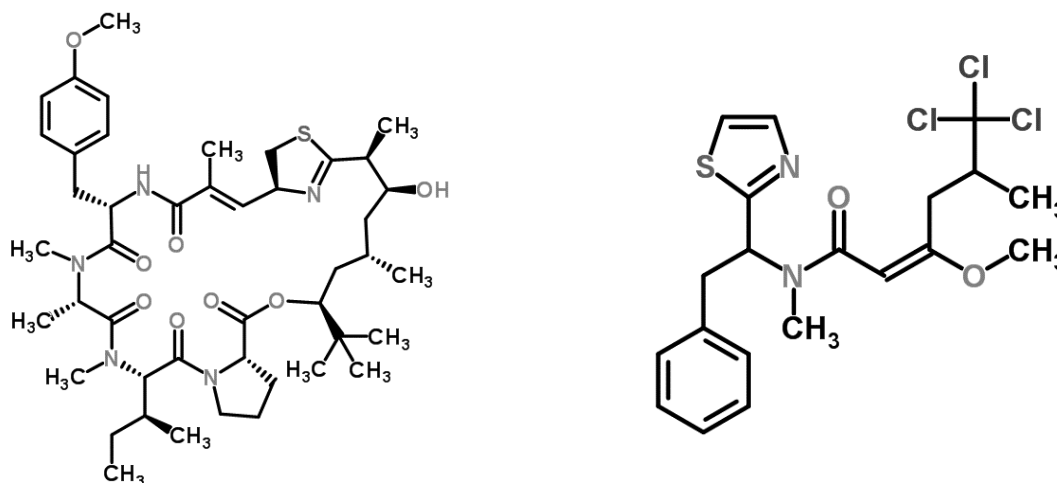


Figure 3 – 2D structure of the secondary metabolites Barbamide (on the left) and Apratoxin A (on the right) (from chemspider.com).

Lyngbya has been collected in various places, from Papua New Guinea to the Bahamas and reported to produce numerous natural products belonging to various chemical classes with anti-proliferative, anti-cancer properties (Nagarajan et al. 2012). Metabolites as malyngamides and its variants reported from *L. majuscula* showed weak toxicity in *in vitro* tests, revealing that this metabolites could be feed deterrents. A group of complex and unique cyanobacterial metabolites named Portoamides isolated from *Oscillatoria sp.* cultures, showed allelopathic activity towards *Chlorella vulgaris* and also cytotoxicity activity, on H460 lung cancer cells (Leão et al. 2010). Portoamides are four compounds, with similar characteristics of families of natural compounds previously described as schyrozins A, pahayokolides and tychonamides (Leão et al. 2010).

Other compounds as the novel apratoxins with both peptide and polyketide moieties have shown potent anti-tumor activity. Apratoxin A (figure 3), for example, has highly varied chemical constituents that include three methylated amino acid moieties, one regular amino acid unit (proline), a tri-substituted double bond containing an unsaturated modified cysteine residue, a new dihydroxylated fatty acid moiety and 3,7-dihydroxy-2,5,8,8-tetramethylnonanoic acid (Luesch et al. 2001). This particular secondary metabolite exhibited significant *in vitro*

cytotoxicity in tumor cell lines and *in vivo* studies revealed complete recovery of an early stage of adenocarcinoma in mice (Luesch et al. 2006). The mechanism proposed is the ability of this metabolite to induce G1 cell cycle arrest in tumor cells (Luesch et al. 2006).

Dolastatin peptides are another group of promising metabolites. Dolastatin 10 was first isolated from sea hare *D. auricularia*, from the Indian Ocean (Poncet 1999), but in fact produced by the cyanobacteria *Symploca hydroides* and *Lyngbya majuscula* (Niedermeyer & Brönstrup 2012). Dolastatin 10 was found to have potent anti-neoplastic activity, with an ED₅₀ in the picomolar range, inhibiting microtubule assembly through the disruption of the microtubule spindle by binding to tubulin (Mitra & Sept 2004). With a simple chemical structure, the total synthesis of the compound was described in 1989 (Pettit et al. 1998). MMAE, the synthetic derivative is coupled to monoclonal antibodies and used as therapeutics to B/T-cell malignancies and acute myeloid leukemia (Pereira et al. 2015).

Other variants of Dolastatin (Dolastatin 3) inhibit HIV integrase (Mitchell et al., 2000). Halogenated compounds are also common, as for the described barbamide (Figure 2), a mixed polypeptide-polyketide that contains an unusual trichloromethyl group (Flatt et al. 2006) with molluscicidal activity (Orjala & Gerwick 1996).

Picocyanobacteria, the simplest cyanobacteria, are also able to produce natural compounds with biomedical applications. Hierridin B was isolated from *Cyanobium sp.*(LEGE 06113) and had selective cytotoxicity towards HT-29 colon adenocarcinoma cells (Leão et al. 2013).

Specific moieties are presumed to be responsible for the activity of certain cyanobacterial products, as unique structural changes in amino acids. Many studies are now focusing on the analysis of structure-activity relationship, towards the synthesis of an active part alone for both medicinal and biology research and aid the screening of potential activities of secondary metabolites.

1.2.2.3. Leads on bioactive compounds from cyanobacteria with anti-obesity activity

Some strains of cyanobacteria are commercially available for consumption due to their beneficial properties to human health as *Arthrospira*, *Nostoc* and *Aphanizomenon* (Pulz & Gross 2004). They are composed of bioactive and beneficial components as carotenoids, γ -linoleic acid, phycocyanin, fibers, and plant sterols (Ku et al. 2013). *Arthrospira*, previously known as *Spirulina*, is a filamentous cyanobacteria belonging to the class III (*Oscillatoriales*) usually found in high salt-alkaline water bodies. As a traditional food in Central Africa, studies proving its beneficial effects on human health has led to its consumption worldwide. The

therapeutic effects, that generally comprise the major three species *Arthrospira platensis*, *Arthrospira maxima*, *Arthrospira fusiformis*, include anti-hypercholesterolemia, anti-hyperglycerolemia, anti-inflammatory, anti-tumour and anti-viral activities; it is also protective of cardiovascular diseases, mainly due to its hypolipidemic, anti-oxidant and anti-inflammatory activities (as reviewed in Deng & Chow 2010). Many preclinical studies have been performed in various animal models that demonstrated the hypolipidemic activity of *Spirulina*. *Spirulina* is well recognized for its high protein content and its richness in minerals, essential fatty acids and carotenoids, as β -carotene, astaxanthin and canthaxanthin (Miranda et al. 1998), phycobiliproteins as c-phycoerythrin (Patel et al. 2005), phenolics as synapic, chlorogenic and caffeic acids, and anti-oxidant vitamins as Vitamin E (Miranda et al. 1998) .

Studies revealed that supplementation in diet of *Arthrospira* species, significantly ameliorated the hyperlipidemic profiles of high fat/high cholesterol diet, high fructose and high sucrose diets, and carbon tetrachloride-induced fatty livers in rats and mice, lowering hepatic cholesterol and triglyceride levels (Iwata et al. 1990; Gonzalez de Rivera et al. 1993; Torres-Duran et al. 1999; Jarouliya et al. 2012; Cheong et al. 2010).

These results were confirmed in human clinical trials, where supplementation with *Spirulina* species resulted in decreases of plasma triglyceride concentrations and of the ratio of high-density lipoprotein (HDL) and low-density lipoprotein (LDL) in subjects with T2DM (Parikh et al. 2001). *Spirulina* also presents a high content of γ -linoleic acid (around 1.3%), which is frequently used to treat rheumatoid arthritis, atopic eczema, acute respiratory distress syndrome, cancer, and asthma, and to improve plasma lipid profiles, for its anti-inflammatory properties (Fan & Chapkin 1998). Recent studies report that the *in vitro* and *in vivo* anti-diabetic effect of *Spirulina* could be from the active component phycocyanin, a phycobiliprotein that lowered body weight, serum and liver triglyceride content and fasting plasma glucose in KK-Ay mice (KK mice strain with the yellow obese gene A^y), most likely by enhancement of insulin sensitivity (Ou et al. 2013). However, the inherent high polysaccharide content itself has the capacity of lowering insulin and glucose blood levels and promote cholesterol elimination in feces (de Jesus Raposo et al. 2013).

The major component of *Spirulina*, phycocyanin, accounting for 14% of the cyanobacteria's dry weight (Romay et al. 2003), has been reported to be a potent anti-inflammatory agent, which abolished the TNF- α response in Kupffer cells from mouse liver after thyroid calorigenesis induction (Remirez et al. 2002) and reduced inflammatory cell infiltration and colonic damage in rats with acetic acid induced colitis (Gonzalez et al. 1999). Other studies

described phycocyanin as a powerful antioxidant agent with neuroprotective effects, able to scavenge reactive oxygen species (Farooq et al. 2014).

Diet supplementation with *Nostoc commune* var *sphaeroides* Kützing (*N. commune*) also showed a hypocholesterolemic effect in mice, reportedly by reducing intestinal cholesterol absorption and stimulating fecal sterol excretion (Rasmussen et al. 2009). Its lipid extract was also seen to significantly lower the expression of 3-hydroxy-3-methyl-glutaryl-CoA reductase (HMG-coA reductase), a key enzyme for cholesterol biosynthesis, and the levels of mature forms of sterol-regulatory element-binding protein 1 and 2 (SREBP-1 and SREBP-2), resulting in the decrease of expression of genes involved in cholesterol and fatty acid metabolism (Rasmussen et al. 2008). Furthermore, another study reported that the lipid extract of *N. commune* is able to decrease proinflammatory gene expression, evaluating the levels of proinflammatory mediators as TNF- α , COX-2, IL-1 β , IL-6 in RAW 264.7 macrophages in a dose-dependent manner (Park et al. 2008). The anti-inflammatory function may be mediated, at least in part, by inhibiting the NF- κ B pathway to decrease the production of proinflammatory mediators (Ku et al. 2013).

Cyanobacteria could have major bioactive compounds other than the ones so far described with effective lipid-profile improving and anti-oxidant properties. Safety assessments of certain cyanobacteria strains are now in development, in order to evaluate if dietary supplementation of cyanobacteria may be consumed without toxic side-effects (Yang et al. 2011).

2. Objectives

Studies performed earlier at the Blue Biotechnology and Ecotoxicology Group of CIIMAR had already established that some cyanobacterial strains are producers of cyanotoxins and secondary metabolites (Martins et al. 2005). The possibility that cyanobacteria could produce secondary metabolites with relevant bioactivity for the treatment of obesity or obesity-related metabolic complications was based on a literature search on bioactive compounds with anti-obesity properties from cyanobacteria and other organisms, and on profiles of compounds found in cyanobacterial strains (Castro et al., submitted; see Appendix II).

Our objective was to screen six cyanobacterial strains for the potential production of secondary metabolites relevant to anti-obesity studies using a bioassay-guided fractionation process. The compounds of cyanobacterial strains were extracted and separated into 62 fractions. Two endpoints were chosen for the analysis of anti-obesity activities: (i) preadipocyte proliferation and (ii) adipogenesis in the 3T3-L1 murine cell line.

The sulforhodamine B (SRB) and 3-(4,5-dimethylthiazol-2-yl)-2,5-diphenyl tetrazolium bromide (MTT) assays were used to estimate the proliferative activity of the prepared fractions. ELISA BrdU assay was used as a complementary method to confirm the observed proliferative bioactivity in selected fractions. Regarding the adipogenic activity, Oil Red O staining was performed after adipocyte differentiation to quantify the intracellular lipid contents, using a combination of imaging and photometrical analyses.

The overall aim of this study was to isolate and identify novel compounds from the selected cyanobacterial strains based on bioactivity screening and subsequent fractionations. For this, several chromatographic techniques (VLC, flash chromatography, HPLC, SPE) were used to isolate compounds and ^1H NMR to characterize each step of fractionation.

3. Materials and Methods

3.1. Cyanobacterial strains and culture

The Blue Biotechnology and Ecotoxicology Group of CIIMAR offers a large collection of cyanobacterial strains isolated from water samples and solid materials from the Portuguese coast and freshwater ecosystems over the years. Culturing of cyanobacteria strains was performed in order to obtain high total biomass. Cyanobacteria were grown in Z8 medium (Kotai, 1972). Cultures were maintained at the constant temperature of 25°C, with a light intensity of approximately 30 $\mu\text{mol photons m}^{-2} \text{s}^{-1}$ and with a light/dark cycle of 14:10h. During the exponential phase, cells were harvested by centrifugation (7 min, 4600 rpm, 4 °C) or filtration, frozen at -80 °C and freeze-dried. The lyophilized biomass was stored until the extraction procedure took place.

3.2. Extraction and bioassay-guided fractionation

The lyophilized biomass from 6 different cyanobacterial strains was used for a simple liquid extraction, which yielded each a cyanobacterial crude extract. A mixture of dichloromethane:methanol (2:1) was employed to extract the cellular components of the biomass. The cyanobacterial biomass was immersed in the mixture for 10 minutes, and then put through the cheese cloth and Whatman N°1 Filter Paper in a Büchner funnel as shown as in Figure 1, with the vacuum on. The resulting liquid phase was collected in a round bottom (RB) flask. This process was repeated twice. Heating (<40 °C) of the mixture using a hotplate was further performed for about four times in order to maximize the amount of cyanobacterial cellular compounds extracted. Following extraction, the liquid phase collected in the RB flask was evaporated in a rotary evaporator. The resulting content in the RB flask was re-suspended in chloroform, transferred to a pre-weighed glass vial and dried under vacuum. The mass of the crude extract was measured in order to calculate the yield of the extraction procedure.

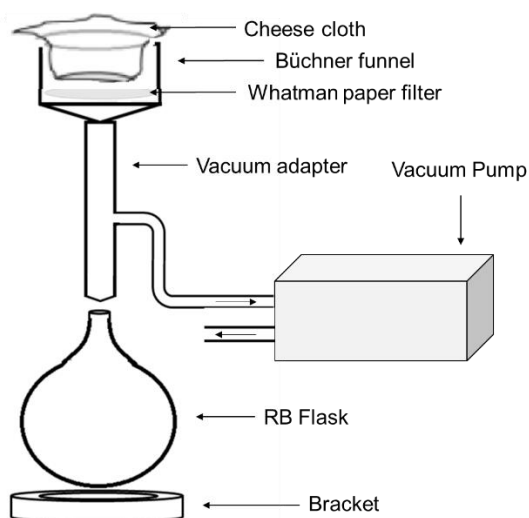


Figure 4 - Apparatus assembly for the extraction of the crude extract, from the lyophilized cyanobacterial biomass.

The crude extracts obtained are then subjected to a normal phase (silica gel 60, 0.0015-0.040 mm, Merck, KGaA, Darmstadt, Germany) vacuum liquid chromatography (NP-VLC). The crude extract was resuspended in the initial eluent mixtures and loaded on top of the silica column. The paper filter is added after loading the sample in the silica, to disturbing the silica bed on the top of the column. Using a gradient of solvents, from 1:9 Ethyl Acetate (EtOAc):Hexane to 1:1000 Trifluoroacetic Acid (TFA):Methanol (MeOH), the crude extract was separated in fractions of increasing polarity. The chromatography eluent solutions were carefully added stepwise, according to Table 1, and 10 solutions were obtained (A-J), collected in RB flasks. These fractions were dried in a rotary evaporator, re-suspended, transferred to pre-weighed vial, dried and weighed before the ^1H nuclear magnetic resonance (NMR) (400 MHz, BrukerAvance III) analysis. This was the general procedure for the first fractionation, whose fractions were later used in the screening for biological activity.

Table 1 - Gradients used in the vacuum liquid chromatography (VLC).

Fraction	EtOAc (%)	Hexane (%)	Methanol (%)	TFA (%)	Volume (mL)
A	10	90	-	-	500
B	20	80	-	-	200-250
C	40	60	-	-	200-250
D	50	50	-	-	200-250
E	60	40	-	-	200-250
F	80	20	-	-	200-250
G	100	-	-	-	200-250
H	75	-	25	-	200-250
I	-	-	100	-	500
J	-	-	99,9	0,1	200-250

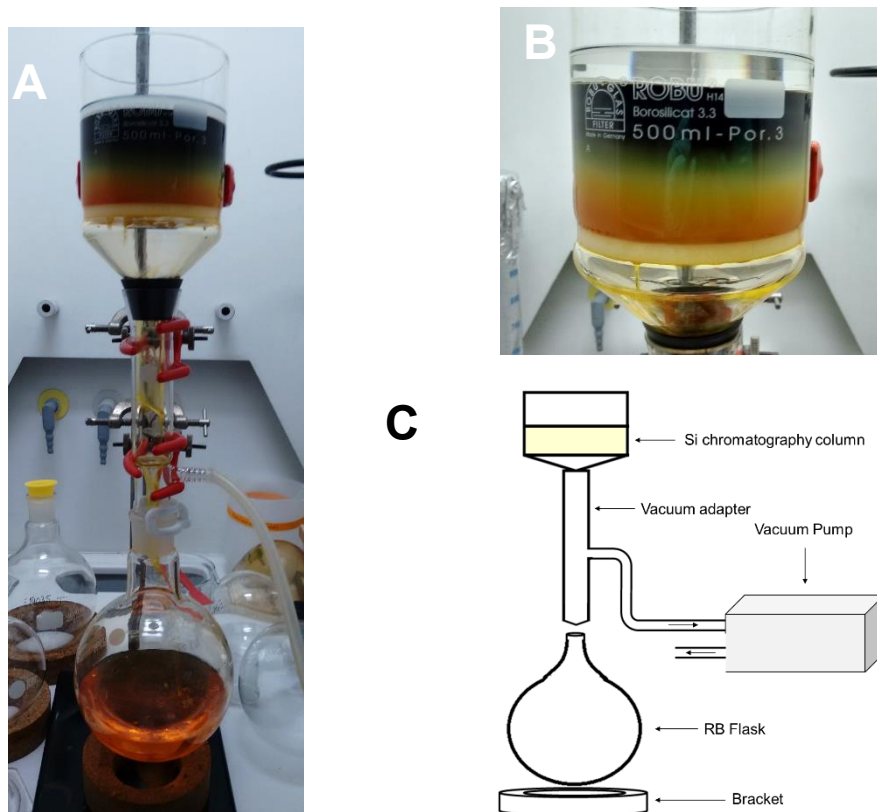


Figure 5 - A) Setup of the fractionation during Fraction B obtainment; B) Close-up of the silica gel column used in the vacuum liquid chromatography; C) Apparatus assembly for the vacuum liquid chromatography.

3.2.1. Normal phase vacuum liquid chromatography of E14028 I

The bioactive fraction E14028 I was subjected again to a normal phase (silica gel 60, 0.0015-0.040 mm, Merck, KgaA, Damstadt, Germany) vacuum liquid chromatography (Figure 4C), a method chosen due to the high mass of this fraction ($m=1.7516$ g), inappropriate for more refined methods as column chromatography. Using a gradient of solvents, from 4:6 EtOAc:Hexane to neat Methanol, seven different fractions were obtained of increased polarity. Fraction E14028 I was suspended in ethyl acetate with the help of ultrasounds, and loaded on top of the silica column. The mixtures were carefully added stepwise, according to Table 2, and 7 solutions were obtained (1-7), collected in RB flasks. The fractions were dried in a rotary evaporator, re-suspended, transferred to pre-weighed vial, dried and weighed before the ^1H NMR (400 MHz, BrukerAvance III) analysis. The obtained fractions were subsequently tested in the biological assays.

Table 2 - Gradients used in the vacuum liquid chromatography (VLC).

Fraction	EtOAc (%)	Hexane (%)	Methanol (%)	Volume (mL)
E14028 I1	40	60	-	400
E14028 I2	80	20	-	300
E14028 I3	100	-	-	300
E14028 I4	90	-	10	300
E14028 I5	75	-	25	300
E14028 I6	50	-	50	300
E14028 I7	0	-	100	400

3.2.2. Flash chromatography of E14028 I7

After the biological assays, the most polar sub-fraction (E14028 I7) was found to be the most active one. We proceeded then to a normal phase 50 cm length silica column (silica gel 60, 0.040-0,063 mm, Merck) flash chromatography (Figure 6). The length of this column was considered appropriate due to the complexity of the sub-fraction, assessed through ^1H NMR (400 MHz, BrukerAvance III) spectrum analysis. Using a gradient of solvents, from 1:9 MeOH:EtOAc to 1:1000 TFA:MeOH, 86 samples were collected in 10 mL tubes. The fraction E14028 I7 (m=891 mg) was resuspended in the mixture corresponding to the Mixture 1 and loaded onto the silica gel column, stabilized with sand (Sigma-Aldrich) on top. The mixtures were carefully added stepwise, according to Table 3. Thin layer chromatography (TLC) (silica 60 F₂₅₄ (Merck)) was performed to every eluate and visualized under UV light in order to assess the efficiency of the chromatography and to extrapolate the composition of each mixture, as elucidated in Figure 7. Some samples in elution tubes were joint due to assumed similar composition as elucidated in Table 4. Sub-fractions were established and evaporated in RB flasks. These mixtures were dried in a rotary evaporator, resuspended, transferred to pre-weighed vial, dried and weighed before the ^1H NMR (400 MHz, BrukerAvance III) analysis. The obtained fractions were later tested in the biological assays.

Table 3 - Gradients used in the flash chromatography, for E1402817 rendering.

Mixture	EtOAc (%)	Methanol (%)	TFA (%)	Volume (mL)
1	90	10	-	100
2	85	15	-	200
3	80	20	-	200
4	75	25	-	200
5	70	30	-	150
6	65	35	-	150
7	60	40	-	200
8	55	45	-	50
9	40	60	-	100
10	30	70	-	100
11	-	100	-	200
12	-	99,9	0,1	100

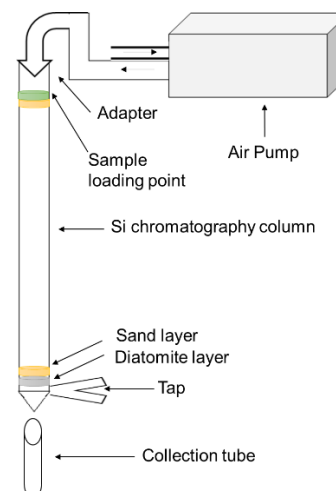
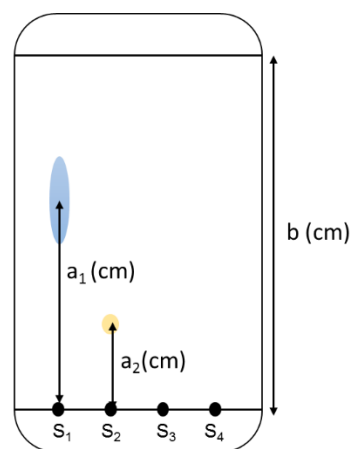


Figure 6 - Elucidatory scheme of flash chromatography procedure.

Table 4 - Fraction pooling after thin layer chromatography for E1402817.

Collection Tubes	Fractions
1-10	1
11,12	2
13-17	3
18-24	4
25-29	5
30-33	6
34-37	7
38-52	8
53-63	9
64-69	10
70,71	11
72-81	12
82-84	13
85,86	14



$$R_f(S_1) = \frac{a_1}{b}$$

$$R_f(S_2) = \frac{a_2}{b}$$

Figure 7 - Elucidatory scheme of thin layer chromatography procedure.

3.2.3. Reverse phase solid phase extraction of E1402817 8A+9

Sub-fraction 8 was difficult to solubilize in chloroform and thus was previously separated into two distinct phases: a phase solubilized in diethyl ether and another phase solubilized in MilliQ water, originating fraction 8A and fraction 8B, respectively. After ^1H NMR (400 MHz,

BrukerAvance III) analysis, the bioactive fractions E14028 I7 8A and 9 were joint due to assumed similar composition. Before processing, sub-fractions were filtered in Whatman N°1 filter paper to remove silica contamination. Reverse phase solid phase extraction (RP-SPE) using a 10g C18-E column (Phenomenex, Torrance, CA, USA) was performed to obtain further simpler sub-fractions. Using a gradient of solvents, from 1:1 H₂O:MeOH to neat Diethyl Ether, 105 solutions were collected in collection tubes. The fraction E14028 I7 8A+9 was resuspended in 1:1 H₂O:MeOH and loaded onto the SPE column. The mixtures were carefully added stepwise, according to Table 5. TLC (silica 60 F₂₅₄ (Merck)) was performed to every eluate, each one visualized under UV light and with PMA (Phosphomolybdic acid) stain, in order to assess the efficiency of the chromatography and to extrapolate the composition of each mixture, as elucidated in Figure 7. Some mixtures were joint due to assumed similar composition as elucidated in Table 6. Sub-fractions were collected and evaporated in RB flasks. These mixtures were dried in a rotary evaporator, resuspended, transferred to pre-weighed vial, dried and weighed before the ¹H NMR (400 MHz, BrukerAvance III) analysis. The obtained 3rd sub-fractions were later tested in the biological assays.

Table 5 - Gradients used in the flash chromatography, for E14028 I7 8A+9 rendering.

Collection Tubes	H ₂ O (%)	Methanol (%)	Diethyl Ether (%)	Volume (mL)
1-6	50	50	-	40
7-13	40	60	-	40
14-20	30	70	-	40
21-24	20	80	-	20
25-43	10	90	-	80
44-56	-	100	-	80
57-62	-	90	20	40
62-65	-	80	20	30
66-70	-	70	30	30
71-82	-	50	50	60
83-89	-	25	75	30
90-105	-	-	100	65

Table 6 - Fraction pooling after TLC for E14028 I7 8A+9.

Collection Tubes	Fractions
1-6	A
7-24	B
25-28	C
29-43	D
44-51	E
52-65	F
66-70	G
71-92	H
93-105	I

3.2.4. Semi-preparative reverse-phase HPLC for E14028 I7 8A+9 E

After biological assays, fraction E was selected for further purification by semi-preparative HPLC. A 1525 Binary HPLC pump and a UV-Vis detector (Waters, Milford, MA, USA) were used in all semi-preparative separations. The separation of process was carried out with a Synergi Fusion-RP column (10 μm , 250 x 10 mm, Phenomenex). Optimization of the separation procedure was previously assessed, in order to assure maximum possible separation of compounds. The conditions used in the separation after optimization are described in Table 7. The chromatogram allowed us to collect the compounds, according to the observed peaks, in RB flasks from multiple injections and evaporated in the rotary evaporator. Sub-fractions were resuspended, transferred to pre-weighed vial, dried and weighed before the ^1H NMR (600 MHz, BrukerAvance III) analysis. The obtained 4th sub-fractions were later used in the biological assays.

Table 7 -Mobile phase gradient used for the semi-preparative HPLC on sub-fraction E14028 I7 8A+9 E.

Time	Flow (mL/min)	H ₂ O (%)	Methanol (%)
0-10	2	40	60
10-20	2	-	100
20-40	2	-	100
40-45	2	40	60
45-60	2	40	60

3.2.5. Semi-preparative reverse-phase HPLC for E14028 I7 8A+9 E7

For the simplification of the active sub-fraction E14028 I7 8A+9 E7, semi-preparative reverse phase HPLC was used. Optimization of the separation procedure was previously assessed, in order to assure maximum possible separation of compounds. The analytical-scale HPLC was performed with a Synergi Fusion-RP column (4 μm , 250 x 4.60 mm, Phenomenex) and with an isocratic program of 75% MeCN/25% H₂O, using a flow of 0.5 mL/min. The chromatogram allowed us to collect the compounds according to the peaks shown, resulting in 10 new sub-fractions (E14028 I7 8A+9 E7 A-J). Sub-fractions were collected in RB flasks from multiple injections and evaporated in the rotary evaporator. Sub-fractions were resuspended and transferred to pre-weighed vial, dried and weighed before the ^1H NMR (600 MHz, BrukerAvance III) analysis.

3.2.6. Semi-preparative reverse-phase HPLC for E14028 I7 8A+9 E7J

For the simplification of the methanol-soluble sub-fraction E14028 I7 8A+9 E7J, semi-preparative reverse phase HPLC was used. Optimization of the separation procedure was previously assessed. We used an isocratic program of 85% MeOH/15% H₂O, using a flow of 0.5 mL/min. The analytical-scale HPLC was performed with a Synergi Fusion-RP column (4 µm, 250 x 4.60 mm, Phenomenex). This process resulted in 7 new sub-fractions ((E14028 I7 8A+9 E7 J 1-7). Preparation of the collected samples was also performed for the biological assays.

3.2.7. Normal phase solid phase extraction of E14031 D

Normal phase solid phase extraction (NP-SPE) using a 50g Strata™ SI-1 Silica column (Phenomenex) was performed to obtain further simpler sub-fractions of the bioactive VLC fraction E14031 D. Using a gradient of solvents, from 100% n-Hexane to 100% MeOH, 10 sub-fractions were collected. The fraction E14031 D was resuspended in 100% n-Hexane and loaded onto the SPE column. The mixtures were carefully added stepwise, according to Table 8. Sub-fractions were dried in a rotary evaporator, resuspended, transferred to pre-weighed vial. Sub-fractions were prepared dried and weighed before the ¹H NMR (400 MHz, BrukerAvance III) analysis and test solutions were prepared for the biological assays.

. Table 8 - Gradients used in the SPE of E14031 D.

Sub-fractions	n-Hexane (%)	EtOAc(%)	Methanol (%)	Volume (mL)
	100	-	-	200
1	95	5	-	700
2-4	90	10	-	500
5	87.5	12.5	-	400
6	85	15	-	300
7	80	20	-	400
8	75	25	-	300
9	-	100	-	500
10	-	50	50	200
10	-	-	100	200

3.3. Cell culture and bioassays

3T3-L1 mouse embryonic fibroblasts (ATCC® CL-173™) were used in this study, obtained from the American Tissue Culture Collection (ATCC) (Manassas, Virginia, EUA). This pre-adipocyte cell line was selected since it has been proven to be a reliable tool in many obesity

studies (MacDougald et al. 1995). Cells were cultured in DMEM Glutamax medium (Dulbecco's modified Eagle Medium DMEM GlutaMAX™) from Life Technologies (Thermo Fisher Scientific, Waltham, Massachusetts, USA), supplemented with 10% (v/v) fetal bovine serum (FBS, Gibco-Invitrogen), 0.1% (v/v) amphotericin B ((Life Technologies)) and 1% (v/v) of penicillin-streptomycin (Pen-Strep 100 IU mL⁻¹ and 10 mg mL⁻¹, respectively) (Life Technologies)). Cells were maintained in a humidified atmosphere with 5% of CO₂, at 37°C in the incubator 8000 DH (Thermo Scientific, Waltham, MA, United States of America). Cells were cultured in cell tissue flasks (Orange Scientific, Braine-l'Alleud, Belgium) and in Petri dishes (Orange Scientific) for the cell differentiation assay. Every two to three days, cultures were split 1:3 using 1 mL of TrypLE™ Express (Life technologies), before they reach confluence (70 to 80%). TrypLE™ Express was used briefly (1-2 minutes) to cause cell detachment, removed and added culture medium to resuspend cells, with the aid of multiple pipetting. Cell density was calculated using Countess™ Automated Cell Counter (Thermo Fisher Scientific) with 10 µL of medium with suspended cells and 10 µL of trypan blue. Cell density for seeding was of approximately 3000 cells cm⁻².

3.3.1. Cell proliferation assays

3.3.1.1. Sulforhodamine B assay

The sulforhodamine B (SRB) assay was used to assess the proliferation rate of the pre-adipocytes of the 3T3-L1 cell line. SRB is a water soluble dye, with the ability to bind to basic amino acid of cellular proteins, hence its use as a measurement of cellular protein content. Pre-adipocytes were seeded in 96-well plates at a concentration of 4 x 10⁴ cells mL⁻¹ and 24 hours later, cells were exposed to fractions and sub-fractions derived from cyanobacteria at a concentration of 100 and 50 µg mL⁻¹, respectively. At the end of each experiment, after 24 or 48 hours of exposure, cells were fixed with ice-cold trichloroacetic acid, adding 25 µL to each well, at a final concentration of 0.1 mg mL⁻¹ SRB (AnaSpec, Inc., Fremont, California, USA), for 1 hour at 4 °C in the dark. Cells were washed with distilled water, air-dried and stained for 15 minutes with 75 µL of 0.4% (wt/vol) SRB dissolved in 1% acetic acid as described in Teixeira et al. (2010). Excess SRB was removed and cells were quickly washed with 1% acetic acid several times to remove all unbound SRB. After being air-dried, the bound dye was solubilized with 150 µl Tris-HCl (10 mmol/l, pH 10.5), and the absorbance was determined at 492 nm with reference at 650 nm on a plate reader (Biotek Synergy HT). The absorbance of cells at Day 0 (before treatment, after 24 hours of seeding) was determined in order to obtain comparable ratios of proliferative activities between treated and untreated cells.

Equation 1 - Formulas used in the calculation of the values for the SRB assay.

$$\% \text{ Cell Proliferation}_{\text{sample}} = \frac{\text{Average Abs}_{492-650 \text{ sample}}}{\text{Average Abs}_{492-650 \text{ Day 0}}} \times 100$$

$$\% \text{ Proliferation rate}_{\text{sample}} = \frac{(\text{Average Abs}_{492-650 \text{ sample}} \div \text{Average Abs}_{492-650 \text{ Day 0}})}{(\text{Average Abs}_{492-650 \text{ solvent control}} \div \text{Average Abs}_{492-650 \text{ Day 0}})} \times 100$$

3.3.2.2. BrdU ELISA assay

Cell proliferation was also assessed using the Cell Proliferation ELISA BrdU kit (Roche Applied Science, Mannheim, Germany) as a more sensitive method for proliferative activity assessment. The principle of the assay is the detection of incorporated 5-bromo-20-deoxyuridine (BrdU) during DNA synthesis by a specific antibody coupled to peroxidase. The test was performed according the manufacturer's protocol. Briefly, pre-adipocytes were seeded in 96-well plates at a concentration of 3×10^4 cells mL^{-1} and 24 hours later, cells were exposed to fractions and sub-fractions derived from cyanobacteria at a concentration of 100 and 50 $\mu\text{g mL}^{-1}$, respectively. After 24 and 48 hours, cells were incubated with 10 μM BrdU labeling solution for two hours. After this, culture medium was removed, cells were fixed and DNA was denatured. Cells were incubated with Anti-BrdU-peroxidase solution for 90 min at room temperature and antibody conjugates were removed by washing three times with PBS. Tetramethyl-benzidine (TMB) substrate was added to each well and absorbance was measured during the course of 30 min (with intervals each 5 min) at 370 nm with reference wavelength at 492 nm in a spectrophotometer (Biotek Synergy HT, Winooski, Vermont, USA), corrected with blank measurements. All tests were run in triplicate and averaged.

Equation 2 - Formula used in the calculation of the values of each time point for the BrdU assay.

$$\% \text{ sample} = \frac{\text{Average Abs}_{370-492 \text{ sample}} - \text{Average Abs}_{370-492 \text{ blank}}}{\text{Average Abs}_{370-492 \text{ solvent control}} - \text{Average Abs}_{370-492 \text{ blank}}} \times 100$$

3.3.2. Cell viability assay / metabolic activity of pre-adipocytes

The cellular viability was evaluated through the 3-(4,5-dimethylthiazol-2-yl)-2,5-diphenyltetrazolium bromide assay (MTT bioassay). The reduction of MTT to formazan is directly proportional to the mitochondrial activity and consequently used to indicate the viability or metabolic activity of the cells. This was found to be a quick and reliable method to evaluate the mitochondrial and metabolic activity of many different compounds, widely used in toxicology (Carmichael et al., 1987). For this test, pre-adipocytes from the cell line 3T3-L1 were seeded in 96-well culture plates at a concentration of 3.3×10^4 cells mL^{-1} . 24 hours later, cells were

exposed to fractions and sub-fractions derived from cyanobacteria at a concentration of 100 and 50 $\mu\text{g mL}^{-1}$, respectively. At the end of the experiment, after 24 or 48 hours of exposure, 10 μL of a 5 mg mL^{-1} MTT solution (final MTT concentration of 0.5 mg/mL) was added to the culture medium. Following, cells were washed once with PBS and the purple-colored formazan salts were dissolved in 100 μL DMSO. The absorbance was measured in a spectrophotometer (Biotek Synergy HT, Winooski, Vermont, USA), at 550 nm. All tests were run in triplicate and averaged.

Equation 3 - Formula used in the calculation of the values for the MTT assay.

$$\% \text{ sample} = \frac{\text{Average } Abs_{550 \text{ sample}}}{\text{Average } Abs_{550 \text{ solvent control}}} \times 100$$

3.3.3. Cell differentiation assay (adipogenesis)

Cells were seeded in 24-well culture plates (Orange Scientific), using the complete culture of one Petri dish for each plate, which makes an approximate concentration of 2×10^4 cells cm^{-2} . Mature adipocytes were obtained after exposing 3T3-L1 pre-adipocytes to differentiating agents. Preadipocytes were allowed to grow to confluence (about 48h to 72h). Two days after reaching full confluence (day 0 of differentiation), cells were exposed to insulin ($10 \mu\text{g mL}^{-1}$) (Sigma-Aldrich, St. Louis, MO, United States of America), IBMX ($500 \mu\text{M}$) (Sigma-Aldrich), and DEX (250nM) (Sigma-Aldrich). The cocktail was removed after three days and cells were maintained in DMEM medium containing insulin ($10 \mu\text{g mL}^{-1}$), the medium was renewed every 2-3 days. From Day 0, cells were exposed to a concentration of $100 \mu\text{g mL}^{-1}$ for fractions and $50 \mu\text{g mL}^{-1}$ for sub-fractions. The medium and fractions or sub-fractions were renewed every 2-3 days.

Following exposure, at Day 12, cells were stained with Oil Red O, a fat soluble dye, which stains intra-cytoplasmic triglyceride and lipid content (Ramírez-Zacarias et al., 1992). Briefly, the culture medium was removed and mature adipocytes were fixed with 500 μL of 4% (w/v) formaldehyde for 1 hour at $2-8^\circ\text{C}$. Cells were washed with ddH₂O, air-dried and stained with 300 μL of a mixture of Oil Red O working solution (0.3 %) in isopropanol/distilled water (3:2). 15 minutes later, after at least two rounds of washing in ddH₂O, cell imaging was performed using an inverted microscope (Olympus, DX71). For photometrical analysis, the intracellular lipid content was dissolved in 100% Dimethyl sulfoxide (DMSO). The absorbance was measured at 492 nm with 650 nm reference in a microplate reader (Thermo Electron, Thermo Fisher Scientific, Waltham, MA, USA). All tests were run in duplicate for fractions and triplicate

for sub-fractions and averaged. For sub-fraction, cell counting was also performed in order to obtain the ratio of lipid content per cell, using the cell count of one well per treatment.

Equation 4 - Formula used in the calculation of the values for the Oil Red O assay.

$$\% \text{ sample} = \frac{\textit{Average Abs}_{492 \textit{ sample}} - \textit{Average Abs}_{650 \textit{ sample}}}{\textit{Average Abs}_{492 \textit{ solvent control}} - \textit{Average Abs}_{650 \textit{ solvent control}}} \times 100$$

4. Results

4.1. Screening of cyanobacterial strains for bioactivity

Cyanobacterial strains were grown during several months in a medium-scale format. When the appropriate collected and lyophilized biomass was achieved, the crude extract of six cyanobacterial strains (*Phormidium* sp. LEGE06363, *Planktothrix planctonica* LEGEXX280, *Synechocystis* sp. LEGE07211, *Oscillatoria limnetica* LEGE00237, *Aphanizomenon* sp. LEGE03283, *Limnothrix* sp. LEGE07212) was obtained and extraction codes were given to each crude extract (Table 9). The crude extracts were submitted to a normal phase vacuum liquid chromatography resulting in several fractions (Table 10).

Table 9 - Data of the extracts obtained of the cultured and collected cyanobacterial strains.

Cynobacterial strain	Extract Number	Aq Number	Biomass/g	Extract/g	Yield/%
<i>Phormidium</i> sp. LEGE06363	E14026	E14026Aq	16.768	1.7445	10.40
<i>Planktothrix planctonica</i> LEGEXX280	E14028	E14028Aq	20.983	3.0227	16.20
<i>Synechocystis</i> sp. LEGE07211	E14031	E14031Aq	24.634	4.4792	18.18
<i>Oscillatoria limnetica</i> LEGE00237	E14032	E14032Aq	13.435	3.5292	26.27
<i>Aphanizomenon</i> sp. LEGE03283	E14035	E14035Aq	28.712	4.4260	15.42
<i>Limnothrix</i> sp. LEGE07212	E14067	E14067Aq	17.114	2.2267	13.10

Table 10 - Data of the VLC fractionations and fractions obtained for the extracts produced.

Extract Number	Fractions	Extract loaded/g	Total mass/mg	Yield/%
E14026	A-K	1,7278	2303.9	100.0
E14028	A-I	2,9458	2693.7	91.4
E14031	A-L	4,4792	3644.5	85.0
E14032	A-J	3,4723	2945.2	84.8
E14035	A-J	3,7979	3060.2	80.6
E14067	A-J	1,8326	1016.3	55.5

VLC is a standard method used at our lab and other natural compound discovery-oriented projects, since it is a quick, simple and inexpensive technique using silica gel and a soft vacuum (Targett et al. 1979; Leão et al. 2013; Leão et al. 2010). VLC allows us to separate complex mixtures of compounds (particle size of stationary phase between 15 to 60 μm), as the extract produced from the simple vacuum filtration of the cyanobacterial biomass, which separates the numerous compounds from the cyanobacterial cells. Using a normal phase gradient and at least 9 different solvent mixtures, we produce several polarity oriented fractions.

Some disadvantages to this method, resulting in lowered method yield, are the uneven packing of the silica gel and sample load. A yield of +100% was obtained for the fractionation of E14026 (Table 10), which is mainly due to the presence of silica contamination, since silica is partially soluble in methanol used in the process. The presence of remaining cyanobacterial cells in the extract produced from the simple vacuum filtration results in a higher dry mass of the extract. Cyanobacterial cells do not cross the silica gel pores and thus a lower yield can be obtained in this step, as happened for E14067 (Table 10). Even though VLC performs with an acceptable final yield, VLC is still a gross method for compound separation, which can ultimately result in a compound or group of compounds to be distributed in neighboring fractions.

Our biological assays rely on spectrophotometric analysis in the visible spectrum. Even though throughout the assay procedure the wells of the well plates are washed with PBS or ddH₂O several times, with the complete removal of the medium, a scan (300-700 nm; Figure 7) of the VLC fractions was performed in order to determine possible interference of the compounds in the readings. Fractions C, D, E and F had higher absorbance values, with peaks at 420 and 675 nm. However, taking into consideration the analyzed wavelengths of the bioassays (MTT, SRB, BrdU), few interference is to be expected, and mostly corrected by the measurement of the reference wavelength.

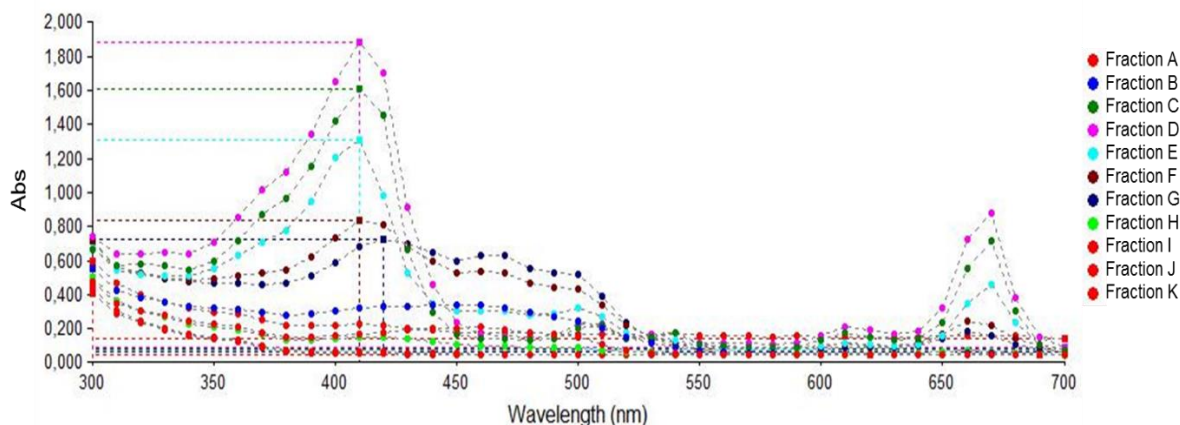


Figure 8 - Visible spectrum (300-700 nm) scanning of the E14026 fractions (A-K) produced after VLC fractionation ($100 \mu\text{g mL}^{-1}$ in DMSO).

4.1.1. Screening for proliferative activity

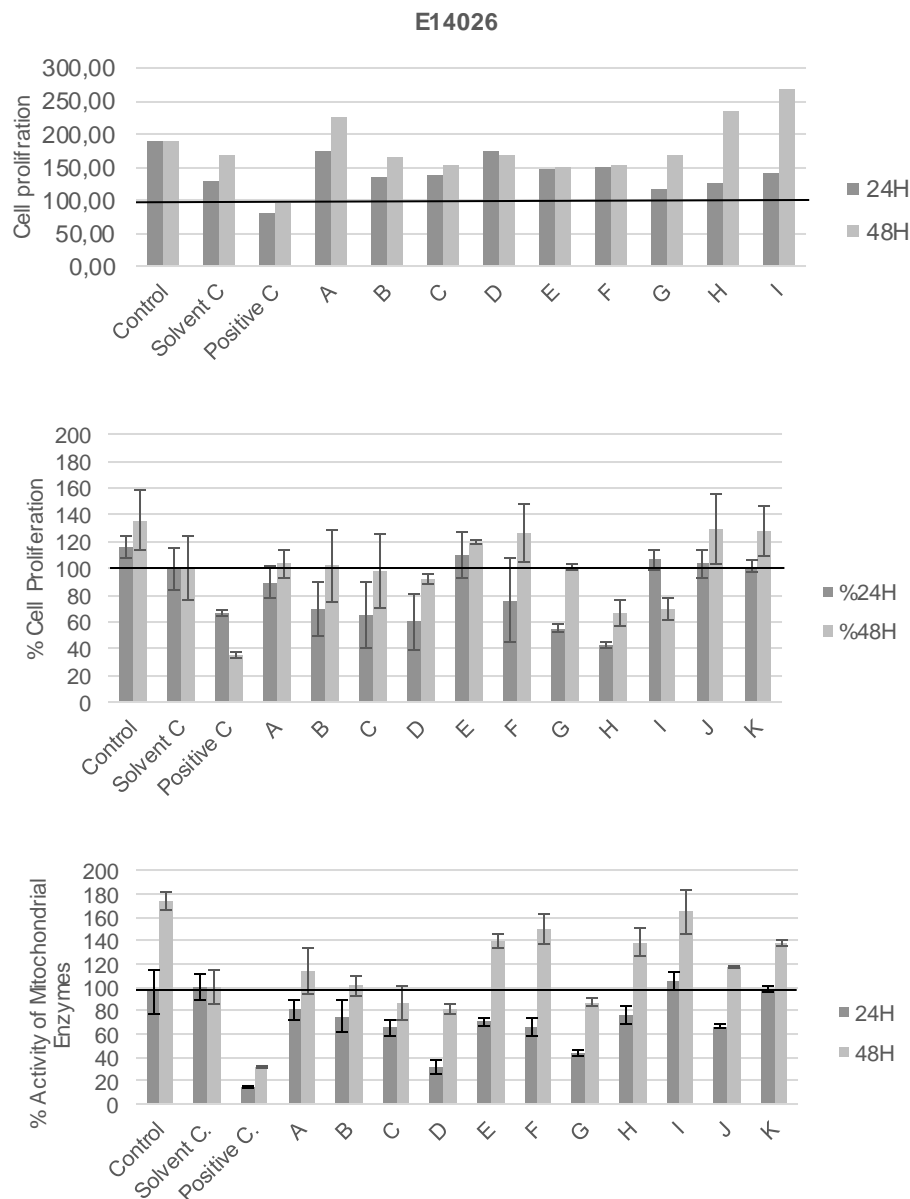


Figure 9 - Cell proliferation (SRB assay, first and second graph, using cell proliferation rate and cell proliferation rate compared to the solvent control, respectively) and activity of mitochondrial enzymes (MTT assay, third graph), in % of solvent control, for the E14026 (*Phormidium* sp. LEGE06363) VLC fractions (A – K) with the concentration of $100 \mu\text{g mL}^{-1}$, after 24 and 48 hours of exposure. Solvent control corresponded to 1% DMSO and positive control to 20% DMSO, using 3 replicate wells per treatment and 6 for control, solvent control and positive control.

In our test designs, the different fractions from every cyanobacterial strain were tested, a control (only medium and cells), a solvent control (1% DMSO), since fraction test-solutions are

dissolved in DMSO, and a positive control (20% DMSO), where it is expected to be observed cell death.

In Figure 9, proliferation rate is presented for each fraction and, in a different graph, in percentage of solvent control. Cell proliferation specific to each fraction gives a better resolution (60 to 250%), however, measurements compared to solvent control will be used throughout as they present a more legible way to interpret activity. Fractions E14026 E and E14026 J (Figure 9) showed proliferative activity both at 24 and 48 hours of exposure. At 48 hours, the differences in cell proliferation between solvent control and both fractions (E, J) were more evident with a proliferative activity of $119.44 \pm 1.56 \%$ and $117.00 \pm 1.01 \%$ in the SRB assay. Similar results were observed in the MTT assay, with an increase of $140.5 \pm 5.93\%$ and $117.0 \pm 1.01 \%$ compared to the solvent control, respectively. E14026 I showed only higher metabolic activity at 48 hours (164.9 ± 18.61), and no effects were seen in the SRB assay.

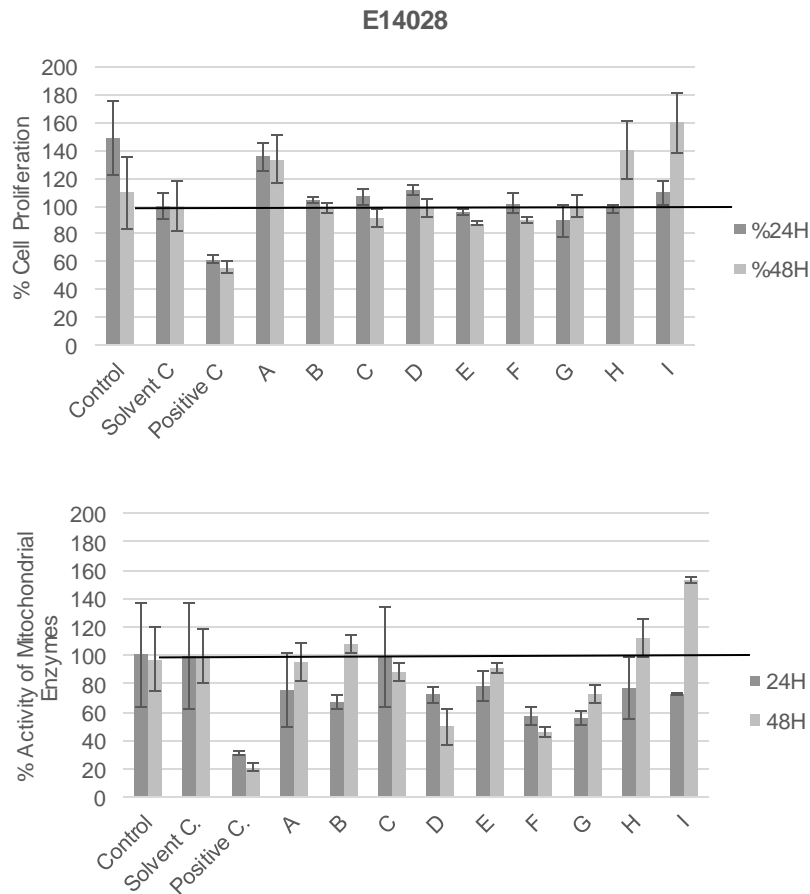


Figure 10 - Cell proliferation (SRB assay, top) and activity of mitochondrial enzymes (MTT assay, bottom), in % of solvent control, for the E14028 (*Planktothrix planctonica* LEGEXX280) VLC fractions (A – I) with the concentration of $100 \mu\text{g mL}^{-1}$, after 24 and 48 hours of exposure. Solvent control corresponded to 1% DMSO and positive control to 20% DMSO, using 3 replicate wells per treatment and 6 for control, solvent control and positive control.

As for the fractions of E14028 (Figure 10), A, H and I showed activity. Fraction E14028 A only showed activity in the SRB assay, with an increase of $135.37 \pm 9.61\%$ and $133.35 \pm 17.27\%$ at 24 and 48 hours, respectively, whereas no alterations were observed for the metabolic activity (MTT). For fractions H and I, the increases of cell proliferation at 48 hours (140.28 ± 21.35 and $159.89 \pm 21.8\%$, respectively) were accompanied by increases in the activity of mitochondrial enzymes (MTT) with 112.10 ± 13.1 and $153.30 \pm 1.82\%$, compared to the solvent control.

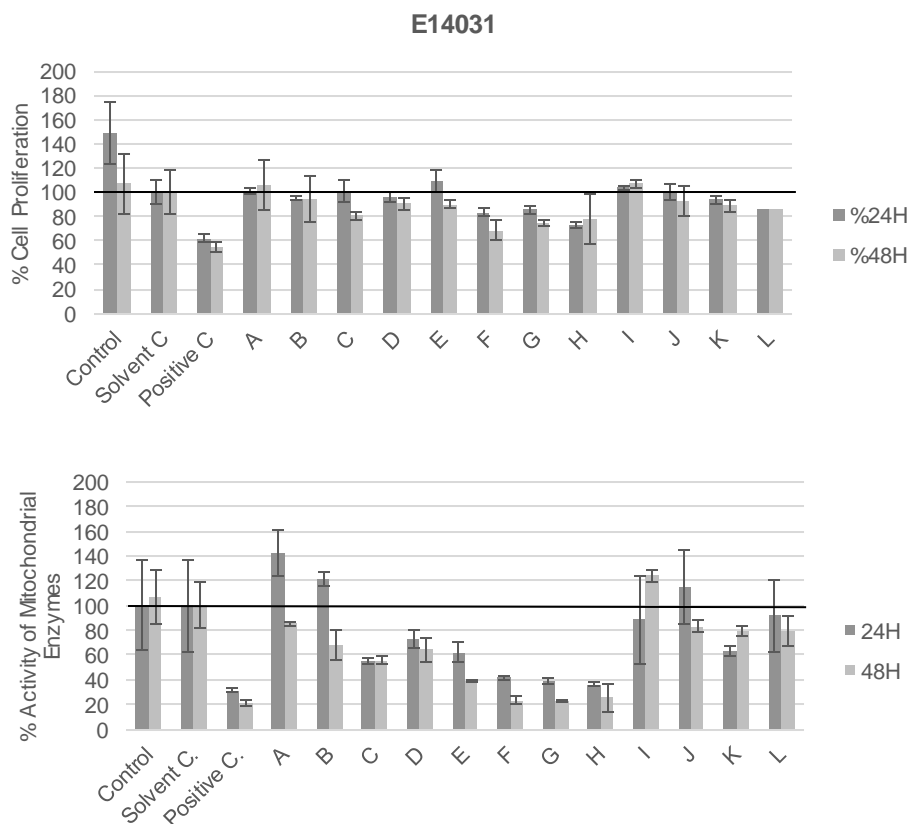


Figure 11 - Cell proliferation (SRB assay, top) and activity of mitochondrial enzymes (MTT assay, bottom), in % of solvent control, for the E14031 (*Synechocystis sp.* LEGE07211) VLC fractions (A – L) with the concentration of $100 \mu\text{g mL}^{-1}$, after 24 and 48 hours of exposure. Solvent control corresponded to 1% DMSO and positive control to 20% DMSO, using 3 replicate wells per treatment and 6 for control, solvent control and positive control.

Regarding E14031 (Figure 11), most of the fractions showed no activity, with little differences in cell proliferation compared to the solvent control. Fractions E14031 A and B showed increases in metabolic activity at 24 hours (142.00 ± 18.68 and $121.15 \pm 5.59\%$, respectively), a result that was not observed, however, at 48 hours of exposure. Fractions E14031 F, G and H showed remarkable activity inhibiting the metabolic activity (MTT) of the

pre-adipocytes (23.10 ± 2.96 , 22.88 ± 0.56 and 25.52 ± 11.53 %, compared to the solvent control). Concomitantly, there was also a decrease in proliferation rate (SRB).

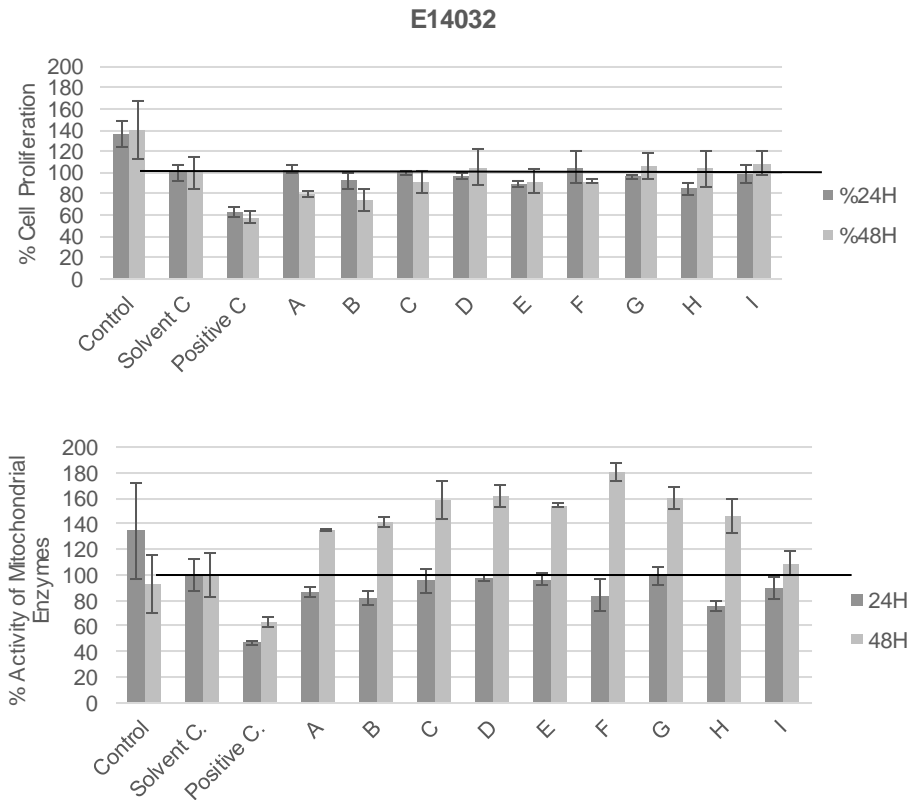


Figure 12 - Cell proliferation (SRB assay, top) and activity of mitochondrial enzymes (MTT assay, bottom), in % of solvent control, for the E14032 (*Oscillatoria limnetica* LEGE00237) VLC fractions (A – I) with the concentration of $100 \mu\text{g mL}^{-1}$, after 24 and 48 hours of exposure. Solvent control corresponded to 1% DMSO and positive control to 20% DMSO, using 3 replicate wells per treatment and 6 for control, solvent control and positive control.

Regarding E14032 (Figure 12), most of the fractions maintained cell proliferation rate compared to the solvent control in the SRB assay. In contrast, most of the fractions induced mitochondrial activity on 3T3-L1 cells (MTT) at 48 hours. Fractions E14032 D, E and F showed the highest increases of 161.76 ± 8.36 , 154.29 ± 1.87 and $179.78 \pm 7.01\%$, respectively.

Fractions from E14035 (Figure 13) showed a similar profile, of an increased metabolic activity at 48 hours in the MTT assay for the exposure of most of the fractions, except for E14035 H and I, which showed decreases in metabolic activity (87.03 ± 8.55 and $80.00 \pm 3.78\%$, respectively). However, in the SRB assay, fractions H and I showed pro-proliferative activity (118.50 ± 18.43 and $138.12 \pm 5.11\%$, respectively, of the solvent control at 24 hours of exposure). Fraction B had one of the highest increases on metabolic activity at 48 hours for this extract ($134.07 \pm 122.75\%$) and no changes in cell proliferation ($105.89 \pm 5.95\%$).

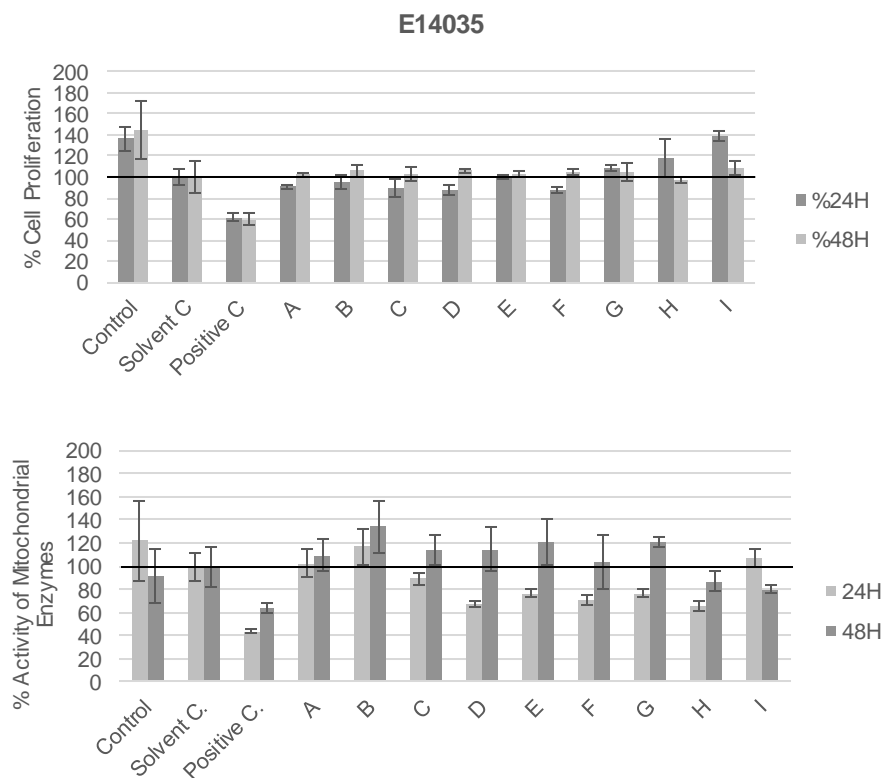


Figure 13 - Cell proliferation (SRB assay, top) and activity of mitochondrial enzymes (MTT assay, bottom), in % of solvent control, for the E14035 (*Aphanizomenon* sp. LEGE03283) VLC fractions (A – I) with the concentration of $100 \mu\text{g mL}^{-1}$, after 24 and 48 hours of exposure. Solvent control corresponded to 1% DMSO and positive control to 20% DMSO, using 3 replicate wells per treatment and 6 for control, solvent control and positive control.

Regarding the E14067 extract (Figure 14), fractions A, J and H exerted increases in mitochondrial activity (MTT) at 24 hours (118.76 ± 10.06 , 132.78 ± 7.10 , 142.89 ± 9.46) and fractions A, J, I and H at 48 hours (145.85 ± 11.75 , 132.47 ± 4.01 , 164.24 ± 11.91 , 143.26 ± 6.36 , respectively). In the SRB assay, fractions C and D showed mild increases in cell proliferation (117.60 ± 4.99 and 101.75 ± 13.10 % at 24 hours of exposure and 109.98 ± 3.93 and 111.08 ± 7.77 % at 48 hours of exposure), while decreases in mitochondrial activity (50–70% compared to the solvent control) at both time points (MTT). Fractions E14067 E and G also strongly inhibited metabolic activity, fraction G accompanied by a decrease in cell proliferation of 76.38 ± 12.89 %, compared to the solvent control. Fraction F exerted increases in the metabolic activity (MTT) at 24 (123.71 ± 6.45 %) and 48 hours (145.45 ± 5.23), but no differences were seen in the SRB assay.

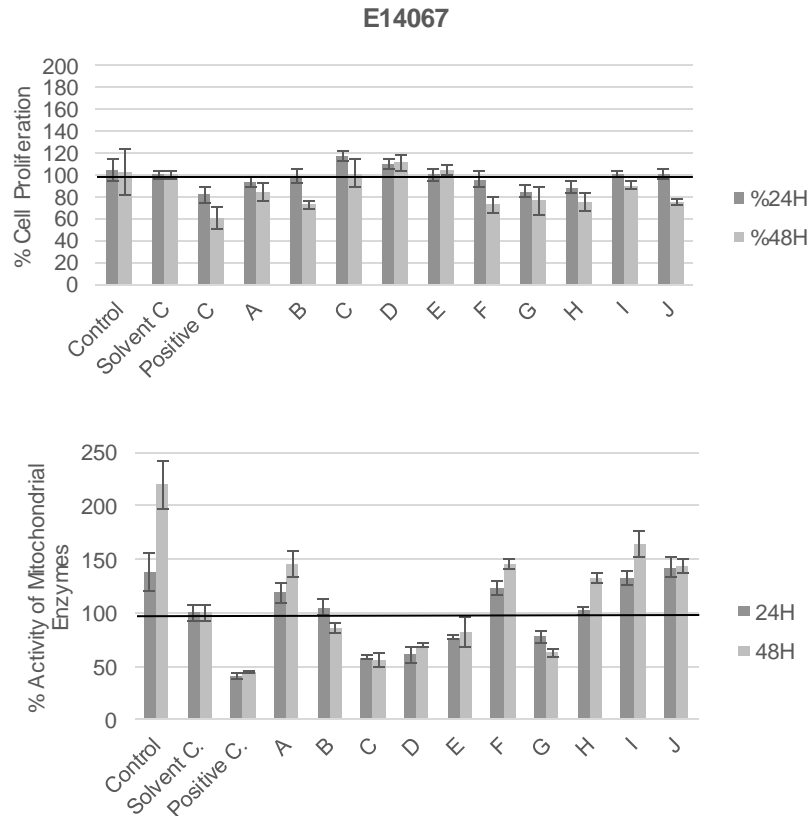


Figure 14 - Cell proliferation (SRB assay, top) and activity of mitochondrial enzymes (MTT assay, bottom), in % of solvent control, for the E14067 (*Limnothrix* sp. LEGE07212) VLC fractions (A – J) with the concentration of 100 $\mu\text{g mL}^{-1}$, after 24 and 48 hours of exposure. Solvent control corresponded to 1% DMSO and positive control to 20% DMSO, using 3 replicate wells per treatment and 6 for control, solvent control and positive control.

Some fractions were chosen to be tested in a more advanced assay for cell proliferation (BrdU ELISA assay), which is based on the specific incorporation of BrdU in the DNA of the dividing cell. In order to determine some of the differences between the MTT and the SRB assay, we selected fractions that showed activity in both assay or in only one of the assays (see Table 11). The specific antibody binding to BrdU was followed by the measurement of colour development for 30 minutes for the determination of highest absorbance time point (Figure 15). In Figure 16, absorbance values after 30 minutes of reaction were normalized to the values of the solvent control, for the 24 and 48 hours of exposure. Differences between treatments were more evident after 48 hours (Figure 15 and 16). After 48 hours of exposure, fractions E14035 B, E14032 H, E14028 A and E14067 D showed increases in cell proliferation (154.50 ± 14.99 , 133.91 ± 16.42 , 129.05 ± 9.57 , 139.73 ± 19.57 , $123.58 \pm 19.43\%$, respectively), whereas E14067 F exerted anti-proliferative effects ($65.54 \pm 12.23\%$).

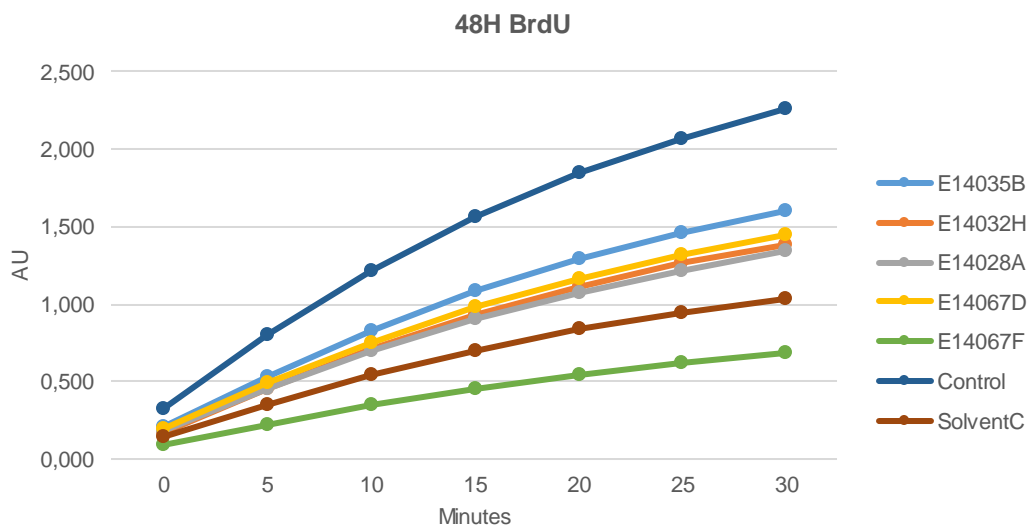


Figure 15 - Measurement of color development from 0 to 30 minutes for cell proliferation assessment through BrdU ELISA assay for VLC fractions E14035B, E14032H, E14028A, E14067D and E14067F with the concentration of 100 $\mu\text{g mL}^{-1}$, control and solvent control (1% DMSO) with 2 hour BrdU pulse, after 48 hours of exposure, using 3 replicate wells per treatment and 6 for control, solvent control and positive control.

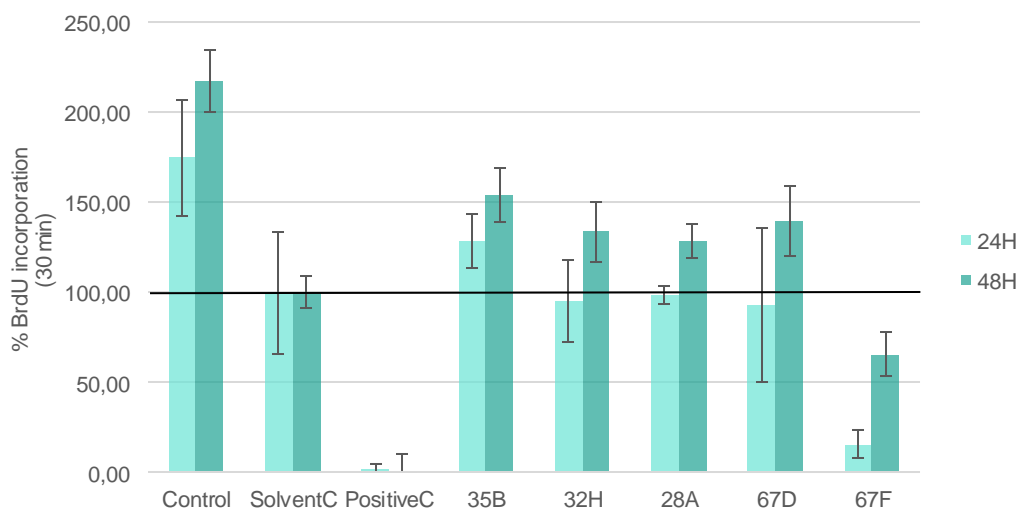


Figure 16 - BrdU incorporation percentage compared to the solvent control for VLC fractions E14035B, E14032H, E14028A, E14067D and E14067F with the concentration of 100 $\mu\text{g mL}^{-1}$, control and solvent control (1% DMSO) with 2 hour BrdU pulse, after 48 hours of exposure, using 3 replicate wells per treatment and 6 for control, solvent control and positive control.

Taking a closer look at all the information we obtained from the cyanobacterial screening, DMSO had different degrees of activities on cell proliferation and metabolic activity through the SRB, BrdU and MTT assay (Table 12). On average, 1% DMSO exerted a decrease on cell proliferation of - 20% for SRB assay and of - 55% through the BrdU ELISA assay. Regarding

the metabolic activity there was, however, an average decrease of – 15% registered through the MTT assay. In the positive control, corresponding to 20% DMSO, where cell death is to be expected, there was an average decrease of – 40% registered for SRB, whilst BrdU ELISA registered a proliferative activity of only 1.30% compared to the control. MTT assay registered a decrease of – 74%.

Table 11 - Summary of the activities obtained in the screening for proliferative activity: comparison between SRB, MTT and BrdU ELISA assay for selected cyanobacterial fractions.

	SRB assay	MTT assay	BrdU ELISA assay
E14035 B	=	↑	↑↑
E14032 H	=	↑↑	↑
E14028 A	↑	=	↑
E14067 D	↑	↓	↑
E14067 F	↓	↑	↓

Table 12 – Average effect of exposure to DMSO after 48 hours, in % of control, through SRB, MTT and BrdU ELISA assay.

	SRB assay	MTT assay	BrdU assay
1% DMSO	79.82	86.36	45.92
20% DMSO	39.28	26.02	1.30

4.1.2. Bioassay-guided fractionation of E14028 I

From the results of the cyanobacterial screening, fraction E14028 I (m=1751.6 mg) was selected as promising candidate for the isolation of the responsible compound(s). Since we had still high fraction mass and a complex mixture (typical of this specific fraction and confirmed after the analysis the NMR spectra (appendix I), another VLC was performed in order to simplify the sample. The sub-fractionation by vacuum liquid chromatography resulted in 7 sub-fractions. Pre-adipocytes were exposed to those sub-fractions at a concentration of 50 $\mu\text{g mL}^{-1}$ with the same experimental design as used in the screening bioassays (Figure 17). Fraction E14028 I7 had the strongest effect on cell proliferation at both 24 ($139.55 \pm 18.71\%$) and 48 hours ($117.52 \pm 5.54\%$), without compromising the activity of mitochondrial enzymes at the 48 hours of exposure, compared to the solvent control. For further characterization of the proliferative activity, the BrdU ELISA proliferation assay (Figure 17) was performed. At 24 hours, a decrease in cell proliferation were observed compared to the solvent control ($83.62 \pm 28.69\%$), while an increase at 48 hours ($123.58 \pm 19.43\%$).

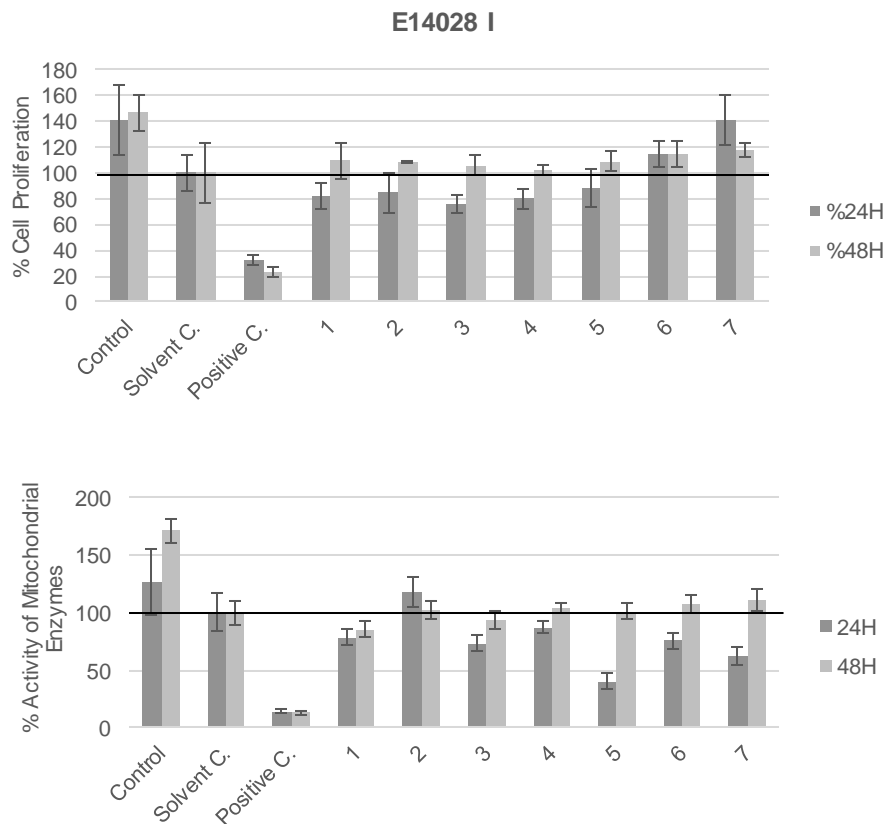


Figure 17 - Cell proliferation (SRB assay, top) and activity of mitochondrial enzymes (MTT assay, bottom), in % of solvent control, for the E14028 I sub-factions (1-7) with the concentration of $50 \mu\text{g mL}^{-1}$, after 24 and 48 hours of exposure. Solvent control corresponded to 1% DMSO and positive control to 20% DMSO, using 3 replicate wells per treatment and 6 for control, solvent control and positive control.

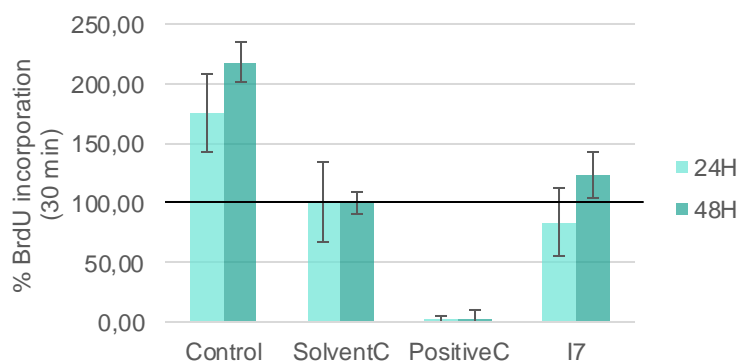


Figure 18 - BrdU incorporation percentage compared to the solvent control for VLC fraction E14028 I7 with the concentration of $50 \mu\text{g mL}^{-1}$, control and solvent control (1% DMSO) with 2 hour BrdU pulse, after 48 hours of exposure, using 3 replicate wells per treatment and 6 for control, solvent control and positive control.

The limited resolution due to the shortness of the column can lead to inefficient separation. The main result is that a compound or a group of compounds may be distributed by neighboring fractions. The use of a narrower column, and longer in length, as in the flash chromatography, increases the column cross section. Sub-fraction E14028 I7 (m=891 mg) was submitted to flash chromatography and TLC was done simultaneously as a screening procedure to extrapolate the composition of each sample; samples were afterwards pooled according to the R_f values (Table 13). TLC is performed with a silica gel plate with a chromophore that absorbs 254 nm UV light. Compounds can screen some of the UV light and therefore can be detected. R_f values from the TLC were calculated as according to Figure 7 (section 3.2.2.) and represent the distance traveled by the solvent mixture front and the compound, which can be unique for each compound. Different solvent mixtures were used according to the ability of the solvent mixture to be able to separate the different samples (Table 13).

Table 13 - Fraction pooling for E14028 I7 with the respective R_f values from TLC after observation under UV light (254 nm).

E14028 I7			
Sub-fraction	Collection Tubes	R_f	Mobile phase
1	1-10	0.929	20% MeOH (EtOAc)
2	11,12	0.704	20% MeOH (EtOAc)
3	13-18	1.000	20% MeOH (EtOAc)
4	19-25	0.948	20% MeOH (EtOAc)
5	26-29	0.692	20% MeOH (EtOAc)
6	30-32	-	30% MeOH (EtOAc)
7	33-37	0.818; 0.945	30% MeOH (EtOAc)
8	38-52	0.741	30% MeOH (EtOAc)
9	53-63	-	30% MeOH (EtOAc)
10	64-69	0.696	30% MeOH (EtOAc)
11	70;71	0.963	50% MeOH (EtOAc)
12	72-81	0.870	60% MeOH (EtOAc)
13	82-84	0.746	60% MeOH (EtOAc)
14	85,86	0.746	60% MeOH (EtOAc)

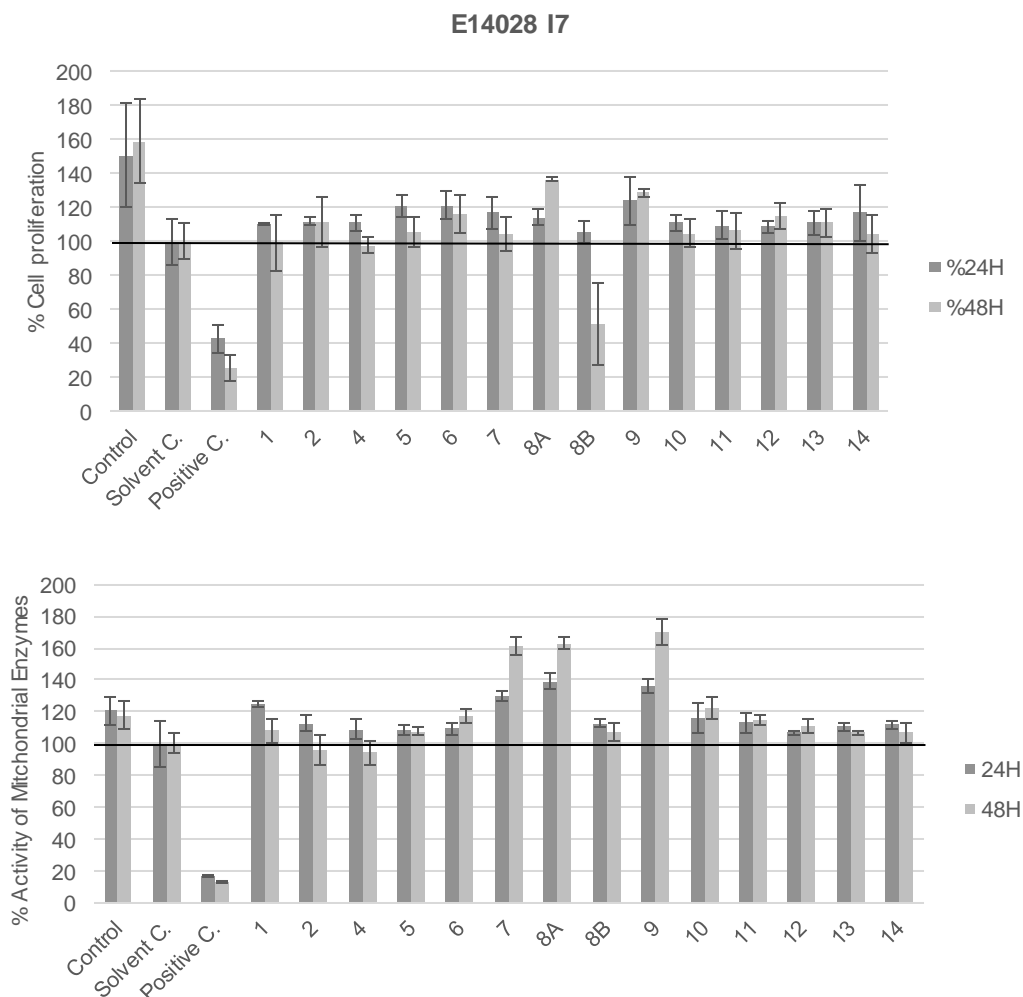


Figure 19 - Cell proliferation (SRB assay, top) and activity of mitochondrial enzymes (MTT assay, bottom), in % of solvent control, for the E14028 I7 sub-fractions (1-14) with the concentration of $50 \mu\text{g mL}^{-1}$, after 24 and 48 hours of exposure. Solvent control corresponded to 1% DMSO and positive control to 20% DMSO, using 3 replicate wells per treatment and 6 for control, solvent control and positive control.

Some samples had compositions which were not detectable through TLC, e.g. sub-fractions E14028 I7 6 and 9 (Table 13). Sub-fraction 8 was separated into two distinct phases previous to the bioassays, due to the distinctive composition of this fraction after collection. Sub-fraction 8A, soluble in ddH₂O, and fraction 9 exerted pro-proliferative effects in 3T3-L1 pre-adipocytes, with a proliferative activity of 136.84 ± 0.88 and 128.77 ± 1.93 % after 48 hours of exposure, respectively, being the highest scores obtained for this group of sub-fractions (Figure 19). Concordantly, the MTT assay revealed increases in the activity of mitochondrial enzymes at 48 hours of 161.01 ± 5.40 , 163.21 ± 3.50 and 169.73 ± 8.26 % for sub-fractions E14028 I7 7, 8 and 9 respectively.

After the close analysis of the $^1\text{H-NMR}$ spectra for sub-fractions 8A and 9 we hypothesized that they had a similar composition (Figure 20). These sub-fractions fractions were joint, originating in sub-fraction E14028 I7 8A+9 with a final mass of 238.9 mg (188.4 mg from sub-fraction E14028 I7 8A and 50.5 mg from sub-fraction E14028 I7 9). NMR, was a crucial method throughout our experiments. NMR is used as a screening technique in several research projects, for both comparison of spectral data found in literature or between fractions. Nuclear magnetic resonance has been a widely used method, extremely important, aiding the bioactivity guided fractionation process and structure elucidation of new metabolites (Pellecchia et al. 2002; Oldoni et al. 2016). Throughout this work, we used $^1\text{H NMR}$ to evaluate the separation procedure, since different NMR spectra are obtained for each fraction. Once the compounds are pure, 1D and 2D NMR can be used to elucidate the structure of the compounds obtained.

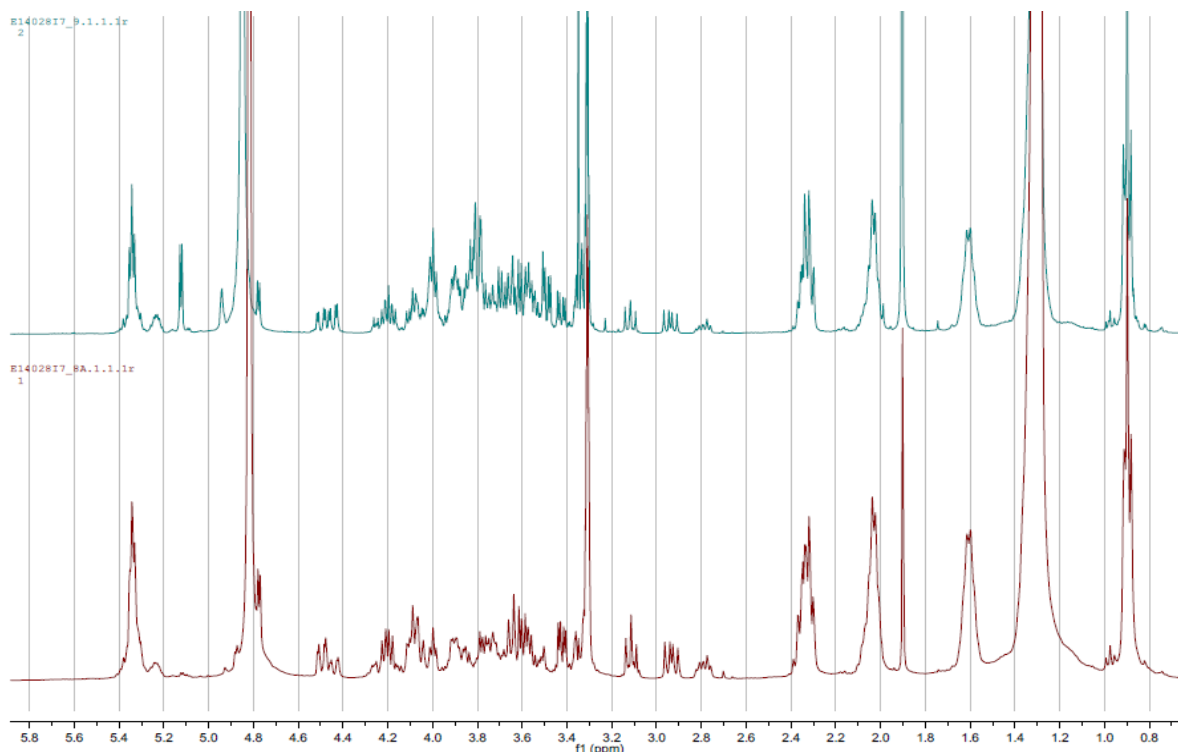


Figure 20 - $^1\text{H-NMR}$ spectra for sub-fractions 9 (top) and 8A (bottom) in CD_3OD (recorded at 400 MHz).

Up until here, silica gel was used in chromatography techniques and contamination of silica occurred, visible at the naked eye. Silica is able to dissolve in mobile phases above 10% MeOH, causing large quantities of amorphous solid to form in samples. Simple filtration using Whatman N^o1 Filter Paper and ddH₂O eliminates silica residues. The following method used to fractionate the bioactive the active sub-fraction E14028 I7 8A+9 was a silica-based C18-E solid

phase extraction, since we still had a considerable amount of mass for this fraction and a rather complex mixture. Final mass of this sub-fraction was 159.5 mg, which was loaded onto SPE C18 column. During SPE separation, several samples were collected and TLC (under UV light and with PMA staining) was performed in order to evaluate the composition of each sample and determine similarity between samples (Table 14). With PMA staining we can identify other compounds as phenolics, alkaloids and steroids. Conjugated organic compounds are able to reduce PMA to a molybdenum blue that upon heating appear as dark green spots on a light green background. Samples that had the same R_f values after TLC were combined to new sub-fractions from this process.

Table 14 - Fraction pooling for E14028 I7 8A+9 with the respective R_f values obtained from TLC after observation under UV light (254 nm) and PMA staining for the samples collected in SPE (left) and after sample assembly in 50% MeOH (EtOAc) (right).

E14028 I7 8A+9 R_f s				E14028 I7 8A+9		
Sub-fraction	Collection Tubes	R_f	Mobile phase	Sub-fraction	R_f	Mobile Phase
A	1-6	0.0	100% MeOH	A	0	50% MeOH (EtOAc)
B	8-14	0.759		B	0.789	
C	26-28	0.781		C	0.758; 0.842	
D	30-42	0.820; 0.902		D	0.758; 0.842	
E	43-50	0.776; 0.862		E	0.926	
F	62-66	0.833		F	0.884; 0.968	
G	68-73	0.667; 0.833		G	0.947	
H	75-86	0.787		H	0.915	
I	86-105	0.820		I	-	

Fractions derived from SPE (Figure 21) were tested again in the proliferation assay with 3T3-L1 cells, except for sub-fraction E14028 I7 8A+9 I that had insufficient mass to prepare the exposure solution of 2.5 mg mL^{-1} . Sub-fraction E14028 I7 8A+9 E seemed to have the highest effect on the cell line, with increases of cell proliferation of $118.33 \pm 13.11 \%$ at 24 hours and $133.28 \pm 34.05\%$ at 48 hours of exposure, compared to the solvent control. Regarding the activity of mitochondrial enzymes, sub-fractions E14028 I7 8A+9 D and E exerted the strongest effects, with increases up to 171.19 ± 13.10 and $199.04 \pm 4.59 \%$ at 24 hours and 172.75 ± 10.86 and $221.27 \pm 6.70 \%$ at 48 hours, respectively, compared to the solvent control.

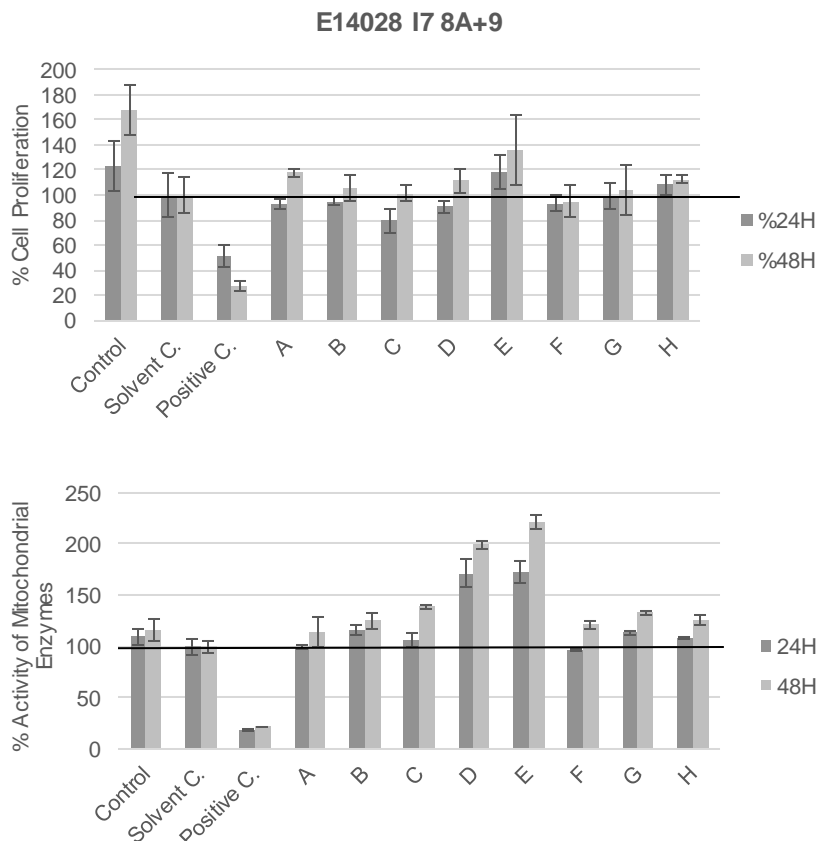


Figure 21 - Cell proliferation (SRB assay, top) and activity of mitochondrial enzymes (MTT assay bottom), in % of solvent control, for the E14028 I7 8A+9 sub-fractions (A-H) with the concentration of $25 \mu\text{g mL}^{-1}$, after 24 and 48 hours of exposure. Solvent control corresponded to 1% DMSO and positive control to 20% DMSO, using 3 replicate wells per treatment and 6 for control, solvent control and positive control.

After the biological assays, fraction E14028 I7 8A+9 E ($m=43.5 \text{ mg}$) was selected to be processed through HPLC UV-Vis. Two wavelengths were selected to follow the chromatogram of the sub-fraction: a wavelength of 280 and 264 nm, which are standard wavelengths used with a UV-Vis detector, since most of the organic compounds absorb in these wavelengths (Bart 2005; Kazakevich & LoBrutto 2006). Run tests were performed in order to determine the mixtures of solvents and the time points for sample collection, in order to achieve maximum compound separation. For this method, a gradient of solvents was used, from 60% MeOH (H_2O) to 100% MeOH, then back to the initial mixture. Samples 1 to 4 were collected at 60% MeOH (H_2O), sample 5 was collected during ramp to 100% MeOH, sample 6 to 9 were collected at 100% MeOH and sample 10 was collected during the return to the initial mixture (Figure 22).

Exposure solutions were prepared from the samples collected from HPLC UV-Vis (1-10) and used in the bioassays (Figure 23). As for the SRB assay, sub-fractions E14028 I7 8A+9 E 6, 7 and 9 showed the highest activities, with increases of protein content of 110.84 ± 7.52 ,

134.94 \pm 20.31 and 106.63 \pm 9.03 % after 24 hours of exposure, respectively. Regarding the metabolic activity (MTT assay), sub-fractions E14028 I7 8A+9 E 1, 6 and 7 had the strongest effects of 132.85 \pm 5.72, 156.82 \pm 5.72 and 140.93 \pm 9.16% for the 48 hours of exposure, respectively, compared to the solvent control. Due to the present bioactivity in the neighboring sub-fraction E14028 I76 8A+9 6, visible in Figure 23, we can expect that the compound is distributed in both samples (E14028 I76 8A+9 6 and 7) and that the chromatogram peak seen in Figure 22, may have underlying not apparent peaks.

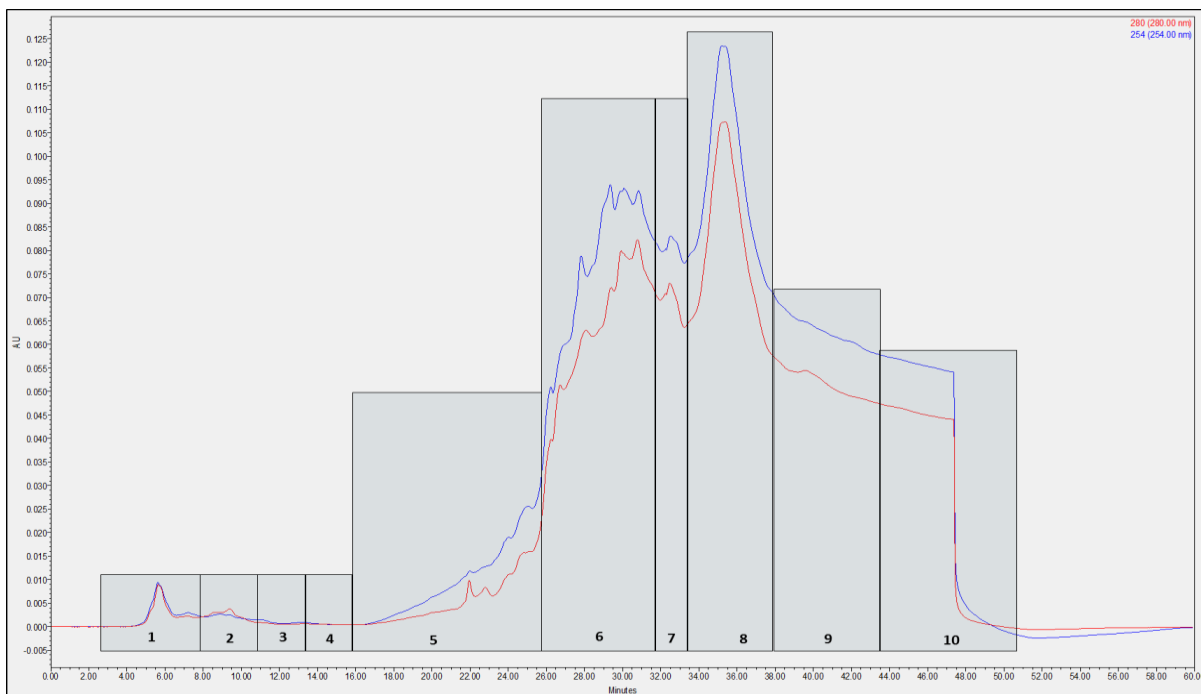


Figure 22 - Chromatogram of E14028 I7 8A+9 E showing highlighted sub-fractions that were collected. Conditions of the injection were 200 μ L at a concentration of approximately 43.5 mg mL⁻¹.

Following these results, sub-fractions E14028 I7 8A+9 E 1, 6, 7 and 9 were also selected for the specific analysis by the BrdU ELISA proliferation assay (Figure 24). Sub-fraction E14028 I7 8A+9 E 1 exerted a negative effect on the proliferation rate, compared to the solvent control, whereas sub-fractions E14028 I7 8A+9 E 6, 7 and 9 increased proliferation in 123.05 \pm 30.57, 119.75 \pm 13.13 and 116.24 \pm 18.49 % at 24 hours compared to the solvent control, respectively. Sub-fraction E14028 I7 8A+9 E7 had a similar pattern to the one obtained in the SRB assay, with an increase of 119.75 \pm 13.13 at the 24 hours of exposure and a lowered rate at 48 hours, compared to the solvent control (106.88 \pm 16.16 % for the BrdU ELISA assay and 102.11 \pm 4.59 for the SRB assay).

Sub-fraction E14028 I7 8A+9 7 was chosen for further fractionation since it is a lowered mass to be processed and thus a higher probability of quickly obtaining the bioactive compounds.

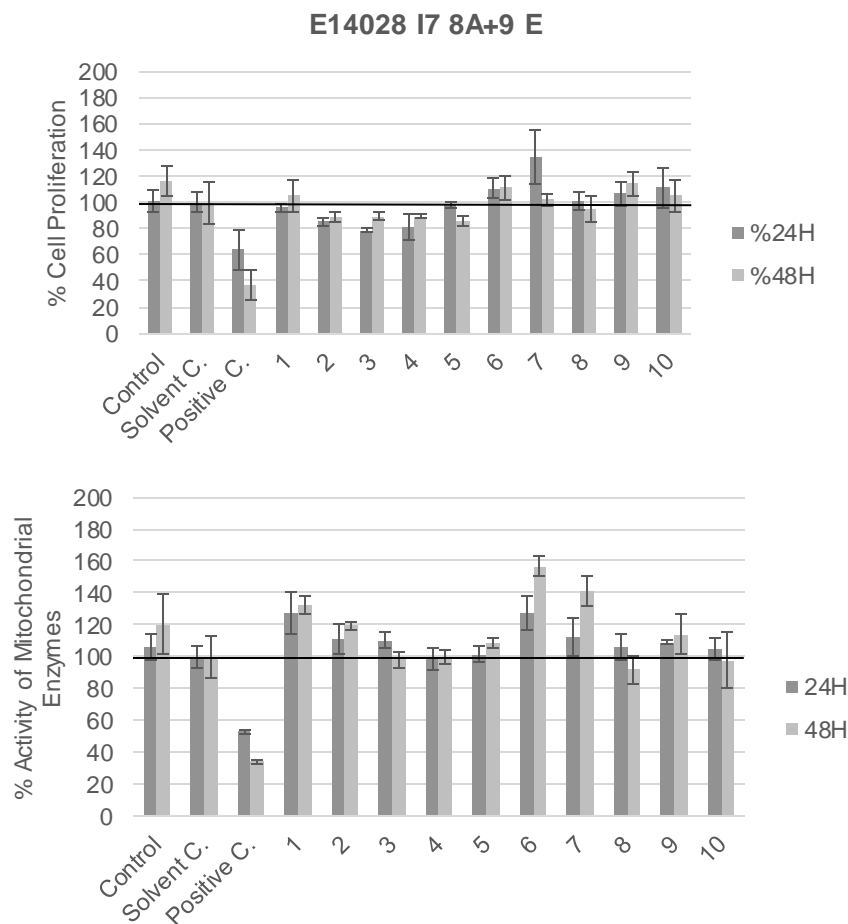


Figure 23 - Cell proliferation (SRB assay, top) and activity of mitochondrial enzymes (MTT assay, bottom), in % of solvent control, for the E14028 I7 8A+9 E sub-fractions (1-10) with the concentration of 25 $\mu\text{g mL}^{-1}$, after 24 and 48 hours of exposure. Solvent control corresponded to 1% DMSO and positive control to 20% DMSO, using 3 replicate wells per treatment and 6 for control, solvent control and positive control.

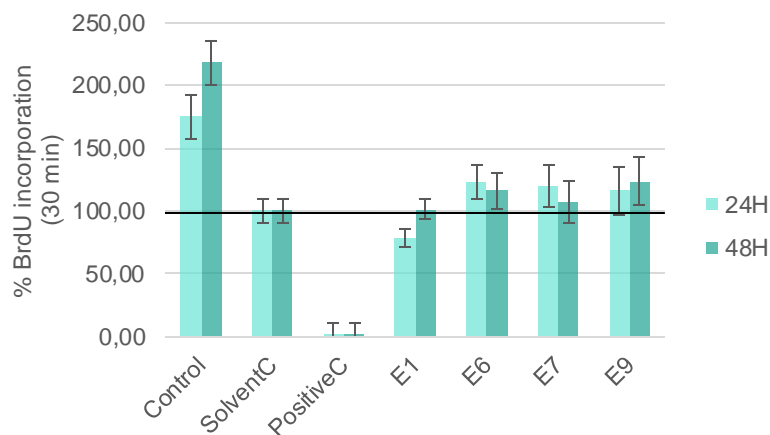


Figure 24 - BrdU incorporation percentage compared to the solvent control for HPLC fractions E14028 I7 8A+9 E 1,6,7 and 9 with the concentration of $25 \mu\text{g mL}^{-1}$, control and solvent control (1% DMSO) with 2 hour BrdU pulse, after 48 hours of exposure, using 3 replicate wells per treatment and 6 for control, solvent control and positive control..

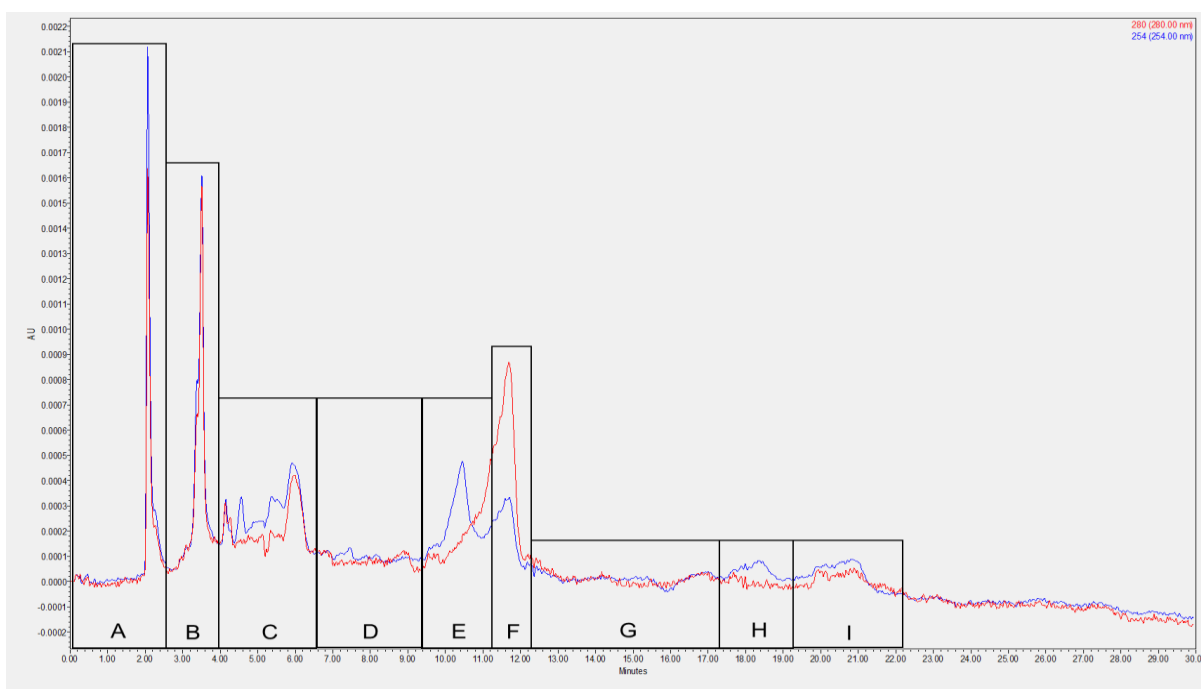


Figure 25 - Chromatogram of E14028 I7 8A+9 E7 showing highlighted sub-fractions that were collected. Conditions of the injection were $35 \mu\text{L}$ at a concentration of approximately 3.8 mg mL^{-1} .

Based on these results, sub-fractions E14028 I7 8A+9 E 6 and 7 were selected as candidates for fractionation. We proceeded to fractionate firstly the sub-fraction E14028 I7 8A+9 E7 ($m=3.8 \text{ mg}$) through HPLC UV-Vis. This sub-fraction was solubilized in MeCN and loaded in the apparatus. Using an isocratic program of 75% MeCN/25% H_2O , fractionation resulted in 10 sub-fractions (Figure 25): A to I recovered directly from the HPLC, with the

absorbance peaks used to determine different resulting fractions, and sub-fraction E14028 I7 8A+9 E7 J that was the mass on the sub-fraction not solubilized in MeCN.

The resulting sub-fractions were tested for bioactivity through SRB and MTT assay (Figure 26). The SRB assay demonstrated that all these sub-fractions had a negative activity on cell proliferation, with values ranging from 60 to 90% compared to the solvent control, except for the sub-fraction E14028 I7 8A+9 E7 J that exerted a positive effect on cell proliferation of 124.80 ± 23.46 and 134.32 ± 25.32 % at 24 and 48 hours of exposure, respectively. The activity of mitochondrial enzymes for this sub-fraction was also positive, 124.35 ± 12.442 and 126.27 ± 1.10 % at 24 and 48 hours of exposure.

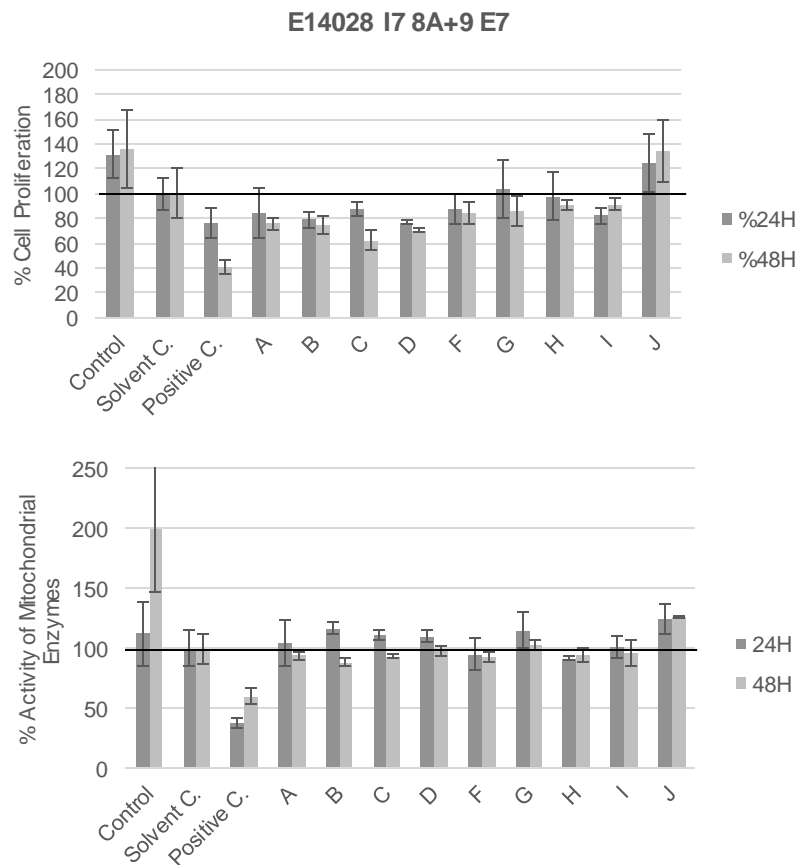


Figure 26 - Cell proliferation (SRB assay, top) and activity of mitochondrial enzymes (MTT assay, bottom), in % of solvent control, for the E14028 I7 8A+9 E7 sub-fractions (A-J) with the concentration of $10 \mu\text{g mL}^{-1}$, after 24 and 48 hours of exposure. Solvent control corresponded to 1% DMSO and positive control to 20% DMSO, using 3 replicate wells per treatment and 6 for control, solvent control and positive control.

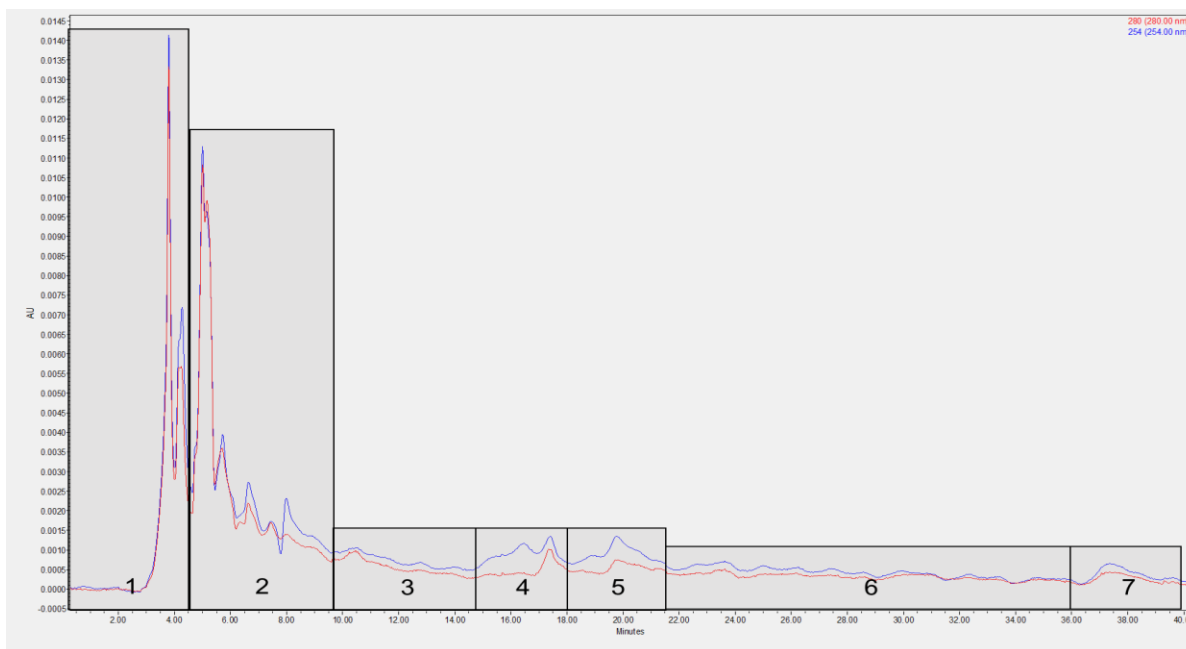


Figure 27 - Chromatogram of E14028 I7 8A+9 E7J showing highlighted sub-fractions that were collected. Conditions of the injection were 50 μL at a concentration of approximately 2.65 mg mL^{-1} .

As described before, the same apparatus and procedure was applied to simplify sub-fraction E14028 I7 8A+9 E7J. With a mass of 2.65 mg, this sub-fraction was solubilized in MeOH and loaded in the HPLC UV-Vis, using an isocratic program of 85% MeOH/15% H₂O (Figure 27). 7 new sub-fractions resulted from this procedure and were further tested in 3T3-L1 pre-adipocytes. Tests through MTT and SRB assay revealed that at a concentration of $25 \mu\text{g mL}^{-1}$, none seem to exert any effects in cell proliferation through SRB assay (Figure 28), with proliferation ratios ranging from 85 to 110%, compared to solvent control. However, for the MTT assay, fraction E14028 I7 8A+9 E7 J 1 revealed a higher score for metabolic activity, with an increase of $165.13 \pm 11.82 \%$ at 48 hours, compared to solvent control.

BrdU ELISA assay, allowed us to confirm that a bioactive compound or a group of bioactive compounds are present in the sub-fractions E14028 I7 8A+9 E6 and 7 (Figure 24). The lowered activity could be a result of the high processing of the sample, which suffered 7 fractionings, and thus some chemical and structural modifications that may have taken place.

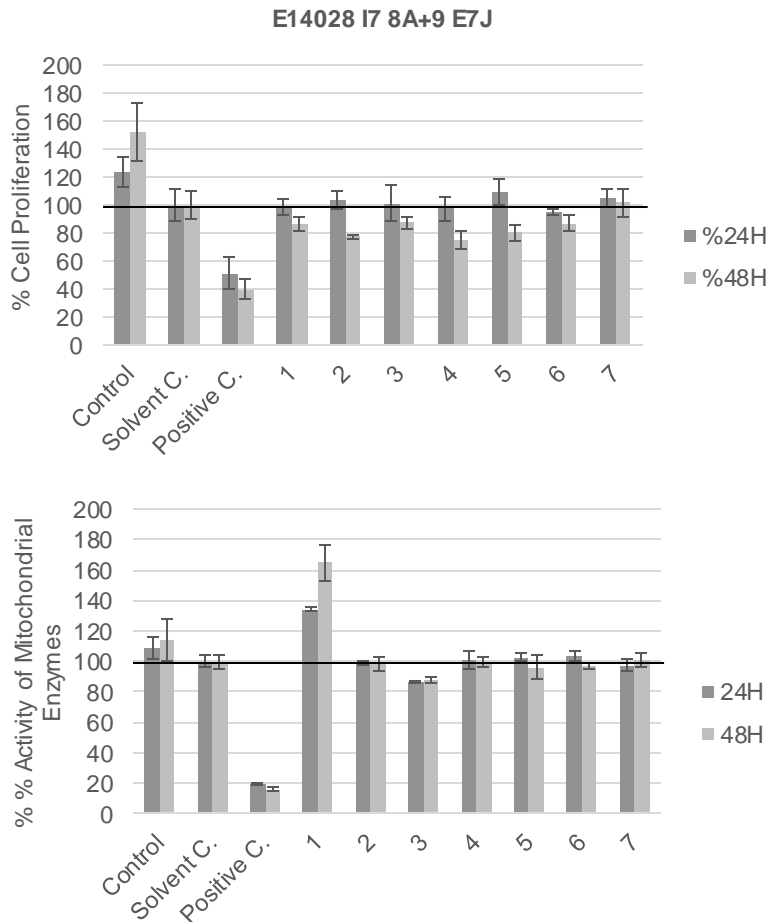


Figure 28 - Cell proliferation (SRB assay, top) and activity of mitochondrial enzymes (MTT assay, bottom), in % of solvent control, for the E14028 I7 8A+9 E7J sub-factions (1-7) with the concentration of $25 \mu\text{g mL}^{-1}$, after 24 and 48 hours of exposure. Solvent control corresponded to 1% DMSO and positive control to 20% DMSO, using 3 replicate wells per treatment and 6 for control, solvent control and positive control.

4.1.3. Screening for adipogenic activity

The following bioassay of preadipocyte differentiation into mature adipocytes was performed at the Department of Biochemistry of the Faculty of Medicine of the University of Porto. Although optimization of differentiation process was carried out at BBE, CIIMAR, we were unable to obtain consistent differentiation rates.

Several tests were conducted for the adipogenesis assay, looking for any significant changes in the differentiation process from the cyanobacterial strains, and for two well-known antidiabetic drugs, troglitazone and rosiglitazone, and the phenol resveratrol (Figure 29). Resveratrol strongly inhibited adipogenesis (51.82 ± 2.43 % of control), as well as the DMSO exposure (0.2%), with an approximate decrease of lipid content of 10% in the adipogenesis process. As for rosiglitazone and troglitazone, increases of 208.59 ± 24.61 and 220.74 ± 44.89

%, respectively, compared to control, were registered. Resveratrol also showed cell detachment and cell death during the differentiation process, along with the poorly differentiated pre-adipocytes (Figure 37).

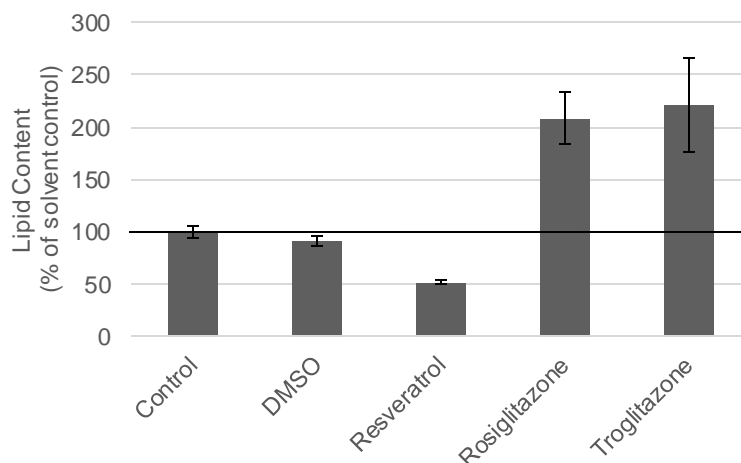


Figure 29 - Results for the adipogenesis assay (Oil Red O staining), in % of control in 3T3-L1 cell line using DMSO (0.2%), resveratrol (100 μ M), rosiglitazone (0.2 μ M) and troglitazone (0.2 μ M), after exposure from day 0 to day 12 of the differentiation process, using 2 replicate wells per treatment and 4 for solvent control.

The most fractions from E14026 (Figure 30) showed inhibiting activity on adipogenesis, which was analyzed by Oil Red O staining and spectrometrical quantification. Fraction E14026 A exerted the strongest inhibitory effect, 62.23 ± 4.79 % compared to the solvent control, followed by fraction E14026 H (69.97 ± 2.31 %).

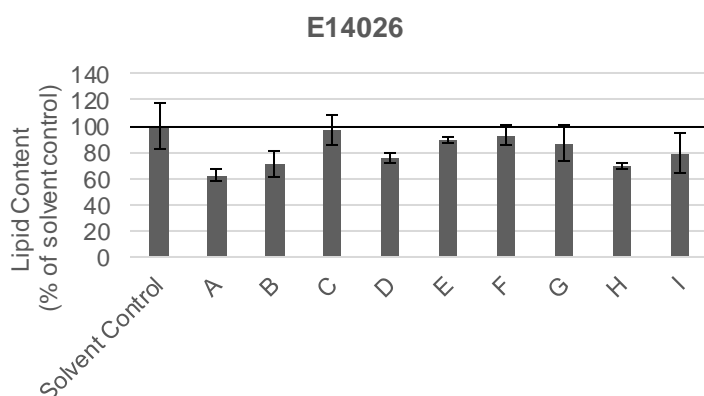


Figure 30 - Results for the adipogenesis assay (Oil Red O staining), in % of solvent control, for the E14026 (*Phormidium* sp. LEGE06363) VLC fractions (A – I) with the concentration of 20 μ g mL⁻¹, after exposure from day 0 to day 12 of the differentiation process. Solvent control corresponded to 0.2% DMSO and 2 replicate wells per treatment and 4 for solvent control were used.

The same activity was observed for the fractions of E14028 (Figure 31). Exposure of pre-adipocytes during adipogenesis to fractions E14028 B, F, H and J caused cell detachment and cell death. Therefore these wells were not used for Oil Red O staining and are not shown in Figure 31. Previously, during our proliferation screening, fractions E14028 B and D exerted detrimental effects in metabolic activity (MTT) and E14028 F in proliferation rate (Figure 10). Fraction E14028 D showed the strongest effect of these fractions inhibiting adipogenesis $77.14 \pm 5.97\%$, compared to the solvent control.

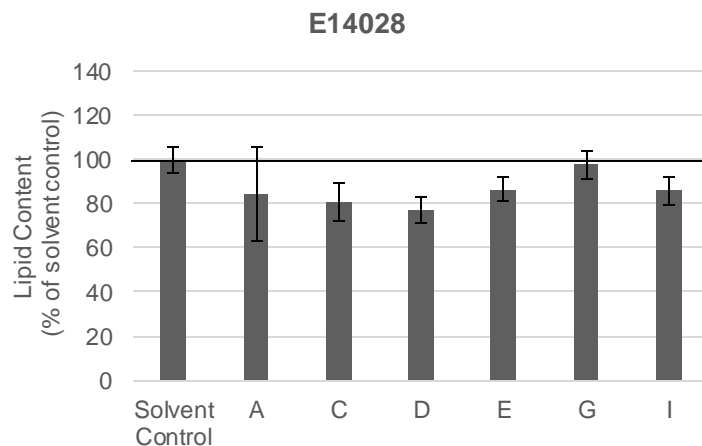


Figure 31 - Results for the adipogenesis assay (Oil Red O staining), in % of solvent control, for the E14028 (*Planktothrix planctonica* LEGEXX280) VLC fractions (A – I) with the concentration of $20 \mu\text{g mL}^{-1}$, after exposure from day 0 to day 12 of the differentiation process. Solvent control corresponded to 0.2% DMSO and 2 replicate wells per treatment and 4 for solvent control were used.

Regarding E14031 (Figure 32), most of the fractions had a stimulatory effect on adipogenesis. Fractions E14031 D and H exerted the strongest effects: 233.30 ± 22.42 and $210.2 \pm 33.76 \%$ compared to the solvent control. In contrast, fraction E14031 B inhibited adipogenesis ($77.23 \pm 1.82 \%$) and fractions E14031 C and G caused cell detachment and cell death, and are not shown in the graph. Fractions E14031 C and G were previously identified as cytotoxic for 3T3-L1, with decreases in proliferation rate (SRB) and metabolic activity (MTT) at 24 and 48 hours of exposure, at a concentration of $100 \mu\text{g mL}^{-1}$ (Figure 11).

Regarding E14032 (Figure 33), exposure to fractions E14032 E, F, G resulted in cell detachment and cell death. In the proliferation assay (SRB) these fractions did not, however, show evident cytotoxic effects (Figure 12). Fractions E14032 A, B, C, D and I reduced adipogenesis ranging from 75 to 96%, the lowest activity corresponding to fraction E14032 A ($75.74 \pm 10.47\%$). Fractions E14032 H and J increased adipogenesis (123.98 ± 6.33 and

122.44 ± 6.73 %, respectively). Fractions E14032 A, B, C and D limited cell proliferation, more evidently at 48 hours of exposure (Figure 12).

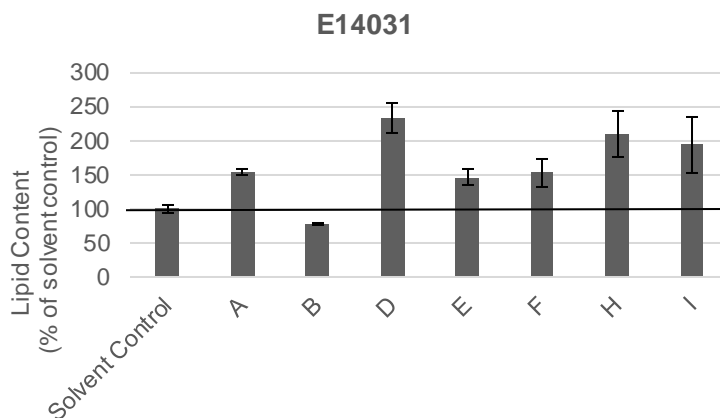


Figure 32 - Results for the adipogenesis assay (Oil Red O staining), in % of solvent control, for the E14031 (*Synechocystis sp.* LEGE07211) VLC fractions (A – I) with the concentration of 20 µg mL⁻¹, after exposure from day 0 to day 12 of the differentiation process. Solvent control corresponded to 0.2% DMSO and 2 replicate wells per treatment and 4 for solvent control were used.

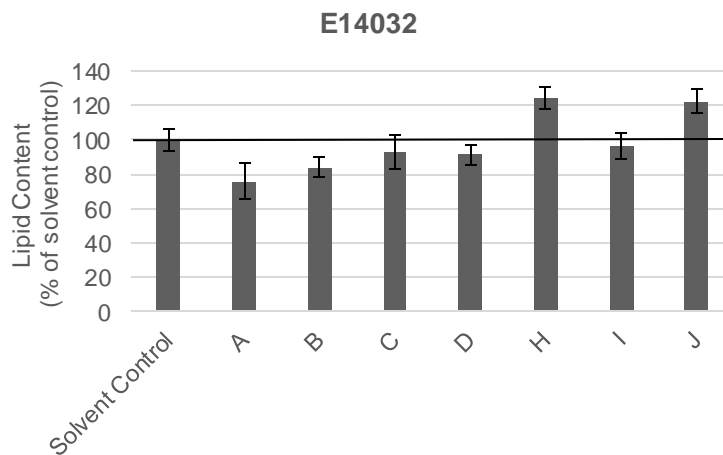


Figure 33 - Results for the adipogenesis assay (Oil Red O staining), in % of solvent control, for the E14032 (*Oscillatoria limnetica* LEGE00237) VLC fractions (A – J) with the concentration of 20 µg mL⁻¹, after exposure from day 0 to day 12 of the differentiation process. Solvent control corresponded to 0.2% DMSO and 2 replicate wells per treatment and 4 for solvent control were used.

Regarding the exposure to E14035 during adipogenesis (Figure 34), only fraction E14035 H was detrimental to cells, causing cell death. This fraction showed cytotoxicity only through the MTT assay, of 65.30 ± 3.93 and 87.03 ± 8.55% at 24 and 48 hours, respectively (Figure 13). The remaining fractions did not exert strong effects on adipogenesis, the lowest value registered for E14035 B (82.58 ± 2.81%) and the highest differentiation score registered for

E14035 J ($113.28 \pm 4.31\%$). Fraction E14035B also inhibited cell proliferation and decreased metabolic activity at 24 hours of exposure (Figure 13).

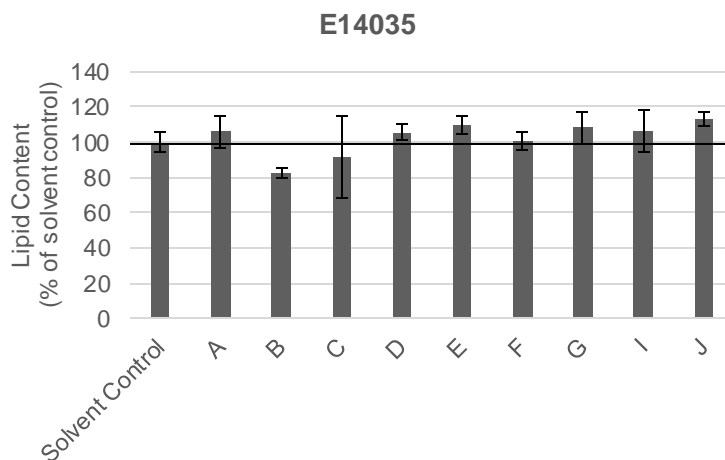


Figure 34 - Results for the adipogenesis assay (Oil Red O staining), in % of solvent control, for the E14035 (*Aphanizomenon* sp. LEGE03283) VLC fractions (A– J) with the concentration of $20 \mu\text{g mL}^{-1}$, after exposure from day 0 to day 12 of the differentiation process. Solvent control corresponded to 1% DMSO and 2 replicate wells per treatment and 4 for solvent control were used.

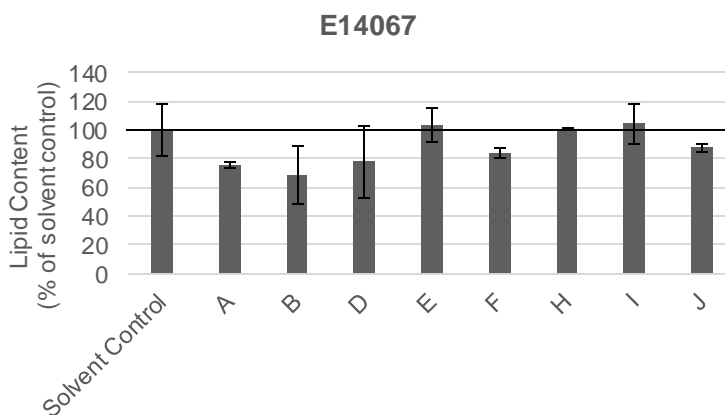


Figure 35 - Results for the adipogenesis assay (Oil Red O staining), in % of solvent control, for the E14067 (*Limnothrix* sp. LEGE07212) VLC fractions (A– J) with the concentration of $20 \mu\text{g mL}^{-1}$, after exposure from day 0 to day 12 of the differentiation process. Solvent control corresponded to 0.2% DMSO and 2 replicate wells per treatment and 4 for solvent control were used.

For E14067 (Figure 35), fractions E14067 C and G caused cell detachment and cell death during adipogenesis. These fractions exerted strong effects in metabolic activity (MTT) at 24 and 48 hours of exposure (Figure 14). Fraction E14067 E also inhibited metabolic activity (MTT), however, no detrimental effects were observed on cell proliferation and adipogenesis were observed. On the other hand, fraction E14067 F increased metabolic activity (MTT) of

pre-adipocytes, but no positive effects were observed on cell proliferation and adipogenesis. Fraction E14067 A inhibited adipogenesis ($75.51 \pm 2.13\%$), followed by fractions E14067 F and J (84.32 ± 3.59 and $88.05 \pm 2.88 \%$, respectively). No pro-adipogenic fractions were identified.

In order to understand the adipogenic effect of the pro-proliferative fractions produced in the screening for proliferative activity on pre-adipocytes (as detailed in section 4.1.1.1.), fractions derived from flash chromatography E14028 I7 were also tested for effects on adipogenesis (Figure 36). Fraction E14028 I7 7 increased adipogenesis ($129.44 \pm 0.75 \%$) and fractions E14028 I7 8A and 9 induced slightly adipogenesis (115.96 ± 12.44 and 109.98 ± 9.07 , respectively).

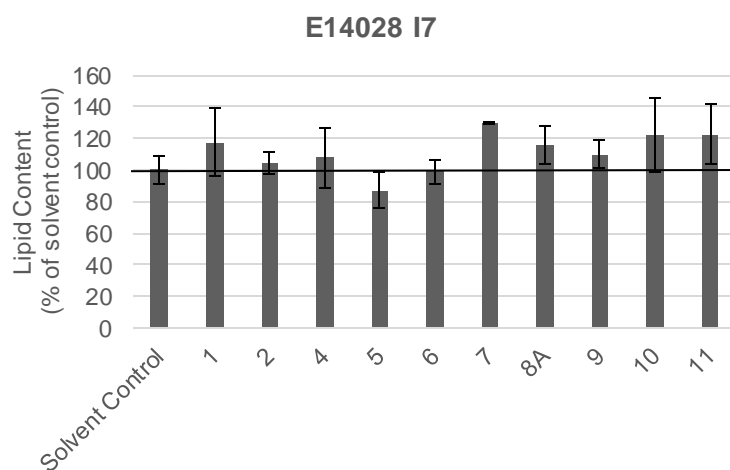


Figure 36 - Results for the adipogenesis assay (Oil Red O staining), in % of solvent control, for the E14028 I7 sub-fractions (1-11) with the concentration of $10 \mu\text{g mL}^{-1}$, after exposure from day 0 to day 12 of the differentiation process. Solvent control corresponded to 0.2% DMSO and 2 replicate wells per treatment and 4 for solvent control were used.

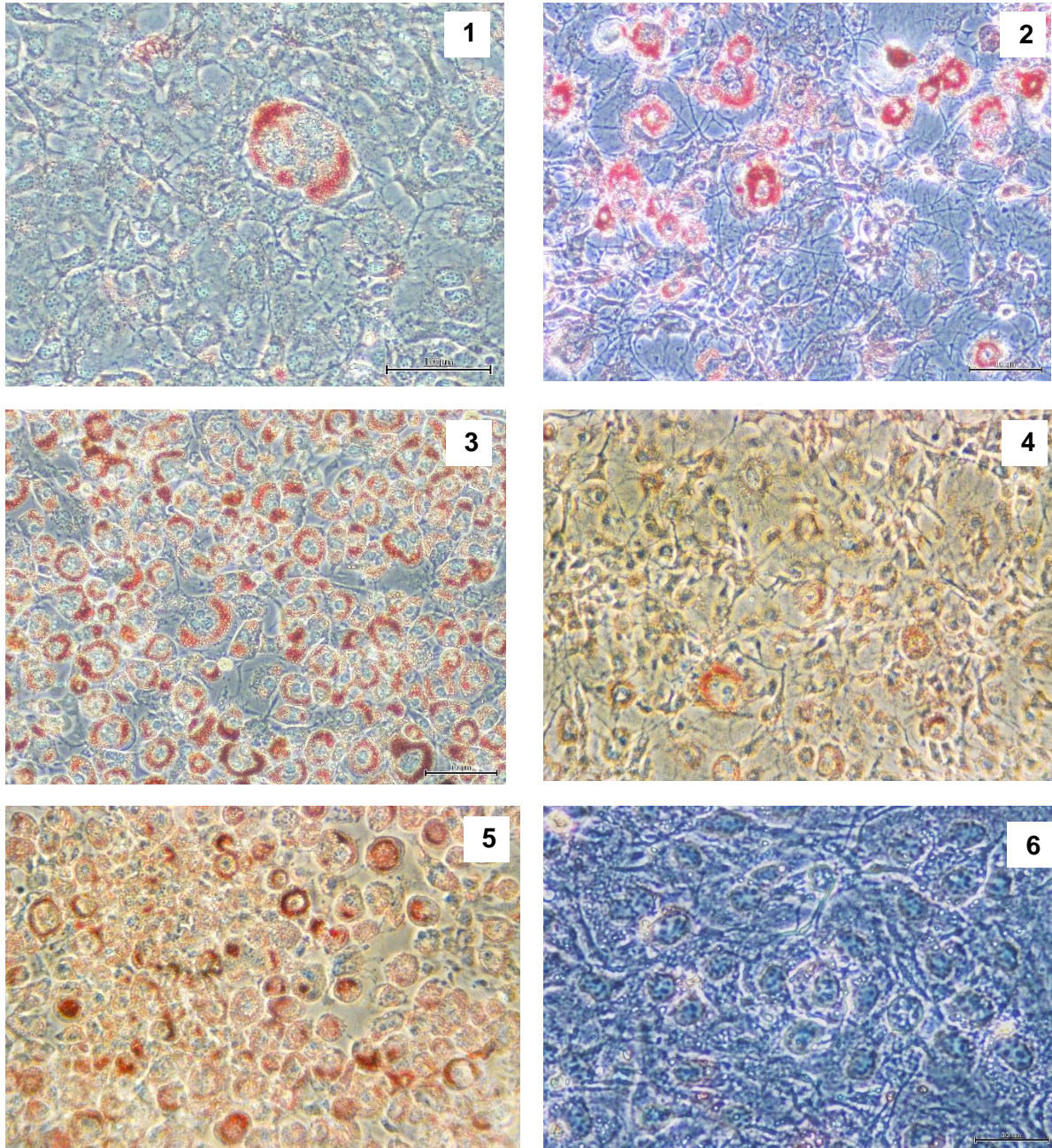


Figure 37 - Mature adipocytes after Oil Red O Staining under the optical microscope (40x). (1) Example of abnormal mature adipocyte; (2) Mature adipocytes exposed to 0.2% DMSO; (3) Mature adipocytes obtained after 12 day exposure to E14032 H; (4) Mature adipocytes after 12 days exposure to E14028 I77; (5) Mature adipocytes obtained after exposure to E14031D; (6) Pre-adipocytes after 12 day exposure to resveratrol.

4.1.4. . Bioassay-guided fractionation of E14031 D

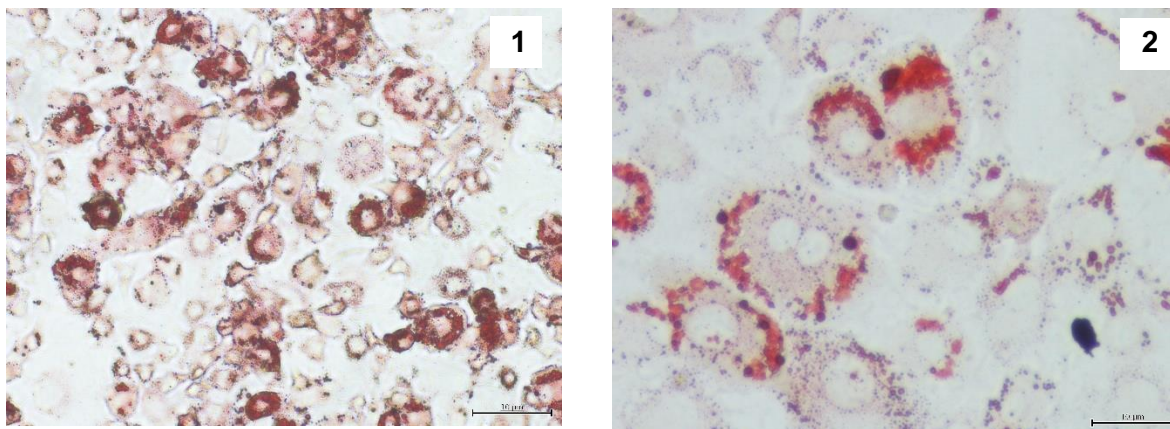


Figure 38 - Mature adipocytes after Oil Red O Staining under the optical microscope after 12 day exposure to cyanobacterial sub-fractions E1431 D 7 (1) and 3 (2), at a concentration of $10 \mu\text{g mL}^{-1}$ (40x).

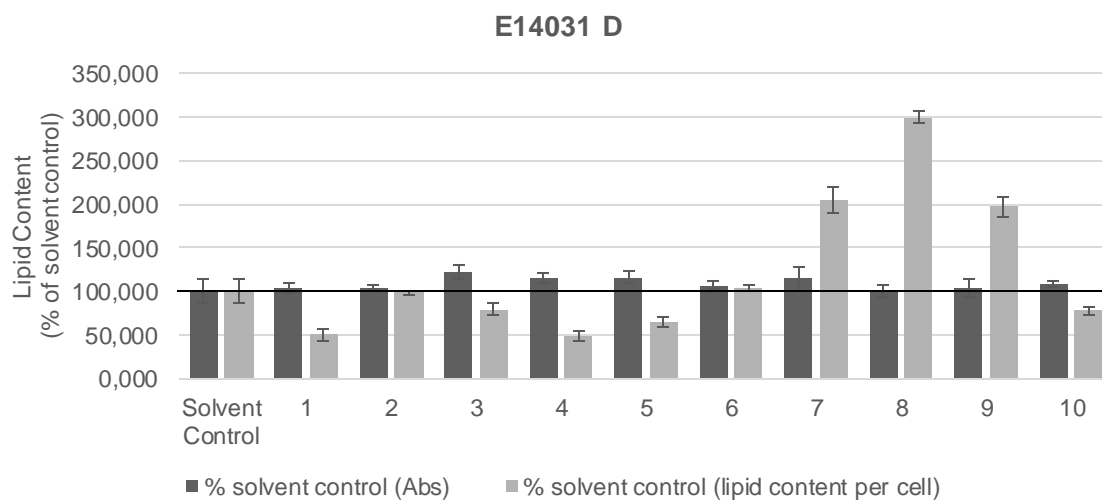


Figure 39 - Results for the adipogenesis assay (Oil Red O staining), in % of solvent control, for the E14031 D sub-fractions (1-10) with the concentration of $10 \mu\text{g mL}^{-1}$, after exposure from day 0 to day 12 of the differentiation process. Solvent control corresponded to 0.2% DMSO and 3 replicate wells per treatment and 4 for solvent control were used.

For the bioactivity test of these sub-fractions, with the Oil Red O staining and the cell count, we are able to adjust the relative lipid content with the cell count for each treatment, in contrast with the relative lipid content per well, obtained from the relative absorbance (Figure 39). Sub-fractions E14031 D 7 and 8 revealed the highest score of Oil Red O per cell of 204.80 ± 14.60 and $300.00 \pm 6.15\%$ compared to the solvent control, respectively. However, from previous observation we registered Oil Red O irremovable precipitates in the wells treated with E14031

D 8 and 9, which with the lower cell number for each treatment accounted for a higher lipid content per cell. Imaging, showing the lowered pre-adipocyte differentiation (Figure 38), substantiate these observations.

5. Discussion

5.1. Pro-proliferative and pro-adipogenic activity as targets for obesity treatment

During obesity, adipocyte hypertrophy and hyperplasia are predominant phenotypes in the adipose tissue. In addition, impaired adipocyte differentiation, enlarged adipose cells, hypoxia, inflammation and fibrosis are related to a dysfunctional adipose tissue. This is a major driving force promoting metabolic disease and the diabetes epidemic (Gustafson et al. 2009; Sun et al. 2011). When adipose tissue stops accommodating excess calorie intake due to expansion or differentiation impairment, lipodystrophy can take place. In this scenario, adipose tissue displays degenerative conditions (macrophage infiltration, cell death, insulin resistance). Excess fat is also detrimental since it may start to accumulate in other tissues as the liver leading to e.g. steatosis, non-alcoholic fatty liver disease (Danforth 2000). The control of adipose tissue processes has a central role in metabolic regulation: recent understandings of strategies for obesity therapeutics indicate that adipocyte hypertrophy and dysfunction could be avoided if preadipocyte recruitment is enabled (Sethi & Vidal-Puig 2007). In fact, anti-diabetic drugs as thiazolidinediones (rosiglitazone, troglitazone and pioglitazone) are currently in the market, used to restore insulin sensitivity and glucose tolerance, which are described as some of the metabolic complications of obesity. These drugs act as PPAR γ agonists, which is beneficial to the enhancement of adipogenesis and glucose uptake. Thus, an important endpoint to reduce the metabolic complications of obesity is the maintenance of the ability to recruit adipocytes and to undergo differentiation in order to distribute the excess calorie intake (energy) among competent adipocytes (Tchoukalova et al. 2008; Gustafson et al. 2013; Henninger et al. 2014). In this context, the stimulation of adipocyte proliferation and differentiation could be beneficial to accommodate the surplus energy and to reduce the obesity associated co-morbidities as diabetes, fatty liver disease or cardiac disease. Following this strategy for the treatment of obesity associated co-morbidities, we aimed to identify novel compounds that could be used to diminish the metabolic complications of obesity.

Regardless of this above described strategy, the inhibition of adipocyte differentiation has been extensively studied and several studies have described that inhibition of adipogenesis can be beneficial and simultaneously ameliorate obesity symptoms when using a whole animal model system. Target herbal ingredient, extract made from two herbs, *Scutellariae Radix* and *Platycodi Radix*, caused the downregulation of adipogenic transcription factors in 3T3-L1 mature adipocytes, as well as adipogenesis (through Oil Red O staining) and triglyceride content. In the animal model, target herbal ingredient caused a reduction of body weight and

total serum cholesterol, and improved the glucose tolerance in high-fat diet induced obese mice, after a daily dose administration for 10 weeks (Han et al. 2011). The ethanol extract of *Laminaria japonica* (Areshoung) also decreased lipid droplets, adipocyte size and body weight gain in Sprague-Dawley male rats (Jang & Choung 2013). Licochalcone A and 18 β -glycyrrhetic acid from licorice, in two distinct studies, decreased body weight and plasma triglycerides in obese animal models and reduced lipid accumulation and key adipogenic genes and receptors (as PPAR- γ , C/EBP α , SREBP-1) in 3T3-L1 adipocytes (Quan et al. 2012; Park et al. 2014). Other compounds, as the antioxidant tanshinone IIA from *Salvia miltiorrhiza* also suppressed adipogenesis through PPAR γ antagonism in 3T3-L1 adipocytes, but reduced adipose tissue mass and body weight and improved glucose tolerance in high fat diet induced obese mice (Gong et al. 2009). This shows that different endpoints (both the inhibition and promotion of adipogenesis) are useful in the study of obesity treatments, since decreases in adipogenesis do translate in lowered body weight gain in the whole animal model system.

However, this approach needs careful analysis of the mechanistic profile and of potential side effects of the studied compounds. 18 β -glycyrrhetic acid is thought to reduce adipogenesis and lipogenesis via cannabinoid receptor type 1 inactivation. Drugs that act as antagonists of this receptor have been known to have serious repercussions in the central nervous system as anxiety and depression, even though they are recognized to effectively lower body weight (Nathan et al. 2011). Many other drugs developed for the treatment of obesity have severe side-effects; diethylpropion increased blood pressure and heart rate; thyroxine leads to hyperthyroidism, anxiety and insomnia; sibutramine, a norepinephrine and serotonin reuptake inhibitor caused headache, insomnia and constipation; phenylpropanol amine, a central α 1-adrenergic receptor agonist caused hemorrhagic stroke and psychosis. These drugs have been withdrawn and banned in most countries (reviewed in Cheung et al. 2013; Kim et al. 2014). Thus, the history of pharmacotherapy for obesity treatment shows that solely inhibiting weight gain may not be a viable solution due to the many secondary effects.

An appropriate methodology to different obesity scenarios should be met in order to treat its complications. In our work, the focus was to identify cyanobacterial secondary metabolites that could treat and prevent metabolic complications of obesity as insulin resistance and adipocyte hypertrophy. In this context, our research focused on the pro-proliferative and pro-adipogenic bioactivity of compounds.

5.2. Cyanobacterial assessment for bioactivity

Many studies have pointed to the benefits of cyanobacteria for human health. Some strains of cyanobacteria effectively ameliorate the hyperlipidemic profile in animal and human models (Iwata et al. 1990; Gonzalez de Rivera et al. 1993; Torres-Duran et al. 1999; Jarouliya et al. 2012; Cheong et al. 2010), or have shown protective properties against inflammatory diseases, cancer, diabetes and hypercholesterolemia (Parikh et al. 2001). Cyanobacterial secondary metabolites are mostly lipopeptides (40%), amino acids (5.6%), fatty acids (4.2%), macrolides (4.2%) and amides (9%). The chemical identity of compounds from cyanobacteria with the highest pharmaceutical and biotechnological interest tends to be lipopeptides (Raja et al. 2015). Cyanobacteria have shown to be prolific in secondary metabolites, with up to 800 described in literature; examples include antioxidant vitamins, phenolic compounds, sterols or polyunsaturated fatty acids. Their array of bioactivity is very wide and, at the same time, they have shown to have specific interactions with cellular targets, which represent a major advantage for pharmaceutical, medicinal and biotechnological fields. Compounds isolated from cyanobacteria have been shown to induce G1 cell cycle arrest in tumor cells (Luesch et al. 2006), inhibit microtubule assembly (Mitra & Sept 2004), inhibit HIV integrase (Mitchell et al., 2000) and can be selectively cytotoxic to a cell line (Leão et al. 2013). As highlighted before (Section 1.2.2.3.), cyanobacteria hold as well many beneficial effects to treat obesity and related co-morbidities. Species of *Arthospira* present anti-hypercholesterolemia, anti-hyperglycemia, anti-inflammatory and anti-oxidant activities in the human and animal model. *N. commune* has also been described to reduce obesity complications *in vivo*. Research is now focusing on describing the bioactive compounds responsible for these valuable activities.

Some studies indicate that phycocyanin, a phycobiliprotein with anti-oxidant activity (Farooq et al. 2014), found in many strains of cyanobacteria (Liu et al. 2014), could act as an anti-diabetic drug (Ou et al. 2013). Phycocyanin significantly decreased the body weight, fasting plasma glucose, serum triglyceride content and enhanced glucose tolerance in KKAY mice (Ou et al. 2013). Scytonemin is a yellow-brown hydrophobic pigment from cyanobacteria that acts as a protection for UV-A radiation. Scytonemin has anti-inflammatory and anti-proliferative activities (Stevenson et al. 2002) and is produced by many cyanobacterial species (Rastogi et al. 2013). γ -Linoleic acid is another cyanobacterial compound under intense study. This rare polyunsaturated fatty acid is 170-fold more effective than linoleic acid and can represent up to 1% of the dry cell mass (Cohen et al. 1993). This compound was isolated in 1967, is easily converted in arachidonic acid and prostaglandin E2 in the human body, which

lowers blood pressure and plays an important role in the lipid metabolism (Euler & Eliassen 1967).

In our work, we tested 62 fractions from six freshwater cyanobacterial strains of three different sub-classes (*Oscillatoriales*, *Chroococcales*, *Nostocales*) for proliferative and adipogenic activity. Summarizing, many of those fractions were able to exert effects in the 3T3-L1 cell line. In total, we observed four different activities: inhibiting or inducing the proliferation or differentiation of the (pre-) adipocytes.

Our present results confirm the ability of cyanobacteria to interact with many cellular targets. Fractions of *Planktothrix planctonica* LEGEXX280 (E14028 I) and *Aphanizomenon* sp. LEGE03283 (E14035 B) exerted strong positive effects in proliferative and metabolic activity of 3T3-L1 pre-adipocytes. Fractions from *Synechocystis* sp. LEGE07211 (E14031 D) and from *Oscillatoria limnetica* LEGE00237 (E14032 H and J) showed remarkable activity in the modulation of adipogenesis of murine pre-adipocytes.

Furthermore, even though we focused on the pro-proliferative and pro-adipogenic activity as strategy for the treatment of obesity-associated co-morbidities (as outlined above), our results show promising bioactivities that can be relevant for other areas of drug discovery (anti-proliferative, anti-adipogenic). Fractions from *Phormidium* sp. LEGE06353 (E14026 A) and *Synechocystis* sp. LEGE07211 (E14031 B) strongly inhibited adipogenesis in 3T3-L1 cells. Since adipogenesis and osteoblastogenesis are tightly connected (Pittenger 1999), each lineage being exclusively induced, many studies have explored the potential of bioactive fractions inhibiting adipogenesis for their effects on the promotion of osteoblastogenesis (Byun et al. 2012; Karadeniz et al. 2014; Kim et al. 2015).

Fractions from *Phormidium* sp. LEGE06353 (E14026 H), *Synechocystis* sp. LEGE07211 (E14031 F and G) effectively decreased cell proliferation. Inhibition of cell proliferation is often used as a method for the screening of new anti-cancer compounds (mainly through anti-proliferative, pro-apoptotic signaling) and to study the etiology of cancer (Shoemaker 2006; Yu et al. 2014; Rubinstein et al. 1990). It has been an endpoint studied in hepatocellular carcinoma (Gedaly et al. 2013), breast cancer (Spink et al. 2006) and several cancer cell lines (Song et al. 2006; Leão et al. 2013; Costa et al. 2014; Catchpole et al. 2015).

5.2.1. E14028 I pro-proliferative activity

From the extract of *Planktothrix planctonica* LEGE XX280, we obtained 9 fractions, E14028 I being the active one. Our bioassay guided activity fractionation of E14028 I yielded up to 44 sub-fractions after 7 fractionation processes: 2 VLCs, a flash chromatography, a SPE and 3

HPLCs. Throughout, several sub-fractions were found to be bioactive; the most promising ones were selected to follow bioactivity. As a result, E14028 I7 8A+9 E7 J1 comprises the bioactive compound responsible for the pro-proliferative activity in 3T3-L1 cells. Hereby, the compound was isolated from *Planktothrix planctonica*, which is a freshwater species. This genus includes filamentous planktonic cyanobacteria that grow through a solitary trichome (filament) without sheaths, and since they present no akinets or heterocysts, they are grouped in the sub-class *Oscillatoriales* (Komárek & Jaroslava 2004). Some strains of this genus are known to produce cyanotoxins as microcystins (Ernst et al. 2001) and other peptides with up to 15 different chemotypes (out of 18 different peptides) (Welker et al. 2004). However, there is no novel secondary metabolite described yet with biotechnological potential from this species or genus of cyanobacteria.

Until now, we can elaborate that this is a polar compound, a secondary metabolite from the cyanobacteria *Planktothrix planctonica* LEGE XX280 that increases both cell proliferation and metabolic activity of 3T3-L1 pre-adipocytes, with a relative high absorbance at 254 and 280 nm, soluble in methanol and water. This compound is now isolated with few impurities in its composition. Due to the lack of purified mass of the isolated compound, we are not able to proceed towards mass spectrometry and compound identification (through e.g. MarinLit, a database of marine natural products). Since this compound may be distributed in another fraction (E14028 I7 8A+9 E6) we will proceed to isolate the compound from this fraction in order to obtain appropriate mass for further identification and characterization.

Compounds like these, acting on the increase of cell proliferation, can contribute to ameliorate the metabolic complications of obesity, since pre-adipocyte proliferation is a key component of adipose tissue development. In other disease areas, a pro-proliferative compound can also be of interest. Cellular proliferation is an important endpoint for therapeutic areas as for neurodegenerative disorders (Popa-Wagner et al. 2015) and fibroblastic wound healing (Werner et al. 2007; Styrzewska et al. 2015; Geller et al. 2015). Specifically in the area of wound healing, where cell proliferation and tissue regeneration is limited, the application of pro-proliferative compounds has been studied. Glycolic acid, a hydroxyacetic acid commonly found in some sugar crops, is a compound used in several cosmetic products to ameliorate photoaging processes and enhance wound healing. In *in vivo* and *in vitro* experiments, treatment with glycolic acid increased collagen mRNA expression and dermal fibroblast proliferation (Kim et al. 1998). In cultured human skin fibroblasts, treatment with glycolic acid resulted in increased cell proliferation and collagen production in a dose-dependent manner (Kim & Won 1998). Studies described that flax fiber hydrophobic extract activated migration

and proliferation of NHDF and NHEK cells (Styrczewska et al. 2015). It is known that this extract contains cannabidiol, phytosterols and unsaturated fatty acids, however, no single compound was described to be responsible for the bioactivity. The ethanolic extract of the leaves of *Hancornia speciosa* Gomes, a medicinal plant from Brazil used to treat wounds and inflammation, revealed *in vitro* wound healing properties. The extract increased cell migration and proliferation of fibroblasts, as well as anti-inflammatory properties. The isolated compounds, bornesitol and quinic acid, were also bioactive (Geller et al. 2015). Thus, cyanobacteria may hold a promising source of pro-proliferative compounds in other disease contexts.

In the context of obesity, proliferative activity has been used as an endpoint in several obesity-related studies (Teixeira et al. 2010b; Marques et al. 2013). In previous studies, natural products inhibiting adipogenesis also decreased pre-adipocyte proliferation. Treatment of 3T3-L1 pre-adipocytes and human pre-adipocytes with curcumin inhibited mitotic clonal expansion and further resulted in the inhibition of mRNA levels of adipogenic transcription factors as PPAR γ and C/EBP α in the early stage of adipocyte differentiation (Kim et al. 2011). The extract of *Populus balsamifera* L. led to a complete inhibition of adipogenesis and severely limited 3T3-L1 proliferation (Martineau et al. 2010). Treatment of 3T3-L1 cells with xanthohumol, a prenylflavonoid from *Humulus lupulus* L., also decreased differentiation, lipid content and PPAR γ expression and the proliferation of pre-adipocytes measured through SRB staining (Mendes et al. 2008). On the other hand, the extracts of the inner bark of *Alnus incana* ssp. *rugosa*, acting as a partial agonist towards PPAR γ , did not affect clonal expansion of pre-adipocytes (Martineau et al. 2010). Hence, studies confirm an intrinsic relation between proliferation and adipogenesis, the two major endpoints controlling the metabolic complications of obesity. Once there is available mass to conduct an adipogenesis study, new information will be obtained on the effects of this compound exerted during adipogenesis. The increase of pre-adipocyte proliferation exerted by the compound present in E14028 I7 8A+9 E7 J1 could all by itself contribute to ameliorate adipocyte hypertrophy and dysfunction as more competent adipocytes may be available to accommodate surplus energy.

5.2.2. Cyanobacterial adipogenic bioactivity

Oil Red O staining was used for the assessment of the effects of the cyanobacterial fractions during adipogenesis, a fat soluble dye. ORO is accepted as the most accurate method for the diagnosis of steatosis in mouse and human liver (Catta-Preta et al. 2011; Levene et al. 2012) and has been widely used in 3T3-L1 adipocytes (Kim et al. 2009; Marques et al. 2013;

Ko et al. 2013; Jung et al. 2014). ORO is a low budget method and requires basic laboratory apparatus. The principle is simple: the dye is minimally soluble in solvent and, when in contact with the cells or tissue, the hydrophobic dye will quickly associate with the lipids. Oil Red O stains hydrophobic and neutral lipids, as triglycerides, diacylglycerols and cholesterol esters, whereas most polar lipids, as phospholipids, sphingolipids and ceramides, are not stained by the dye (Fowler & Greenspan 1985).

Imaging is a crucial tool to understand phenotypic variations of adipocytes when exposed to fractions or compounds. A high Oil Red O score means higher lipid content per well and the lipid content may be distributed in many and small adipocytes or in few and large adipocytes. The latter case is an undesirable result, since this correlates with a hypertrophic phenotype and dysfunctional adipose tissue due to lack of adipogenesis committed cells. Moreover, even though each well is seeded with the same cell density, the cell number per well may vary from the beginning of the treatment until the end of the experiment. In Figure 37 (1), we captured an abnormal adipocyte, high in size and lipid content, in contrast with a lack of differentiation in the rest of the well. This result was obtained during optimization of the differentiation process. In Figure 37 (2), the effect of 0.2% DMSO is shown on adipogenesis. Some differentiation takes place and clear lipid droplets are formed, however, not in every treated cell. In contrast, fractions E14031 D (Figure 37 (5)) and E14032 H (Figure 37 (3)) showed increased adipogenesis that resulted in higher scores of Oil Red O and in the desired phenotypic changes of mature adipocytes with more than 80% of differentiated cells after the 12 day treatment. Imaging allowed us to conclude that E14031D exerted stronger effects, with a higher number of differentiated cells after 12 days and a uniform lipid accumulation, without the formation of hypertrophic adipocytes.

Fractions E14031 D (*Synechocystis* sp. LEGE07211) and E14032 H (*Oscillatoria limnetica* LEGE00237) exerted the most substantial effects on adipogenesis. These are derived from two strains of distinct classes of cyanobacteria, *Synechocystis* sp. LEGE07211 belongs to the sub-class *Chroococales* and *Oscillatoria limnetica* LEGE00237 to the sub-class *Oscillatoriales*. Researchers have pointed to more complex bacteria (from sub-class *Oscillatoriales*, *Nostocales* or *Stigonematales*) as more prolific in secondary metabolites. However, our bioassays show that simpler cyanobacteria can also possess novel secondary metabolites with pharmaceutical and biotechnological potential. This is in agreement with a previous work done at our laboratory (Costa et al. 2014). *Synechocystis* sp. is a unicellular picoplanktonic cyanobacterial genus. Strains of this genus have been identified to have a high carotenoid content (mainly β -carotene and zeaxanthin) and thus could present anti-oxidant properties.

Several fatty acids and volatile compounds with antimicrobial activity, and pigments were already isolated from this genus (Plaza et al. 2010). However, no bioactive anti-obesity compounds were identified yet.

The bioactive fraction was chosen for further fractionation through SPE and resulted in 10 new fractions (E14031D 1-10). In order to overcome the existing differences in cell number per well, an extra well was added that was used for cell counting after trypsinization in the end of the experiment. Cell number registered for each treatment varied between 1.9 and 8.5×10^5 cells/well. In comparison, the addition of the cell count showed a more pronounced effect of the sub-fraction E14031 D 7, the most active sub-fraction of the group (Figure 38). From imaging, E14031 D 7 also exerted an apparent evenly differentiation of the pre-adipocytes (Figure 39 (1)).

Sub-fraction E14031 D 7 was eluted in 20% EtOAc (n-Hexane) and has a blue color in this solution. Analysis of the ^1H NMR spectra indicated us this is a fairly simple sub-fraction and thus HPLC separation will be performed. Phycocyanin is a known blue pigment with anti-diabetic properties and could be suspected to be present in our cyanobacterial extracts. Most of the described optimized techniques for phycocyanin isolation are, briefly, aqueous extraction and precipitation of the protein in ammonium sulfate followed by centrifugation, ultracentrifugation or filtration (Furuki et al. 2003; Gantar et al. 2012; Kumar et al. 2014; Chethana et al. 2015). The aqueous extract we prepared in our work should contain the protein extract of the cyanobacterial strains. However, we assume that phycocyanin was not solubilized in our organic solvent mixture dichloromethane:methanol (2:1) and is not present in this fraction. Further tests will be necessary to characterize the composition of our active E14031 D7 sub-fraction.

In our *in vitro* tests, we assayed the activity of resveratrol, a phenol known for its biological and pharmacological properties, and two thiazolidinediones: troglitazone and rosiglitazone. Resveratrol caused a decrease on adipogenesis of 51.82 ± 2.43 % compared to the control (Figure 37 (6)), as well as cell death and detachment after the 12 day exposure at a concentration of $100 \mu\text{M}$. This is in agreement with the literature, which described an inhibition of adipogenesis (Zhang et al. 2012; Santos et al. 2014) and apoptosis on doses above $10 \mu\text{M}$ of resveratrol in differentiating cells (Hu et al. 2014; S. Chen et al. 2015). Hu et al. (2014) described, however, that under physiologically achievable doses (1 and $10 \mu\text{M}$) adipogenesis is enhanced, as well as increases of the glucocorticoid receptor and PPAR γ , possibly synergistic. Resveratrol exposure in 3T3-L1 pre-adipocytes, however, did not affect cell viability at concentrations up to 1.8 mM (Zhang et al. 2012).

The same pattern was obtained for several cyanobacterial fractions, as for E14026 A (Figure 30) and E14067 A (Figure 35) that inhibited cell differentiation. Cell death and cell detachment were observed in response to the exposure to fractions E14035 H, E14028 B, F, H and J, and E14032 E, F and G at a concentration of 20 $\mu\text{g mL}^{-1}$.

Thiazolidinediones are recognized as beneficial molecules for the treatment of T2DM (Oakes et al., 1994, Young et al., 1995, Petersen et al., 2000, Smith et al., 2000), acting as agonists of PPAR γ . PPAR γ controls many cellular events as adipocyte differentiation and lipid, carbohydrate and amino acid metabolism. Thiazolidinediones are heterocyclic organic compounds that share a thiazolidine, a saturated ring with a thioether and an amine group in the 1 and 3 positions, respectively (Schoonjans & Auwerx 2000). They are able to reverse the insulin resistance by restoring insulin-induced translocation of the glucose transporter GLUT4 towards the cell membrane in adipocytes. This results in a lowered blood glucose levels, beneficial to T2DM patients (Anil Kumar & Marita 2000; Martinez et al. 2010; Karimfar et al. 2015). 3T3-L1 pre-adipocytes treated with troglitazone also showed enhancements on the rate of differentiation of adipocytes, by increasing the expression of the adipocyte-specific transcription factor, C/EBP α , as well as increased uptake of glucose (Tafari 1996). In addition, these molecules seem to have anti-inflammatory activity, since NF- κ B levels were decreased after administration of rosiglitazone in patients (Pan et al. 2014; Chen et al. 2015). Our results were in agreement with the literature, balanced increases of adipocyte differentiation and lipid accumulation occurred when cells were treated for 12 days with 0.2 μM of troglitazone and rosiglitazone.

During our cyanobacterial screening, many fractions could act as potential PPAR γ agonists, as remarkable increases in adipogenesis were observed after a 12 day exposure to 20 $\mu\text{g mL}^{-1}$. Once a cyanobacterial compound is isolated and characterized, future studies will focus on the mechanistic pathway through which these compounds are able to exert their effects. Previous studies have used this approach on natural product discovery: PUFAs from fish oil (Flachs & Hal 2005), dysidine, a sesquiterpene quinone from the Hainan sponge *Dysidea villosa* (Zhang et al. 2009), two plastoquinones, sargaquinoic acid and sargahydroquinoic acid, from *Sargassum yezoense* (Kim et al. 2008) and the extract of *Alnus incana* (Martineau et al. 2010) acted as agonists for PPAR γ and led to increased adipogenesis. Although most research on natural compound discovery focuses on the inhibition of weight gain and adipogenesis, this approach is beneficial for the enhancement of glucose tolerance, for the prevention of fat accumulation in non-fat depots, and to ameliorate metabolic complications.

The combination of both activities, the pro-proliferative and pro-adipogenic effect on 3T3-L1, is also beneficial since the recruitment of pre-adipocytes and the presence of competent adipocytes are equally important, as discussed before. During our bioactivity guided fractionation for pro-proliferative effects on 3T3-L1 adipocytes, 11 fractions resulting from the flash chromatography (E14028 I7 1-11) were tested in pre-adipocytes in order to evaluate their effects in adipogenesis (Figure 36). Our fractions of interest, E14028 I7 7, 8A and 9, showed increases in adipogenesis compared to the solvent control. The highest score was obtained for E14028 I7 7 (Figure 37 (4)). The bioactive fractions E14031D and E14032 H increased the adipogenesis and no changes were registered in the proliferation rate, compared to the solvent control. These are promising activities in this context. The approach on drug discovery can focus on peripheral or central targets, although a combined approach can lead to more efficient strategies (Dietrich & Horvath 2012). A combination therapy, with one compound increasing pre-adipocyte proliferation and another compound increasing adipogenesis, could be a valuable tool for the disease. However, since these two endpoints are tightly connected, different natural cyanobacterial compounds can be obtained from this research work, with different mechanism of action.

5.3. Methodology for the analysis of cell proliferation

Two tests were performed routinely for the screening assay on cell proliferation, one measuring protein content that correlates with cell proliferation (SRB assay) and another one used for measuring the metabolic activity (MTT assay). Sulforhodamine B is a red dye used for protein stain. This amino heterocyclic dye binds to basic amino-acid residues, under low pH conditions. The use of tris-HCl (pH 10.5) results in the dissociation of the dye and suitable spectrophotometric analysis (Vichai & Kirtikara 2006). This method has been used for cytotoxicity assays and cell proliferation assessment (Teixeira et al. 2010b; Faria et al. 2010). The MTT assay requires cellular metabolic activity to reduce the tetrazole ring of MTT into purple formazan crystals. Conversion of the tetrazolium ring to the formazan crystals is mainly performed by mitochondrial succinic dehydrogenases, the crystals accumulating in endosomal and/or lysosomal compartments, being later transported out of the cell by exocytosis (Liu et al. 1997).

The used of these two assays is beneficial and helps avoiding technical misinterpretation. Some compounds that affect pH can directly interfere with MTT-formazan absorption (λ_{max}), without compromising cell viability, or with the cell density itself (Plumb et al. 1989), which does not happen for SRB assay. The MTT assay is classically used for cell viability but can also be

a measure of cell proliferation and metabolic activity (Sieuwert et al. 1995; Grenho et al. 2015; Lee et al. 2015), although it may overestimate the number of viable cells, when compared to other methods as trypan blue determinations (Wang et al. 2010). Previous studies indicated that SRB assay has a smaller variability on cell enumeration than the MTT assay (van Tonder et al. 2015) and has been described to provide a better linearity with cell number (Keepers et al. 1991) which are major advantages for scientific research and medicine. Due to its high reproducibility, at the present, the SRB assay is preferred by the National Cancer Institute in the USA as a high-throughput assay, used widely for compound screening (Shoemaker 2006). Nonetheless, MTT assay is still considered as a golden standard, an assay similarly suitable for high-throughput screening (Hamid et al. 2004) and important in this context of metabolic research.

To understand the effects of cyanobacterial fractions in the 3T3-L1 pre-adipocytes we further compared selected results obtained by MTT and SRB to the BrdU ELISA assay. BrdU ELISA is a frequently used semi-quantitative method applied to measure cell proliferation, as an alternative to the radioactive nucleoside ^3H -thymidine labelling in newly synthesized DNA. The colorimetric assay based on the anti-BrdU-POD reaction is suitable for routine screening for studies that need to elaborate on cell proliferation mechanisms and regulation. BrdU is the non-radioactive chemical analog of ^3H -thymidine. This assay involves the incorporation of BrdU into newly synthesized DNA, a DNA denaturation step and immobilization with an anti-BrdU antibody and quantification of incorporated BrdU through a peroxidase-conjugated anti-BrdU antibody (Magaud et al. 1988; Muir et al. 1990). This technique is a rapid and sensitive quantification of DNA synthesis through a colorimetric detection, suitable for experiments in cell lines, and *in vivo* and *ex vivo* experiments (Behl et al. 2006). For our fast growing cells, a 2 hour exposure for the BrdU incorporation was found to be necessary to establish the minimum interval for the maintenance of the linearity of the results – between 0.5 to 1.5 absorbance units.

BrdU ELISA assay confirmed that the selected cyanobacterial fractions are commonly beneficial for cell fitness and proliferation (Figure 16). A similar pattern to the one obtained for the regular tests with MTT and SRB assays is also observed, in which most of the pro-proliferative effects are more evident at 48 hours of exposure.

Comparing these three assays (Table 11), both SRB and MTT assay are important to the study of proliferation of pre-adipocytes. The most active fractions on proliferation through BrdU ELISA assay (E14035 B and E14032 H) had a concomitant increased activity through MTT assay, where an increase of metabolic activity is observed. However, for fractions E14067 D

and E14067 F, BrdU ELISA was in agreement with the results obtained through the SRB assay, but not with the MTT assay (Table 11).

Looking at the average effect of exposure of the pre-adipocytes to DMSO (Table12), the MTT underestimated the inhibitory activity of 1% DMSO exposure in cell metabolism, a phenomenon already described for this assay (Wang et al. 2010). However, for the 20% DMSO exposure, where cell death is expected, the MTT assay was more sensitive and presented closer values to the ones obtained with the BrdU ELISA assay. This can be explained since SRB does not distinguish dead cells from live cells, whereas MTT only detects viable cells.

Summarizing, BrdU is a more sensitive assay but comparatively more expensive as it uses an ELISA detection. This makes it not suitable for the medium scale screening of cyanobacterial compounds, but aids in the confirmation of results. Bioactivity may be detected either through MTT or SRB assays, although BrdU was seen to be generally in accordance with the SRB assay. The use of both methods seem to be a cost-effective methodology to screen bioactive compounds with proliferative activity.

5.4. Bioactivity-guided fractionation for compound discovery

Bioactivity guided-fractionation is a classic method for novel natural compound discovery that relies on extract preparation, fractionation, biological screening with relevant assays and the isolation, purification and structural elucidation of the active compounds. This process has been very helpful for the discovery of compounds for specific targets, usually with the aid of chromatographic techniques as liquid chromatography, HPLC, liquid-liquid or solid phase extraction (Oldoni et al. 2016). Bioactivity guided fractionation can be time consuming and expensive, since high volumes of solvents are used. Moreover, this process can often result in the elucidation of a compound already described in literature and has the limitation of occurrence of synergisms and antagonisms between compounds that can ultimately result in the loss of activity or the blocking of the activity of a compound, respectively. Another disadvantage is that this method is resource consuming. After each step of fractionation, preparation of exposure solutions is needed, which results in losses of biomass of the sub-fractions. In case of bioassay failure or need for concentration readjustment, extra mass for solution preparation is required. However, this approach ensures that a compound with a specific biological activity is identified. This is the case of the discovery of hexapeptides with anti-fouling activity (Sera et al. 2003), proanthocyanidins with anti-oxidant activity (Oldoni et al. 2016), α -glucosidase Inhibitors from *Vauquelinia corymbosa* (Flores-Bocanegra et al. 2015), lignans from the root of *Machilus obovatifolia* (Lin et al. 2015), among others.

Other approaches allow the identification of novel secondary metabolites. Some research is based upon the identification of new compounds and the consequent purification from a mother mixture without the previous knowledge about bioactivity. Isolated compounds with chemical identities of interest are further screened for specific bioactivities, a process that contrasts with the classic bioactivity guided-fractionation. This has resulted in the isolation of several natural products of interest from varied organisms as xanthenes from *Garcinia succifolia* (Duangrisai et al. 2014), sansalvamide, a cyclic depsipeptide from a marine fungus of the genus *Fusarium* (Belofsky et al. 1999).

Dereplication techniques is often used in novel natural compound discovery to discriminate previously characterized compounds in an early stage of the research, before pursuing the process of isolation and characterization. This process is based on analyzing the spectroscopic features at the level of the crude extract and following the compounds with non-characterized features, increasing the potential to elucidate and identify novel secondary metabolites. The most common uses of dereplication are UV spectroscopy and mass spectrometry combined with HPLC (LC-UV/PDA, LC-MS) that allow the identification of certain structural classes and gives leads on the molecular weight and formula (Hubert et al. 2014).

Another recent approach is the on-line coupling of biochemical detection assays with HPLC. As reviewed in Malherbe et al. (2012), enzyme activity/affinity detection and receptor affinity detection are some types of biochemical detection that have been developed for the detection of acetylcholinesterase inhibitors, α -glucosidase inhibitors, liver cytochrome P450 ligands, HIV-protease inhibitors, estrogen receptor ligands, among others. This technique uses a conventional HPLC as a first step and then the mobile phase gets separated into two distinct branches: one to the biochemical detector and another one for substance detection (e.g. UV detector) and identification (e.g. ESI-TOF-MS). Some limitations to these processes can be the lack of sensitivity for bioactivity testing, the bioactivity can be too complex to be automated (poor availability or stability of biocomponents and targets) and, as this is a complex setup, there is a need for an extensive and expensive method development.

Intricate and complex models can be used in mass identification of novel compounds. However, they often lack in flexibility and a previous method development is needed, which is time consuming. In this perspective, a bioactivity guided fractionation is a more versatile technique. In our lab, this approach allows to find novel secondary metabolites with a bigger range of bioactivities and to explore the cyanobacterial biotechnological and pharmaceutical potential.

6. Conclusion

The present work aimed to identify novel cyanobacterial secondary metabolites that could be useful for the treatment of the metabolic complications of obesity. 60 fractions derived from six cyanobacterial strains were screened for activity on preadipocyte proliferation, metabolic activity and adipogenesis.

The results showed that the selected fractions of cyanobacteria possess activities that can aid in the treatment of obesity and two distinct groups of compounds are to be isolated. Sub-fractions of *Planktothrix planctonica* LEGEXX280 (E14028 I), from *Oscillatoriales*, and *Aphanizomenon* sp. LEGE03283 (E14035 B), from *Nostocales*, exerted strong effects in proliferative and metabolic activity of 3T3-L1 pre-adipocytes. A sub-fraction from *Synechocystis* sp. LEGE07211 (E14031 D), a more simple cyanobacteria belonging to the *Chroococales* genus, also showed interesting activity in the modulation of adipogenesis of murine pre-adipocytes. These results confirm that unicellular free-living species of cyanobacteria are prolific in secondary metabolites with bioactivity of interest.

The polar bioactive compound present in E14028 I7 8A+9 E7 J1 is now isolated and ready for chemical identification and structure elucidation with the aid of mass spectrometry and NMR spectroscopy, respectively. Sub-fraction E14031 D7 is being processed through HPLC, and further isolation of the bioactive compound will follow. We expect to obtain at least two bioactive secondary metabolites from this work. Once the pure bioactive compounds are obtained and fully characterized, our future work will focus on the mode of action of these compounds using molecular biological tools.

These compounds may be significant tools to treat the metabolic complications of obesity, through the increase pre-adipocytes available in the adipose tissue and through the increase of differentiated and competent adipocytes to accommodate surplus energy. Further tests on adipocytes and other adipose tissue related cell lines will allow us to characterize the effects of the compound(s) on obesity-related co-morbidities in more details.

To the best of our knowledge, this is the first work focusing on bioactivity guided isolation of novel cyanobacterial secondary metabolites for the treatment of obesity and obesity related co-morbidities.

7. References

- Ahmad, R.S., Butt, M.S., Sultan, M.T., Mushtaq, Z., Ahmad, S., Dewanjee, S., De Feo, V. & Zia-Ul-Haq, M., 2015. Preventive role of green tea catechins from obesity and related disorders especially hypercholesterolemia and hyperglycemia. *Journal of translational medicine*, 13(1), p.79.
- Anil Kumar, K.L. & Marita, A.R., 2000. Troglitazone prevents and reverses dexamethasone induced insulin resistance on glycogen synthesis in 3T3 adipocytes. *British journal of pharmacology*, 130(2), pp.351–358.
- Ansell, S.M., 2014. Brentuximab vedotin. *Blood*, 124(22), pp.3197–3200.
- Baptista, T., 1999. Body weight gain induced by antipsychotic drugs: mechanisms and management. *Acta psychiatrica Scandinavica*, 100(1), pp.3–16.
- Barbatelli, G., Murano, I., Madsen, L., Hao, Q., Jimenez, M., Kristiansen, K., Giacobino, J.P., De Matteis, R. & Cinti, S., 2010. The emergence of cold-induced brown adipocytes in mouse white fat depots is determined predominantly by white to brown adipocyte transdifferentiation. *American journal of physiology. Endocrinology and metabolism*, 298(6), pp.E1244–E1253.
- Bart, J.C.J., 2005. *Additives in Polymers: Industrial Analysis and Applications*,
- Bartness, T.J., Vaughan, C.H. & Song, C.K., 2010. Sympathetic and sensory innervation of brown adipose tissue. *International journal of obesity (2005)*, 34 Suppl 1, pp.S36–S42.
- Bays, H. & Dujovne, C., 2002. Anti-obesity drug development. *Expert opinion on investigational drugs*, 11(9), pp.1189–1204.
- Behl, B., Klos, M., Serr, M., Ebert, U., Janson, B., Drescher, K., Gross, G. & Schoemaker, H., 2006. An ELISA-based method for the quantification of incorporated BrdU as a measure of cell proliferation in vivo. *Journal of Neuroscience Methods*, 158(1), pp.37–49.
- Belofsky, G.N., Jensen, P.R. & Fenical, W., 1999. Sansalvamide: A new cytotoxic cyclic depsipeptide produced by a marine fungus of the genus *Fusarium*. *Tetrahedron Letters*, 40(15), pp.2913–2916. Available at: <http://www.sciencedirect.com/science/article/pii/S0040403999003937> [Accessed September 1, 2015].
- Blüher, M., 2014. Adipokines - removing road blocks to obesity and diabetes therapy. *Molecular Metabolism*, 3(January), pp.230–240.
- Boone, D.R. & Castenholz, R.W., 2001. The Archaea and the Deeply Branching and Phototrophic Bacteria. In *Bergey's Manual of Systematic Bacteriology*. p. 1 (2).

- Bush, J.A., Kraemer, W.J., Mastro, A.M., Triplett-McBride, N.T., Volek, J.S., Putukian, M., Sebastianelli, W.J. & Knuttgen, H.G., 1999. *Exercise and recovery responses of adrenal medullary neurohormones to heavy resistance exercise.*
- Butler, M.S., Robertson, A.A.B. & Cooper, M.A., 2014. Natural product and natural product derived drugs in clinical trials. *Nat. Prod. Rep.*, 31, pp.1612–1661. Available at: <http://dx.doi.org/10.1038/nrclinonc.2011.62>.
- Byun, M.R., Kim, A.R., Hwang, J.-H., Sung, M.K., Lee, Y.K., Hwang, B.S., Rho, J.-R., Hwang, E.S. & Hong, J.-H., 2012. Phorbaketal A stimulates osteoblast differentiation through TAZ mediated Runx2 activation. *FEBS letters*, 586(8), pp.1086–1092.
- Catchpole, O., Mitchell, K., Bloor, S., Davis, P. & Suddes, A., 2015. Antiproliferative Activity of New Zealand Propolis and Phenolic Compounds vs Human Colorectal Adenocarcinoma Cells. *Fitoterapia*.
- Catta-Preta, M., Mendonca, L.S., Fraulob-Aquino, J., Aguila, M.B. & Mandarin-de-Lacerda, C.A., 2011. A critical analysis of three quantitative methods of assessment of hepatic steatosis in liver biopsies. *Virchows Archiv: an international journal of pathology*, 459(5), pp.477–85. Available at: <http://www.ncbi.nlm.nih.gov/pubmed/21901430>.
- Chatzigeorgiou, a., Kandaraki, E., Papavassiliou, a. G. & Koutsilieris, M., 2014. Peripheral targets in obesity treatment: A comprehensive update. *Obesity Reviews*, (June), pp.487–503.
- Chen, S., Zhou, N., Zhang, Z., Li, W. & Zhu, W., 2015. Resveratrol induces cell apoptosis in adipocytes via AMPK activation. *Biochemical and biophysical research communications*, 457(4), pp.608–613.
- Chen, X., Liu, X., Wang, Q., Zhang, M., Guo, M., Liu, F., Jiang, W. & Zhou, L., 2015. Pioglitazone inhibits angiotensin II-induced atrial fibroblasts proliferation via NF-kappaB/TGF-beta1/TRIF/TRAF6 pathway. *Experimental cell research*, 330(1), pp.43–55.
- Cheong, S.H., Kim, M.Y., Sok, D.-E., Hwang, S.-Y., Kim, J.H., Kim, H.R., Lee, J.H., Kim, Y.-B. & Kim, M.R., 2010. Spirulina prevents atherosclerosis by reducing hypercholesterolemia in rabbits fed a high-cholesterol diet. *Journal of nutritional science and vitaminology*, 56(1), pp.34–40.
- Chethana, S., Nayak, C.A., Madhusudhan, M.C. & Raghavarao, K.S.M.S., 2015. Single step aqueous two-phase extraction for downstream processing of C-phycoerythrin from *Spirulina platensis*. *Journal of food science and technology*, 52(4), pp.2415–2421.
- Cheung, B.M.Y., Cheung, T.T. & Samaranyake, N.R., 2013. Safety of antiobesity drugs. *Therapeutic advances in drug safety*, 4(4), pp.171–181.
- Cohen, Z., Reungjitchachawali, M., Siangdung, W. & Tanticharoen, M., 1993. Production and partial purification of γ -linolenic acid and some pigments from *Spirulina platensis*. *Journal of Applied Phycology*, 5(1), pp.109–115. Available at: <http://dx.doi.org/10.1007/BF02182428>.

- Costa, M., Garcia, M., Costa-Rodrigues, J., Costa, M.S., Ribeiro, M.J., Fernandes, M.H., Barros, P., Barreiro, A., Vasconcelos, V. & Martins, R., 2014. Exploring bioactive properties of marine cyanobacteria isolated from the Portuguese coast: High potential as a source of anticancer compounds. *Marine Drugs*, 12(December 2013), pp.98–114.
- Cruz-Rivera, E. & Paul, V.J., 2007. Chemical deterrence of a cyanobacterial metabolite against generalized and specialized grazers. *Journal of chemical ecology*, 33(1), pp.213–217.
- D'Esposito, V., Passaretti, F., Hammarstedt, A., Liguoro, D., Terracciano, D., Molea, G., Canta, L., Miele, C., Smith, U., Beguinot, F. & Formisano, P., 2012. Adipocyte-released insulin-like growth factor-1 is regulated by glucose and fatty acids and controls breast cancer cell growth in vitro. *Diabetologia*, 55(10), pp.2811–2822.
- Deng, R. & Chow, T.-J., 2010. Hypolipidemic, antioxidant, and antiinflammatory activities of microalgae *Spirulina*. *Cardiovascular therapeutics*, 28(4), pp.e33–45.
- Dietrich, M.O. & Horvath, T.L., 2012. Limitations in anti-obesity drug development: the critical role of hunger-promoting neurons. *Nature Reviews Drug Discovery*, 11(9), pp.675–691.
- Duangsrirai, S., Choowongkamon, K., Bessa, L., Costa, P., Amat, N. & Kijjoa, A., 2014. Antibacterial and EGFR-Tyrosine Kinase Inhibitory Activities of Polyhydroxylated Xanthenes from *Garcinia succifolia*. *Molecules*, 19(12), pp.19923–19934. Available at: <http://www.mdpi.com/1420-3049/19/12/19923/>.
- Ehrenkranz, J.R.L., Lewis, N.G., Kahn, C.R. & Roth, J., 2005. Phlorizin: a review. *Diabetes/metabolism research and reviews*, 21(1), pp.31–38.
- Eisenhut, M., 2012. Inflammation-induced Desensitization of β -Receptors in Acute Lung Injury. *American Journal of Respiratory and Critical Care Medicine*, 185(8), p.894. Available at: <http://dx.doi.org/10.1164/ajrccm.185.8.894>.
- Ekanem, A.P., Wang, M., Simon, J.E. & Moreno, D.A., 2007. Antiobesity properties of two African plants (*Afromomum meleguetta* and *Spilanthes acmella*) by pancreatic lipase inhibition. *Phytotherapy Research*, 21, pp.1253–1255.
- Eom, S.H., Lee, M.S., Lee, E.W., Kim, Y.M. & Kim, T.H., 2013. Pancreatic lipase inhibitory activity of phlorotannins isolated from *Eisenia bicyclis*. *Phytotherapy Research*, 27(1), pp.148–151.
- Ernst, B., Hitzfeld, B. & Dietrich, D., 2001. Presence of *Planktothrix* sp. and cyanobacterial toxins in Lake Ammersee, Germany and their impact on whitefish (*Coregonus lavaretus* L.). *Environmental Toxicology*, 16(6), pp.483–488.
- Esposito, K., Pontillo, A., Ciotola, M., Di Palo, C., Grella, E., Nicoletti, G. & Giugliano, D., 2002. Weight loss reduces interleukin-18 levels in obese women. *Journal of Clinical Endocrinology and Metabolism*, 87(8), pp.3864–3866.
- Euler, U.S. & Eliassen, R., 1967. Prostaglandins. *New York: Academic Press*.

- Fan, Y.Y. & Chapkin, R.S., 1998. Importance of dietary gamma-linolenic acid in human health and nutrition. *The Journal of nutrition*, 128(9), pp.1411–1414.
- Faria, A., Pestana, D., Teixeira, D., De Freitas, V., Mateus, N. & Calhau, C., 2010. Blueberry anthocyanins and pyruvic acid adducts: Anticancer properties in breast cancer cell lines. *Phytotherapy Research*, 24(12), pp.1862–1869.
- Farmer, S.R., 2008. Molecular determinants of brown adipocyte formation and function. *Genes and Development*, 22(10), pp.1269–1275.
- Farooq, S.M., Boppana, N.B., Devarajan, A., Sekaran, S.D., Shankar, E.M., Li, C., Gopal, K., Bakar, S.A., Karthik, H.S. & Ebrahim, A.S., 2014. C-phycoyanin confers protection against oxalate-mediated oxidative stress and mitochondrial dysfunctions in MDCK cells. *PloS one*, 9(4), p.e93056.
- Finking, R. & Marahiel, M.A., 2004. Biosynthesis of nonribosomal peptides1. *Annual review of microbiology*, 58, pp.453–488.
- Finucane, O.M., Reynolds, C.M., McGillicuddy, F.C. & Roche, H.M., 2012. Insights into the role of macrophage migration inhibitory factor in obesity and insulin resistance. *The Proceedings of the Nutrition Society*, 71(4), pp.622–33. Available at: <http://www.ncbi.nlm.nih.gov/pubmed/22914223>.
- Flachs, A.P.P.J.J. & Hal, F., 2005. Polyunsaturated fatty acids of marine origin upregulate mitochondrial biogenesis and induce β -oxidation in white fat. , pp.2365–2375.
- Flatt, P.M., O'Connell, S.J., McPhail, K.L., Zeller, G., Willis, C.L., Sherman, D.H. & Gerwick, W.H., 2006. Characterization of the initial enzymatic steps of barbamide biosynthesis. *Journal of natural products*, 69(6), pp.938–944.
- Flores-Bocanegra, L., Perez-Vasquez, A., Torres-Piedra, M., Bye, R., Linares, E. & Mata, R., 2015. alpha-Glucosidase Inhibitors from *Vauquelinia corymbosa*. *Molecules (Basel, Switzerland)*, 20(8), pp.15330–15342.
- Foltin, R.W., Fischman, M.W. & Nautiyal, C., 1990. The effects of cocaine on food intake of baboons before, during, and after a period of repeated desipramine. *Pharmacology Biochemistry and Behavior*, 36(4), pp.869–874.
- Fowler, S.D. & Greenspan, P., 1985. Application of Nile red, a fluorescent hydrophobic probe, for the detection of neutral lipid deposits in tissue sections: comparison with oil red O. *The journal of histochemistry and cytochemistry : official journal of the Histochemistry Society*, 33(8), pp.833–836.
- Fox, C.S., Massaro, J.M., Hoffmann, U., Pou, K.M., Maurovich-Horvat, P., Liu, C.Y., Vasan, R.S., Murabito, J.M., Meigs, J.B., Cupples, L.A., D'Agostino, R.B. & O'Donnell, C.J., 2007. Abdominal visceral and subcutaneous adipose tissue compartments: Association with metabolic risk factors in the framingham heart study. *Circulation*, 116(1), pp.39–48.

- Furuki, T., Maeda, S., Imajo, S., Hiroi, T., Amaya, T., Hirokawa, T., Ito, K. & Nozawa, H., 2003. Rapid and selective extraction of phycocyanin from *Spirulina platensis* with ultrasonic cell disruption. *Journal of Applied Phycology*, 15(4), pp.319–324.
- Fusco, R., Galgani, M., Procaccini, C., Franco, R., Pirozzi, G., Fucci, L., Laccetti, P. & Matarese, G., 2010. Cellular and molecular crosstalk between leptin receptor and estrogen receptor- α in breast cancer: molecular basis for a novel therapeutic setting. *Endocrine-related cancer*, 17(2), pp.373–382.
- Gantar, M., Simović, D., Djilas, S., Gonzalez, W.W. & Miksovská, J., 2012. Isolation, characterization and antioxidative activity of C-phycocyanin from *Limnospira* sp. strain 37-2-1. *Journal of Biotechnology*, 159(1-2), pp.21–26.
- Gedaly, R., Galuppo, R., Musgrave, Y., Angulo, P., Hundley, J., Shah, M., Daily, M.F., Chen, C., Cohen, D.A., Spear, B.T. & Evers, B.M., 2013. PKI-587 and sorafenib alone and in combination on inhibition of liver cancer stem cell proliferation. *Journal of Surgical Research*, 185(1), pp.225–230.
- Geller, F.C., Teixeira, M.R., Pereira, A.B.D., Dourado, L.P.A., Souza, D.G., Braga, F.C. & Simoes, C.M.O., 2015. Evaluation of the Wound Healing Properties of *Hancornia speciosa* Leaves. *Phytotherapy research : PTR*.
- Geloen, A., Roy, P.E. & Bukowiecki, L.J., 1989. Regression of white adipose tissue in diabetic rats. *American Journal of Physiology - Endocrinology and Metabolism*, 257(4), pp.E547–E553. Available at: <http://ajpendo.physiology.org/content/257/4/E547.abstract>.
- Gerwick, W.H., Coates, R.C., Engene, N., Gerwick, L., Grindberg, R. V, Jones, A.C. & Sorrels, C.M., 2008. Giant Marine Cyanobacteria Produce Exciting Potential Pharmaceuticals. *Microbe*, 3(6), pp.277–284.
- Gerwick, W.H. & Moore, B.S., 2012. Lessons from the past and charting the future of marine natural products drug discovery and chemical biology. *Chemistry & biology*, 19(1), pp.85–98.
- Gong, Z., Huang, C., Sheng, X., Zhang, Y., Li, Q., Wang, M.-W., Peng, L. & Zang, Y.Q., 2009. The Role of Tanshinone IIA in the Treatment of Obesity through Peroxisome Proliferator-Activated Receptor γ Antagonism. *Endocrinology*, 150(1), pp.104–113. Available at: <http://dx.doi.org/10.1210/en.2008-0322>.
- Gonzalez de Rivera, C., Miranda-Zamora, R., Diaz-Zagoya, J.C. & Juarez-Oropeza, M.A., 1993. Preventive effect of *Spirulina maxima* on the fatty liver induced by a fructose-rich diet in the rat, a preliminary report. *Life sciences*, 53(1), pp.57–61.
- Gonzalez, R., Rodriguez, S., Romay, C., Ancheta, O., Gonzalez, A., Armesto, J., Ramirez, D. & Merino, N., 1999. Anti-inflammatory activity of phycocyanin extract in acetic acid-induced colitis in rats. *Pharmacological research : the official journal of the Italian Pharmacological Society*, 39(1), pp.55–59.
- Green, H. & Meuth, M., 1974. An established pre-adipose cell line and its differentiation in culture. *Cell*, 3(2), pp.127–133. Available at:

<http://www.sciencedirect.com/science/article/pii/S092867474901160> [Accessed January 12, 2015].

- Grenho, L., Barros, J., Ferreira, C., Santos, V.R., Monteiro, F.J., Ferraz, M.P. & Cortes, M.E., 2015. *In vitro* antimicrobial activity and biocompatibility of propolis containing nanohydroxyapatite. *Biomedical Materials*, 10(2), p.025004. Available at: <http://stacks.iop.org/1748-605X/10/i=2/a=025004?key=crossref.9cca1c39a6d297f2f7005d7c0fa8c4dc>.
- Guilherme, A., Virbasius, J. V, Puri, V. & Czech, M.P., 2008. Adipocyte dysfunctions linking obesity to insulin resistance and type 2 diabetes. *Nature reviews. Molecular cell biology*, 9(5), pp.367–377.
- Gupta, R.K., Mepani, R.J., Kleiner, S., Lo, J.C., Khandekar, M.J., Cohen, P., Frontini, A., Bhowmick, D.C., Ye, L., Cinti, S. & Spiegelman, B.M., 2012. Zfp423 expression identifies committed preadipocytes and localizes to adipose endothelial and perivascular cells. *Cell Metabolism*, 15(2), pp.230–239.
- Gustafson, B., Gogg, S., Hedjazifar, S., Jenndahl, L., Hammarstedt, A. & Smith, U., 2009. Inflammation and impaired adipogenesis in hypertrophic obesity in man. *AJP: Endocrinology and Metabolism*, 297(5), pp.E999–E1003.
- Gustafson, B., Hammarstedt, A., Hedjazifar, S. & Smith, U., 2013. Restricted adipogenesis in hypertrophic obesity: The role of WISP2, WNT, and BMP4. *Diabetes*, 62(9), pp.2997–3004.
- Gutiérrez, M., Tidgewell, K., Capson, T.L., Engene, N., Almanza, A., Schemies, J., Jung, M. & Gerwick, W.H., 2010. Malyngolide dimer, a bioactive symmetric cyclodepside from the panamanian marine cyanobacterium *lyngbya majuscula*. *Journal of Natural Products*, 73(4), pp.709–711.
- Hainer, V., Kabrnova, K., Aldhoon, B., Kunesova, M. & Wagenknecht, M., 2006. Serotonin and norepinephrine reuptake inhibition and eating behavior. In *Annals of the New York Academy of Sciences*. pp. 252–269.
- Hamid, R., Rotshteyn, Y., Rabadi, L., Parikh, R. & Bullock, P., 2004. Comparison of alamar blue and MTT assays for high through-put screening. *Toxicology in vitro: an international journal published in association with BIBRA*, 18(5), pp.703–710.
- Han, S., Oh, K.S., Yoon, Y., Park, J.S., Park, Y.S., Han, J.H., Jeong, A.L., Lee, S., Park, M., Choi, Y. a., Lim, J.S. & Yang, Y., 2011. Herbal extract TH1 improves metabolic abnormality in mice fed a high-fat diet. *Nutrition Research and Practice*, 5(3), pp.198–204.
- Henninger, a. M.J., Eliasson, B., Jenndahl, L.E. & Hammarstedt, A., 2014. Adipocyte Hypertrophy, Inflammation and Fibrosis Characterize Subcutaneous Adipose Tissue of Healthy, Non-Obese Subjects Predisposed to Type 2 Diabetes. *PLoS ONE*, 9(8), p.e105262. Available at: <http://dx.plos.org/10.1371/journal.pone.0105262>.

- Himms-Hagen, J., Melnyk, A., Zingaretti, M.C., Ceresi, E., Barbatelli, G. & Cinti, S., 2000. Multilocular fat cells in WAT of CL-316243-treated rats derive directly from white adipocytes. *American journal of physiology. Cell physiology*, 279(3), pp.C670–C681.
- Hirata, Y. & Uemura, D., 1986. Halichondrins - antitumor polyether macrolides from a marine sponge. *Pure and Applied Chemistry*, 58(5), pp.701–710.
- Van Der Horst, D.J., Van Marrewijk, W.J.A., Vullings, H.G.B. & Diederens, J.H.B., 1999. Metabolic neurohormones: Release, signal transduction and physiological responses of adipokinetic hormones in insects. *European Journal of Entomology*, 96(3), pp.299–308.
- Hu, P., Zhao, L. & Chen, J., 2014. Physiologically achievable doses of resveratrol enhance 3T3-L1 adipocyte differentiation. *European Journal of Nutrition*.
- Hubert, J., Nuzillard, J.M., Purson, S., Hamzaoui, M., Borie, N., Reynaud, R. & Renault, J.H., 2014. Identification of natural metabolites in mixture: A pattern recognition strategy based on ¹³C NMR. *Analytical Chemistry*, 86, pp.2955–2962.
- Ishibashi, J. & Seale, P., 2010. Medicine. Beige can be slimming. *Science (New York, N.Y.)*, 328(5982), pp.1113–1114.
- Iwata, K., Inayama, T. & Kato, T., 1990. Effects of *Spirulina platensis* on plasma lipoprotein lipase activity in fructose-induced hyperlipidemic rats. *Journal of nutritional science and vitaminology*, 36(2), pp.165–171.
- Jang, W.S. & Choung, S.Y., 2013. Antiobesity effects of the ethanol extract of *Laminaria japonica* Areshoung in high-fat-diet-induced obese rat. *Evidence-based Complementary and Alternative Medicine*, 2013.
- Jarouliya, U., Zacharia, J.A., Kumar, P., Bisen, P.S. & Prasad, G.B.K.S., 2012. Alleviation of metabolic abnormalities induced by excessive fructose administration in Wistar rats by *Spirulina maxima*. *The Indian journal of medical research*, 135, pp.422–428.
- De Jesus Raposo, M.F., de Moraes, R.M.S.C. & de Moraes, A.M.M.B., 2013. Bioactivity and Applications of Sulphated Polysaccharides from Marine Microalgae. *Marine Drugs*, 11(1), pp.233–252. Available at: <http://www.ncbi.nlm.nih.gov/pmc/articles/PMC3564169/>.
- John, U., Beszteri, B., Derelle, E., Van de Peer, Y., Read, B., Moreau, H. & Cembella, A., 2008. Novel Insights into Evolution of Protistan Polyketide Synthases through Phylogenomic Analysis. *Protist*, 159(1), pp.21–30.
- Jung, H.A., Jung, H.J., Jeong, H.Y., Kwon, H.J., Ali, M.Y. & Choi, J.S., 2014. Phlorotannins isolated from the edible brown alga *Ecklonia stolonifera* exert anti-adipogenic activity on 3T3-L1 adipocytes by downregulating C/EBP α and PPAR γ . *Fitoterapia*, 92, pp.260–269. Available at: <http://dx.doi.org/10.1016/j.fitote.2013.12.003>.
- Kadowaki, T. & Yamauchi, T., 2005. Adiponectin and adiponectin receptors. *Endocrine Reviews*, 26(3), pp.439–451.

- Karadeniz, F., Kim, J., Ahn, B.-N., Kwon, M. & Kong, C.-S., 2014. Effect of *Salicornia herbacea* on Osteoblastogenesis and Adipogenesis in Vitro. *Marine Drugs*, 12(10), pp.5132–5147. Available at: <http://www.mdpi.com/1660-3397/12/10/5132/>.
- Karimfar, M.H., Haghani, K., Babakhani, A. & Bakhtiyari, S., 2015. Rosiglitazone, but not epigallocatechin-3-gallate, attenuates the decrease in PGC-1alpha protein levels in palmitate-induced insulin-resistant C2C12 cells. *Lipids*, 50(6), pp.521–528.
- Kazakevich, Y. & LoBrutto, R., 2006. *HPLC for Pharmaceutical Scientists*,
- Keepers, Y.P., Pizao, P.E., Peters, G.J., van Ark-Otte, J., Winograd, B. & Pinedo, H.M., 1991. Comparison of the sulforhodamine B protein and tetrazolium (MTT) assays for in vitro chemosensitivity testing. *European journal of cancer (Oxford, England : 1990)*, 27(7), pp.897–900.
- Kim, C.Y., Le, T.T., Chen, C., Cheng, J.-X. & Kim, K.-H., 2011. Curcumin inhibits adipocyte differentiation through modulation of mitotic clonal expansion. *The Journal of nutritional biochemistry*, 22(10), pp.910–920.
- Kim, G.W., Lin, J.E., Blomain, E.S. & Waldman, S. a, 2014. Antiobesity pharmacotherapy: new drugs and emerging targets. *Clinical pharmacology and therapeutics*, 95(1), pp.53–66. Available at: <http://www.pubmedcentral.nih.gov/articlerender.fcgi?artid=4054704&tool=pmcentrez&rendertype=abstract>.
- Kim, J.-A., Karadeniz, F., Ahn, B.-N., Kwon, M.S., Mun, O.-J., Bae, M.J., Seo, Y., Kim, M., Lee, S.-H., Kim, Y.Y. & Kong, C.-S., 2015. Bioactive quinone derivatives from marine brown algae *Sargassum thunbergii* induce anti-adipogenic and pro-osteoblastogenic activities. *Journal of the Science of Food and Agriculture*, p.n/a–n/a. Available at: <http://doi.wiley.com/10.1002/jsfa.7148>.
- Kim, M.J., Chang, U.J. & Lee, J.S., 2009. Inhibitory effects of fucoidan in 3T3-L1 adipocyte differentiation. *Marine Biotechnology*, 11(5), pp.557–562.
- Kim, S.J., Park, J.H., Kim, D.H., Won, Y.H. & Maibach, H.I., 1998. Increased in vivo collagen synthesis and in vitro cell proliferative effect of glycolic acid. *Dermatologic surgery : official publication for American Society for Dermatologic Surgery [et al.]*, 24(10), pp.1054–1058.
- Kim, S.J. & Won, Y.H., 1998. The effect of glycolic acid on cultured human skin fibroblasts: cell proliferative effect and increased collagen synthesis. *The Journal of dermatology*, 25(2), pp.85–89.
- Kim, S.N., Choi, H.Y., Lee, W., Park, G.M., Shin, W.S. & Kim, Y.K., 2008. Sargaquinoic acid and sargahydroquinoic acid from *Sargassum yezoense* stimulate adipocyte differentiation through PPAR α/γ activation in 3T3-L1 cells. *FEBS Letters*, 582(23-24), pp.3465–3472. Available at: <http://dx.doi.org/10.1016/j.febslet.2008.09.011>.
- Ko, S.C., Lee, M., Lee, J.H., Lee, S.H., Lim, Y. & Jeon, Y.J., 2013. Dieckol, a phlorotannin isolated from a brown seaweed, *Ecklonia cava*, inhibits adipogenesis through AMP-

- activated protein kinase (AMPK) activation in 3T3-L1 preadipocytes. *Environmental Toxicology and Pharmacology*, 36(3), pp.1253–1260. Available at: <http://dx.doi.org/10.1016/j.etap.2013.10.011>.
- Komárek, J. & Jaroslava, K., 2004. Taxonomic review of the cyanoprokaryotic genera Planktothrix and Planktothricoides Taxonomický přehled rodů Planktothrix a. *Czech Phycology*, 4(4), pp.1–18. Available at: <http://scholar.google.com/scholar?hl=en&btnG=Search&q=intitle:Taxonomic+review+of+the+cyanoprokaryotic+genera+Planktothrix+and+Planktothricoides#0>.
- Kraus, R.M., Houmard, J. a, Kraus, W.E., Tanner, C.J., Pierce, J.R., Choi, M.D. & Hickner, R.C., 2012. Obesity, insulin resistance, and skeletal muscle nitric oxide synthase. *Journal of applied physiology (Bethesda, Md. : 1985)*, 113(5), pp.758–65. Available at: <http://www.pubmedcentral.nih.gov/articlerender.fcgi?artid=3472472&tool=pmcentrez&rendertype=abstract>.
- Ku, C.S., Yang, Y., Park, Y. & Lee, J., 2013. Health benefits of blue-green algae: prevention of cardiovascular disease and nonalcoholic fatty liver disease. *Journal of medicinal food*, 16(2), pp.103–11. Available at: <http://www.pubmedcentral.nih.gov/articlerender.fcgi?artid=3576896&tool=pmcentrez&rendertype=abstract>.
- Kumar, D., Dhar, D.W., Pabbi, S., Kumar, N. & Walia, S., 2014. Extraction and purification of C-phycoerythrin from *Spirulina platensis* (CCC540). *Indian Journal of Plant Physiology*, 19(2), pp.184–188.
- Kumar, S. & Alagawadi, K.R., 2013. Anti-obesity effects of galangin, a pancreatic lipase inhibitor in cafeteria diet fed female rats. *Pharmaceutical biology*, 51(5), pp.607–613.
- Lai, J.R., Koglin, A. & Walsh, C.T., 2006. Carrier protein structure and recognition in polyketide and nonribosomal peptide biosynthesis. *Biochemistry*, 45(50), pp.14869–14879.
- Leão, P.N., Costa, M., Ramos, V., Pereira, A.R., Fernandes, V.C., Domingues, V.F., Gerwick, W.H., Vasconcelos, V.M. & Martins, R., 2013. Antitumor Activity of Hierridin B, a Cyanobacterial Secondary Metabolite Found in both Filamentous and Unicellular Marine Strains. *PLoS ONE*, 8(7).
- Leão, P.N., Pereira, A.R., Liu, W.-T., Ng, J., Pevzner, P. a, Dorrestein, P.C., König, G.M., Vasconcelos, V.M. & Gerwick, W.H., 2010. Synergistic allelochemicals from a freshwater cyanobacterium. *Proceedings of the National Academy of Sciences of the United States of America*, 107(25), pp.11183–11188.
- Lee, J., Kim, D., Choi, J., Choi, H., Ryu, J.H., Jeong, J., Park, E.J., Kim, S.H. & Kim, S., 2012. Dehydrodiconiferyl alcohol isolated from *Cucurbita moschata* shows anti-adipogenic and anti-lipogenic effects in 3T3-L1 cells and primary mouse embryonic fibroblasts. *Journal of Biological Chemistry*, 287(12), pp.8839–8851.

- Lee, J.S., Lee, S.U., Che, C.-Y. & Lee, J.-E., 2015. Comparison of cytotoxicity and wound healing effect of carboxymethylcellulose and hyaluronic acid on human corneal epithelial cells. *International Journal of Ophthalmology*, 8(2), pp.215–221.
- Lee, O.H., Kwon, Y.I., Apostolidis, E., Shetty, K. & Kim, Y.C., 2011. Rhodiola-induced inhibition of adipogenesis involves antioxidant enzyme response associated with pentose phosphate pathway. *Phytotherapy Research*, 25(1), pp.106–115.
- Levene, A.P., Kudo, H., Armstrong, M.J., Thursz, M.R., Gedroyc, W.M., Anstee, Q.M. & Goldin, R.D., 2012. Quantifying hepatic steatosis - more than meets the eye. *Histopathology*, 60(6), pp.971–981.
- Li, C.R., Potenza, M.N., Lee, D.E., Planeta, B., Gallezot, J., Labaree, D., Henry, S., Nabulsi, N., Sinha, R., Ding, Y., Carson, R.E. & Neumeister, A., 2014. NeuroImage Decreased norepinephrine transporter availability in obesity: Positron Emission Tomography imaging with (S , S) - [11 C] O-methylreboxetine. *NeuroImage*, 86, pp.306–310. Available at: <http://dx.doi.org/10.1016/j.neuroimage.2013.10.004>.
- Liang, L.-F., Wang, T., Cai, Y.-S., He, W.-F., Sun, P., Li, Y.-F., Huang, Q., Tagliatalata-Scafati, O., Wang, H.-Y. & Guo, Y.-W., 2014. Brominated polyunsaturated lipids from the Chinese sponge *Xestospongia testudinaria* as a new class of pancreatic lipase inhibitors. *European Journal of Medicinal Chemistry*, 79, pp.290–297. Available at: <http://linkinghub.elsevier.com/retrieve/pii/S0223523414003122>.
- Lin, S.-Y., Ko, H.-H., Lee, S.-J., Chang, H.-S., Lin, C.-H. & Chen, I.-S., 2015. Biological Evaluation of Secondary Metabolites from the Root of *Machilus obovatifolia*. *Chemistry & biodiversity*, 12(7), pp.1057–1067.
- Liu, H., Jing, H., Wong, T.H.C. & Chen, B., 2014. Co-occurrence of phycocyanin- and phycoerythrin-rich *Synechococcus* in subtropical estuarine and coastal waters of Hong Kong. *Environmental Microbiology Reports*, 6(1), pp.90–99.
- Liu, Y., Peterson, D.A., Kimura, H. & Schubert, D., 1997. Mechanism of cellular 3-(4,5-dimethylthiazol-2-yl)-2,5-diphenyltetrazolium bromide (MTT) reduction. *Journal of neurochemistry*, 69(2), pp.581–593.
- Luesch, H., Chanda, S.K., Raya, R.M., DeJesus, P.D., Orth, A.P., Walker, J.R., Izipisua Belmonte, J.C. & Schultz, P.G., 2006. A functional genomics approach to the mode of action of apratoxin A. *Nature chemical biology*, 2(3), pp.158–167.
- Luesch, H., Yoshida, W.Y., Moore, R.E., Paul, V.J. & Corbett, T.H., 2001. Total structure determination of apratoxin A, a potent novel cytotoxin from the marine cyanobacterium *Lyngbya majuscula*. *Journal of the American Chemical Society*, 123(23), pp.5418–5423.
- MacDougald, O.A., Hwang, C.S., Fan, H. & Lane, M.D., 1995. Regulated expression of the obese gene product (leptin) in white adipose tissue and 3T3-L1 adipocytes. *Proceedings of the National Academy of Sciences of the United States of America*, 92(20), pp.9034–9037.

- Madigan, M., Martinko, J., Stahl, D. & Clark, D., 2010. *Brock Biology of Microorganisms (13th Edition)* 13th ed., Benjamin Cummings. Available at: citeulike-article-id:10894293.
- Magaud, J.P., Sargent, I. & Mason, D.Y., 1988. Detection of human white cell proliferative responses by immunoenzymatic measurement of bromodeoxyuridine uptake. *Journal of Immunological Methods*, 106(1), pp.95–100.
- Malherbe, C.J., de Beer, D. & Joubert, E., 2012. Development of on-line high performance liquid chromatography (HPLC)-biochemical detection methods as tools in the identification of bioactives. *International journal of molecular sciences*, 13(3), pp.3101–3133.
- Malloy, K.L., Villa, F. a., Engene, N., Matainaho, T., Gerwick, L. & Gerwick, W.H., 2011. Malyngamide 2, an oxidized lipopeptide with nitric oxide inhibiting activity from a Papua New Guinea marine cyanobacterium. *Journal of Natural Products*, 74(1), pp.95–98.
- Marques, C., Teixeira, D., Cunha, A., Meireles, M., Pestana, D., Keating, E., Calhau, C., Monteiro, R. & Faria, A., 2013. Methotrexate enhances 3T3-L1 adipocytes hypertrophy. *Cell Biology and Toxicology*, 29, pp.293–302.
- Martel, P. & Fantino, M., 1996. Mesolimbic dopaminergic system activity as a function of food reward: a microdialysis study. *Pharmacology, biochemistry, and behavior*, 53(1), pp.221–226.
- Martineau, L.C., Herve, J., Muhamad, A., Saleem, A., Harris, C.S., Arnason, J.T. & Haddad, P.S., 2010. Anti-adipogenic activities of *Alnus incana* and *Populus balsamifera* bark extracts, part I: sites and mechanisms of action. *Planta medica*, 76(13), pp.1439–1446.
- Martinez, L., Berenguer, M., Bruce, M.C., Le Marchand-Brustel, Y. & Govers, R., 2010. Rosiglitazone increases cell surface GLUT4 levels in 3T3-L1 adipocytes through an enhancement of endosomal recycling. *Biochemical Pharmacology*, 79(9), pp.1300–1309.
- Martins, R., Pereira, P., Welker, M., Fastner, J. & Vasconcelos, V.M., 2005. Toxicity of culturable cyanobacteria strains isolated from the Portuguese coast. *Toxicon: official journal of the International Society on Toxinology*, 46(4), pp.454–464.
- McTernan, P.G., Kusminski, C.M. & Kumar, S., 2006. Resistin. *Current opinion in lipidology*, 17(2), pp.170–175.
- Mendes, V., Monteiro, R., Pestana, D., Teixeira, D., Calhau, C. & Azevedo, I., 2008. Differentiation: Implication of Antiproliferative and Apoptotic Effects. *J. Agric. Food Chem.*, (56), pp.11631–11637.
- Mendes, V., Monteiro, R., Pestana, D., Teixeira, D., Calhau, C. & Azevedo, I., 2008. Xanthohumol influences preadipocyte differentiation: Implication of antiproliferative and apoptotic effects. *Journal of Agricultural and Food Chemistry*, 56(24), pp.11631–11637.
- Miranda, M.S., Cintra, R.G., Barros, S.B. & Mancini Filho, J., 1998. Antioxidant activity of the microalga *Spirulina maxima*. *Brazilian journal of medical and biological research* =

Revista brasileira de pesquisas medicas e biologicas / Sociedade Brasileira de Biofisica ... [et al.], 31(8), pp.1075–1079.

- Mitra, A. & Sept, D., 2004. Localization of the antimitotic peptide and depsipeptide binding site on beta-tubulin. *Biochemistry*, 43(44), pp.13955–13962.
- Miyashita, K., Nishikawa, S., Beppu, F., Tsukui, T., Abe, M. & Hosokawa, M., 2011. The allenic carotenoid fucoxanthin, a novel marine nutraceutical from brown seaweeds. *Journal of the Science of Food and Agriculture*, 91(7), pp.1166–1174.
- Muir, D., Varon, S. & Manthorpe, M., 1990. An enzyme-linked immunosorbent assay for bromodeoxyuridine incorporation using fixed microcultures. *Analytical biochemistry*, 185(2), pp.377–382.
- Nagarajan, M., Maruthanayagam, V. & Sundararaman, M., 2012. A review of pharmacological and toxicological potentials of marine cyanobacterial metabolites. *Journal of Applied Toxicology*, 32(3), pp.153–185.
- Nathan, P.J., O'Neill, B. V., Napolitano, A. & Bullmore, E.T., 2011. Neuropsychiatric Adverse Effects of Centrally Acting Antiobesity Drugs. *CNS Neuroscience and Therapeutics*, 17(5), pp.490–505.
- Newman, D.J., Cragg, G.M. & Battershill, C.N., 2009. Therapeutic agents from the sea: biodiversity, chemo-evolutionary insight and advances to the end of Darwin's 200th year. *Diving and hyperbaric medicine*, 39(4), pp.216–225.
- Niedermeyer, T. & Brönstrup, M., 2012. Natural product drug discovery from microalgae. In *Microalgal Biotechnology: Integration and Economy*. pp. 169–200.
- Nukitragasan, N., Okabe, T., Toda, T., Inafuku, M., Iwasaki, H. & Oku, H., 2012. Effect of Peucedanum japonicum Thunb Extract on High-fat Diet-induced Obesity and Gene Expression in Mice. *Journal of Oleo Science*, 61(2), pp.89–101.
- Ogden, C.L., Carroll, M.D., Kit, B.K. & Flegal, K.M., 2012. Prevalence of obesity and trends in body mass index among US children and adolescents, 1999-2010. *JAMA : the journal of the American Medical Association*, 307(5), pp.483–90. Available at: <http://jama.jamanetwork.com/article.aspx?articleid=1104932>.
- Oldoni, T.L.C., Melo, P.S., Massarioli, A.P., Moreno, I. a. M., Bezerra, R.M.N., Rosalen, P.L., da Silva, G.V.J., Nascimento, A.M. & Alencar, S.M., 2016. Bioassay-guided isolation of proanthocyanidins with antioxidant activity from peanut (*Arachis hypogaea*) skin by combination of chromatography techniques. *Food Chemistry*, 192, pp.306–312. Available at: <http://linkinghub.elsevier.com/retrieve/pii/S0308814615010092>.
- Olivera, B.M., 2000. -Conotoxin MVIIA: From Marine Snail Venom to Analgesic Drug. *Drugs from the Sea*, pp.74–85.
- Orjala, J. & Gerwick, W.H., 1996. Barbamide, a chlorinated metabolite with molluscicidal activity from the Caribbean cyanobacterium *Lyngbya majuscula*. *Journal of natural products*, 59(4), pp.427–430.

- Ou, Y., Lin, L., Yang, X., Pan, Q. & Cheng, X., 2013. Antidiabetic potential of phycocyanin: effects on KKAY mice. *Pharmaceutical biology*, 51(5), pp.539–44. Available at: <http://www.scopus.com/inward/record.url?eid=2-s2.0-84876571017&partnerID=tZOtx3y1>.
- Pan, S., Lei, L., Chen, S., Li, H. & Yan, F., 2014. Rosiglitazone impedes Porphyromonas gingivalis-accelerated atherosclerosis by downregulating the TLR/NF-kappaB signaling pathway in atherosclerotic mice. *International immunopharmacology*, 23(2), pp.701–708.
- Parikh, P., Mani, U. & Iyer, U., 2001. Role of Spirulina in the Control of Glycemia and Lipidemia in Type 2 Diabetes Mellitus. *Journal of medicinal food*, 4(4), pp.193–199.
- Park, M., Lee, J., Choi, J., Hong, Y., Bae, I., Lim, K., Park, Y. & Ha, H., 2014. 18B-Glycyrrhetic Acid Attenuates Anandamide-Induced Adiposity and High-Fat Diet Induced Obesity. *Molecular Nutrition and Food Research*, 58(7), pp.1436–1446.
- Park, Y.-K., Rasmussen, H.E., Ehlers, S.J., Blobaum, K.R., Lu, F., Schlegel, V.L., Carr, T.P. & Lee, J.-Y., 2008. Repression of proinflammatory gene expression by lipid extract of Nostoc commune var sphaeroides Kützing, a blue-green alga, via inhibition of nuclear factor-kappaB in RAW 264.7 macrophages. *Nutrition research (New York, N. Y.)*, 28(2), pp.83–91. Available at: <http://www.sciencedirect.com/science/article/pii/S0271531707002813> [Accessed April 29, 2015].
- Patel, A., Mishra, S., Pawar, R. & Ghosh, P.K., 2005. Purification and characterization of C-Phycocyanin from cyanobacterial species of marine and freshwater habitat. *Protein expression and purification*, 40(2), pp.248–55. Available at: <http://www.sciencedirect.com/science/article/pii/S1046592804003742> [Accessed June 4, 2015].
- Pellecchia, M., Sem, D.S. & Wüthrich, K., 2002. NMR in drug discovery. *Nature reviews. Drug discovery*, 1(3), pp.211–219.
- Pereira, D.S., Guevara, C.I., Jin, L., Mbong, N., Verlinsky, A., Hsu, S.J., Avina, H., Karki, S., Abad, J.D., Yang, P., Moon, S.-J., Malik, F., Choi, M.Y., An, Z., Morrison, K., Challita-Eid, P.M., Donate, F., Joseph, I.B.J., Kipps, T.J., Dick, J.E. & Stover, D.R., 2015. AGS67E, an Anti-CD37 Monomethyl Auristatin E Antibody-Drug Conjugate as a Potential Therapeutic for B/T-Cell Malignancies and AML: A New Role for CD37 in AML. *Molecular cancer therapeutics*.
- Pereira-Fernandes, A., Vanparys, C., Vergauwen, L., Knapen, D., Jorens, P.G. & Blust, R., 2014. Toxicogenomics in the 3T3-L1 Cell Line, a New Approach for Screening of Obesogenic Compounds. *Toxicological sciences : an official journal of the Society of Toxicology*, 140(2), pp.352–63. Available at: <http://www.ncbi.nlm.nih.gov/pubmed/24848799>.
- Petrovic, N., Walden, T.B., Shabalina, I.G., Timmons, J.A., Cannon, B. & Nedergaard, J., 2010. Chronic peroxisome proliferator-activated receptor γ (PPAR γ) activation of epididymally derived white adipocyte cultures reveals a population of thermogenically

- competent, UCP1-containing adipocytes molecularly distinct from classic brown adipocytes. *Journal of Biological Chemistry*, 285(10), pp.7153–7164.
- Pettit, G.R., Kamano, Y., Herald, C.L., Tuinman, A.A., Boettner, F.E., Kizu, H., Schmidt, J.M., Baczynskyj, L., Tomer, K.B. & Bontems, R.J., 1987. The isolation and structure of a remarkable marine animal antineoplastic constituent: dolastatin 10. *Journal of the American Chemical Society*, 109(22), pp.6883–6885. Available at: <http://dx.doi.org/10.1021/ja00256a070>.
- Pettit, G.R., Srirangam, J.K., Barkoczy, J., Williams, M.D., Boyd, M.R., Hamel, E., Pettit, R.K., Hogan, F., Bai, R., Chapuis, J.C., McAllister, S.C. & Schmidt, J.M., 1998. Antineoplastic agents 365. Dolastatin 10 SAR probes. *Anti-cancer drug design*, 13(4), pp.243–277.
- Phielers, J., Chung, K.-J., Chatzigeorgiou, A., Klotzsche-von Ameln, A., Garcia-Martin, R., Sprott, D., Moisdou, M., Tzanavari, T., Ludwig, B., Baraban, E., Ehrhart-Bornstein, M., Bornstein, S.R., Mziaut, H., Solimena, M., Karalis, K.P., Economopoulou, M., Lambris, J.D. & Chavakis, T., 2013. The complement anaphylatoxin C5a receptor contributes to obese adipose tissue inflammation and insulin resistance. *Journal of immunology (Baltimore, Md. : 1950)*, 191(8), pp.4367–74. Available at: <http://www.ncbi.nlm.nih.gov/pubmed/24043887>.
- Pittenger, M.F., 1999. Multilineage Potential of Adult Human Mesenchymal Stem Cells. *Science*, 284(5411), pp.143–147.
- Plaza, M., Santoyo, S., Jaime, L., García-Blairsy Reina, G., Herrero, M., Señoráns, F.J. & Ibáñez, E., 2010. Screening for bioactive compounds from algae. *Journal of Pharmaceutical and Biomedical Analysis*, 51(2), pp.450–455.
- Plumb, J.A., Milroy, R. & Kaye, S.B., 1989. Effects of the pH dependence of 3-(4,5-dimethylthiazol-2-yl)-2,5-diphenyl-tetrazolium bromide-formazan absorption on chemosensitivity determined by a novel tetrazolium-based assay. *Cancer research*, 49(16), pp.4435–4440.
- Polak, J., Klimcakova, E., Moro, C., Viguerie, N., Berlan, M., Hejnova, J., Richterova, B., Kraus, I., Langin, D. & Stich, V., 2006. Effect of aerobic training on plasma levels and subcutaneous abdominal adipose tissue gene expression of adiponectin, leptin, interleukin 6, and tumor necrosis factor ?? in obese women. *Metabolism: Clinical and Experimental*, 55(10), pp.1375–1381.
- Poncet, J., 1999. The dolastatins, a family of promising antineoplastic agents. *Current pharmaceutical design*, 5(3), pp.139–162.
- Popa-Wagner, A., Filfan, M., Uzoni, A., Pourgolafshan, P. & Buga, A.-M., 2015. Poststroke Cell Therapy of the Aged Brain. *Neural plasticity*, 2015, p.839638.
- Pulz, O. & Gross, W., 2004. Valuable products from biotechnology of microalgae. *Applied Microbiology and Biotechnology*, 65(6), pp.635–648. Available at: <http://dx.doi.org/10.1007/s00253-004-1647-x>.

- Quan, H.-Y., Baek, N.I. & Chung, S.H., 2012. Licochalcone A prevents adipocyte differentiation and lipogenesis via suppression of peroxisome proliferator-activated receptor gamma and sterol regulatory element-binding protein pathways. *Journal of agricultural and food chemistry*, 60(20), pp.5112–5120.
- Raja, R., Hemaiswarya, S., Ganesan, V. & Carvalho, I.S., 2015. Recent developments in therapeutic applications of Cyanobacteria. *Critical Reviews in Microbiology*, 00(00), pp.1–12. Available at: <http://dx.doi.org/10.3109/1040841X.2014.957640>.
- Rao, V.S., de Melo, C.L., Queiroz, M.G.R., Lemos, T.L.G., Menezes, D.B., Melo, T.S. & Santos, F.A., 2011. Ursolic acid, a pentacyclic triterpene from *Sambucus australis*, prevents abdominal adiposity in mice fed a high-fat diet. *Journal of medicinal food*, 14(11), pp.1375–1382.
- Rasmussen, H.E., Blobaum, K.R., Jesch, E.D., Ku, C.S., Park, Y.-K., Lu, F., Carr, T.P. & Lee, J.-Y., 2009. Hypocholesterolemic effect of *Nostoc commune* var. *sphaeroides* Kutzing, an edible blue-green alga. *European journal of nutrition*, 48(7), pp.387–394.
- Rasmussen, H.E., Blobaum, K.R., Park, Y.-K., Ehlers, S.J., Lu, F. & Lee, J.-Y., 2008. Lipid extract of *Nostoc commune* var. *sphaeroides* Kutzing, a blue-green alga, inhibits the activation of sterol regulatory element binding proteins in HepG2 cells. *The Journal of nutrition*, 138(3), pp.476–481.
- Rastogi, R.P., Sinha, R.P. & Incharoensakdi, A., 2013. Partial characterization, UV-induction and photoprotective function of sunscreen pigment, scytonemin from *Rivularia* sp. HKAR-4. *Chemosphere*, 93(9), pp.1874–1878.
- Remirez, D., Fernandez, V., Tapia, G., Gonzalez, R. & Videla, L.A., 2002. Influence of C-phycoyanin on hepatocellular parameters related to liver oxidative stress and Kupffer cell functioning. *Inflammation research: official journal of the European Histamine Research Society ... [et al.]*, 51(7), pp.351–356.
- Rippka, R., Deruelles, J., Waterbury, J.B., Herdman, M. & Stanier, R.Y., 1979. Generic Assignments, Strain Histories and Properties of Pure Cultures of Cyanobacteria. *Journal of General Microbiology*, 111(1), pp.1–61.
- Romay, C., Gonzalez, R., Ledon, N., Remirez, D. & Rimbau, V., 2003. C-phycoyanin: a biliprotein with antioxidant, anti-inflammatory and neuroprotective effects. *Current protein & peptide science*, 4(3), pp.207–216.
- Rosen, E.D. & MacDougald, O.A., 2006. Adipocyte differentiation from the inside out. *Nature reviews. Molecular cell biology*, 7(12), pp.885–896.
- Rubinstein, L. V., Shoemaker, R.H., Paull, K.D., Simon, R.M., Tosini, S., Skehan, P., Scudiero, D.A., Monks, A. & Boyd, M.R., 1990. Comparison of in vitro anticancer-drug-screening data generated with a tetrazolium assay versus a protein assay against a diverse panel of human tumor cell lines. *Journal of the National Cancer Institute*, 82(13), pp.1113–1118.

- Vom Saal, F.S., Nagel, S.C., Coe, B.L., Angle, B.M. & Taylor, J.A., 2012. The estrogenic endocrine disrupting chemical bisphenol A (BPA) and obesity. *Molecular and Cellular Endocrinology*, 354(1-2), pp.74–84.
- Santos, J.C., Gotardo, E.M.F., Brianti, M.T., Pirae, M., Gambero, A. & Ribeiro, M.L., 2014. Effects of yerba mate, a plant extract formulation (“YGD”) and resveratrol in 3T3-L1 adipogenesis. *Molecules (Basel, Switzerland)*, 19(10), pp.16909–16924.
- Sarjeant, K. & Stephens, J.M., 2012. Adipogenesis. *Cold Spring Harbor perspectives in biology*, 4.
- Schneider, A. & Marahiel, M.A., 1998. Genetic evidence for a role of thioesterase domains, integrated in or associated with peptide synthetases, in non-ribosomal peptide biosynthesis in *Bacillus subtilis*. *Archives of microbiology*, 169(5), pp.404–410.
- Schoonjans, K. & Auwerx, J., 2000. Thiazolidinediones: an update. *Lancet*, 355(9208), pp.1008–1010.
- Sera, Y., Adachi, K., Fujii, K. & Shizuri, Y., 2003. A new antifouling hexapeptide from a Palauan sponge, *Haliclona* sp. *Journal of Natural Products*, 66(5), pp.719–721.
- Sethi, J.K. & Vidal-Puig, A.J., 2007. Thematic review series: adipocyte biology. Adipose tissue function and plasticity orchestrate nutritional adaptation. *Journal of lipid research*, 48(6), pp.1253–1262.
- Sharif, D.I., Gallon, J., Smith, C.J. & Dudley, E., 2008. Quorum sensing in Cyanobacteria: N-octanoyl-homoserine lactone release and response, by the epilithic colonial cyanobacterium *Gloeotheca* PCC6909. *The ISME journal*, 2(12), pp.1171–1182.
- Shoemaker, R.H., 2006. The NCI60 human tumour cell line anticancer drug screen. *Nature reviews. Cancer*, 6(10), pp.813–823.
- Sieuwert, A.M., Klijn, J.G., Peters, H.A. & Foekens, J.A., 1995. The MTT tetrazolium salt assay scrutinized: how to use this assay reliably to measure metabolic activity of cell cultures in vitro for the assessment of growth characteristics, IC50-values and cell survival. *European journal of clinical chemistry and clinical biochemistry : journal of the Forum of European Clinical Chemistry Societies*, 33(11), pp.813–823.
- Smith, C.J., Morin, N.R., Bills, G.F., Dombrowski, A.W., Salituro, G.M., Smith, S.K., Zhao, A. & MacNeil, D.J., 2002. Novel sesquiterpenoids from the fermentation of *Xylaria persicaria* are selective ligands for the NPY Y5 receptor. *Journal of Organic Chemistry*, 67(14), pp.5001–5004.
- Song, L., Luo, Y. & Shi, J., 2006. Inhibition of conjugated linoleic acid isomers on the proliferation of tumor cells. *Wei sheng yan jiu = Journal of hygiene research*, 35(2), pp.191–193.
- Spink, B.C., Cole, R.W., Katz, B.H., Gierthy, J.F., Bradley, L.M. & Spink, D.C., 2006. Inhibition of MCF-7 breast cancer cell proliferation by MCF-10A breast epithelial cells in coculture. *Cell Biology International*, 30(3), pp.227–238.

- Stathis, A. & Younes, A., 2015. The new therapeutical scenario of Hodgkin lymphoma. *Annals of oncology : official journal of the European Society for Medical Oncology / ESMO*.
- Stephens, J.M., 2012. The Fat Controller: Adipocyte Development. *PLoS Biology*, 10(11), pp.11–13.
- Stevenson, C.S., Capper, E.A., Roshak, A.K., Marquez, B., Eichman, C., Jackson, J.R., Mattern, M., Gerwick, W.H., Jacobs, R.S. & Marshall, L.A., 2002. The identification and characterization of the marine natural product scytonemin as a novel antiproliferative pharmacophore. *The Journal of pharmacology and experimental therapeutics*, 303(2), pp.858–866.
- Styrczewska, M., Kostyn, A., Kulma, A., Majkowska-Skrobek, G., Augustyniak, D., Prescha, A., Czuj, T. & Szopa, J., 2015. Flax Fiber Hydrophobic Extract Inhibits Human Skin Cells Inflammation and Causes Remodeling of Extracellular Matrix and Wound Closure Activation. *BioMed research international*, 2015, p.862391.
- Sun, K., Kusminski, C.M. & Scherer, P.E., 2011. Adipose tissue remodeling and obesity. *The Journal of clinical investigation*, 121(6), pp.2094–2101.
- Surmi, B.K. & Hasty, A.H., 2008. Macrophage infiltration into adipose tissue: initiation, propagation and remodeling. *Future Lipidology*, 3(5), pp.545–556.
- Tafari, S.R., 1996. Troglitazone enhances differentiation, basal glucose uptake, and Glut1 protein levels in 3T3-L1 adipocytes. *Endocrinology*, 137(11), pp.4706–4712.
- Tang-Péronard, J.L., Andersen, H.R., Jensen, T.K. & Heitmann, B.L., 2011. Endocrine-disrupting chemicals and obesity development in humans: A review. *Obesity Reviews*, 12(8), pp.622–636.
- Targett, N.M., Kilcoyne, J.P. & Green, B., 1979. Vacuum liquid chromatography: an alternative to common chromatographic methods. *J. Org. Chem.*, 44(26), pp.4962–4964.
- Tchoukalova, Y.D., Koutsari, C., Karpayak, M. V, Votruba, S.B., Wendland, E. & Jensen, M.D., 2008. Subcutaneous adipocyte size and body fat distribution. *The American journal of clinical nutrition*, 87(1), pp.56–63.
- Teixeira, D., Pestana, D., Faria, A., Calhau, C., Azevedo, I. & Monteiro, R., 2010a. Modulation of adipocyte biology by $\delta(9)$ -tetrahydrocannabinol. *Obesity (Silver Spring, Md.)*, 18(11), pp.2077–2085. Available at: <http://dx.doi.org/10.1038/oby.2010.100>.
- Teixeira, D., Pestana, D., Faria, A., Calhau, C., Azevedo, I. & Monteiro, R., 2010b. Modulation of adipocyte biology by $\delta(9)$ -tetrahydrocannabinol. *Obesity (Silver Spring, Md.)*, 18(11), pp.2077–2085. Available at: <http://dx.doi.org/10.1038/oby.2010.100>.
- Van Tonder, A., Joubert, A.M. & Cromarty, A.D., 2015. Limitations of the 3-(4,5-dimethylthiazol-2-yl)-2,5-diphenyl-2H-tetrazolium bromide (MTT) assay when compared to three commonly used cell enumeration assays. *BMC research notes*, 8, p.47.

- Torres-Duran, P. V, Miranda-Zamora, R., Paredes-Carbajal, M.C., Mascher, D., Ble-Castillo, J., Diaz-Zagoya, J.C. & Juarez-Oropeza, M.A., 1999. Studies on the preventive effect of *Spirulina maxima* on fatty liver development induced by carbon tetrachloride, in the rat. *Journal of ethnopharmacology*, 64(2), pp.141–147.
- Towell, A., Muscat, R. & Willner, P., 1988. Behavioural microanalysis of the role of dopamine in amphetamine anorexia. *Pharmacology, biochemistry, and behavior*, 30(3), pp.641–648.
- Tripathi, A., Puddick, J., Prinsep, M.R., Rottmann, M., Chan, K.P., Chen, D.Y.K. & Tan, L.T., 2011. Lagunamide C, a cytotoxic cyclodepsipeptide from the marine cyanobacterium *Lyngbya majuscula*. *Phytochemistry*, 72(18), pp.2369–2375. Available at: <http://dx.doi.org/10.1016/j.phytochem.2011.08.019>.
- Vichai, V. & Kirtikara, K., 2006. Sulforhodamine B colorimetric assay for cytotoxicity screening. *Nature protocols*, 1(3), pp.1112–1116.
- Wang, P., Henning, S.M. & Heber, D., 2010. Limitations of MTT and MTS-based assays for measurement of antiproliferative activity of green tea polyphenols. *PLoS one*, 5(4), p.e10202.
- Wang, Z.Q., Ribnicky, D., Zhang, X.H., Zuberi, A., Raskin, I., Yu, Y. & Cefalu, W.T., 2011. An extract of *Artemisia dracunculoides* L. enhances insulin receptor signaling and modulates gene expression in skeletal muscle in KK-Ay mice. *Journal of Nutritional Biochemistry*, 22(1), pp.71–78.
- Welker, M., Christiansen, G. & Von Döhren, H., 2004. Diversity of coexisting Planktothrix (cyanobacteria) chemotypes deduced by mass spectral analysis of microcystins and other oligopeptides. *Archives of Microbiology*, 182(4), pp.288–298.
- Werner, S., Krieg, T. & Smola, H., 2007. Keratinocyte-fibroblast interactions in wound healing. *The Journal of investigative dermatology*, 127(5), pp.998–1008.
- Wright, A.E., Forleo, D.A., Gunawardana, G.P., Gunasekera, S.P., Koehn, F.E. & McConnell, O.J., 1990. Antitumor tetrahydroisoquinoline alkaloids from the colonial ascidian *Ecteinascidia turbinata*. *The Journal of Organic Chemistry*, 55(15), pp.4508–4512. Available at: <http://dx.doi.org/10.1021/jo00302a006>.
- Yang, Y., Park, Y., Cassada, D.A., Snow, D.D., Rogers, D.G. & Lee, J., 2011. In vitro and in vivo safety assessment of edible blue-green algae, *Nostoc commune* var. *sphaeroides* Kützing and *Spirulina plantensis*. *Food and chemical toxicology : an international journal published for the British Industrial Biological Research Association*, 49(7), pp.1560–1564.
- Yao, L., Herlea-Pana, O., Heuser-Baker, J., Chen, Y. & Barlic-Dicen, J., 2014. Roles of the chemokine system in development of obesity, insulin resistance, and cardiovascular disease. *Journal of Immunology Research*, 2014.

Yu, L., Ding, G.F., He, C., Sun, L., Jiang, Y. & Zhu, L., 2014. MicroRNA-424 is down-regulated in hepatocellular carcinoma and suppresses cell migration and invasion through c-Myb. *PLoS ONE*, 9(3).

Zhang, X.H., Huang, B., Choi, S.K. & Seo, J.S., 2012. Anti-obesity effect of resveratrol-amplified grape skin extracts on 3T3-L1 adipocytes differentiation. *Nutrition Research and Practice*, 6(4), pp.286–293.

Zhang, Y., Li, Y., Guo, Y., Jiang, H. & Shen, X., 2009. A sesquiterpene quinone, dysidine, from the sponge *Dysidea villosa*, activates the insulin pathway through inhibition of PTPases. *Acta pharmacologica Sinica*, 30(3), pp.333–345.

Zhang, Y., Proenca, R., Maffei, M., Barone, M., Leopold, L. & Friedman, J.M., 1994. Positional cloning of the mouse obese gene and its human homologue. *Nature*, 372(6505), pp.425–432.

8. Appendixes

Appendix I – ^1H NMR data for sub-fractions resulting from E14028I successive fractionings.

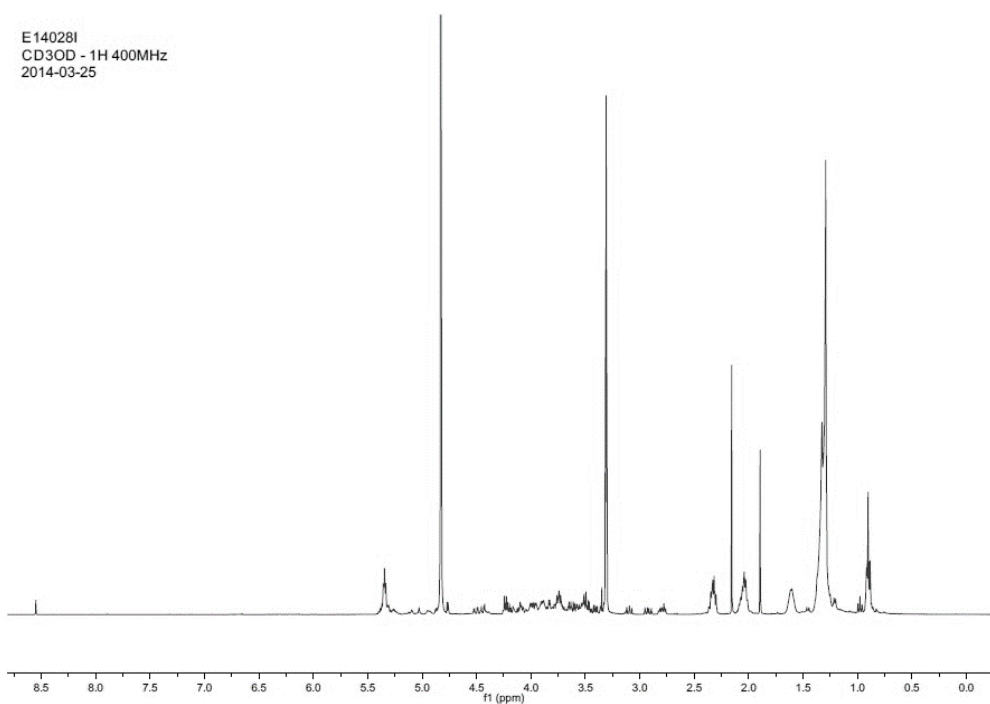


Figure 1 – ^1H NMR spectral data for E14028I in CD_3OD (recorded at 400 MHz).

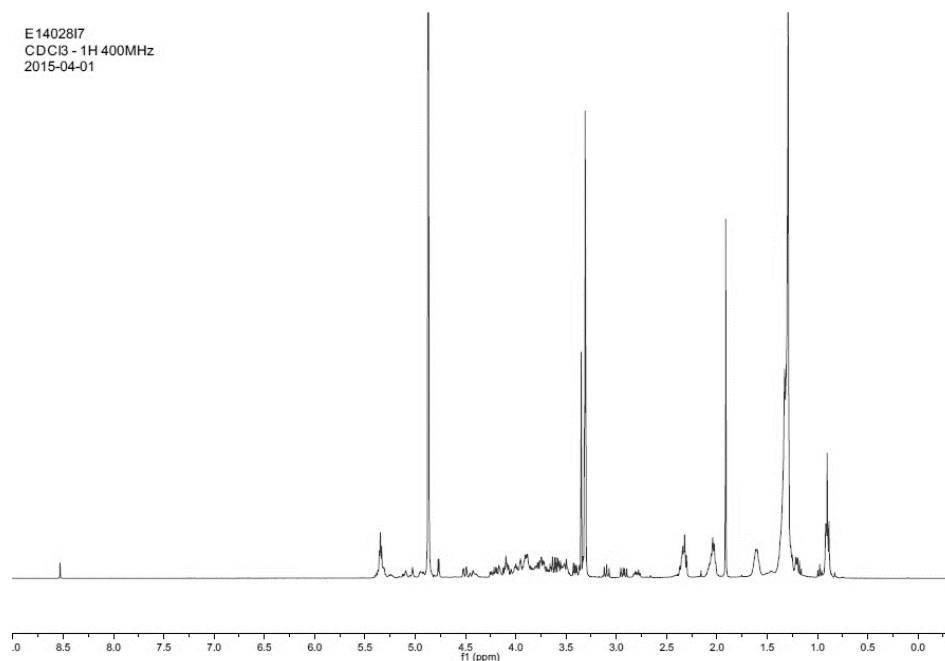


Figure 2 – ¹H NMR spectral data for E1402817 in CDCl₃ (recorded at 400 MHz).

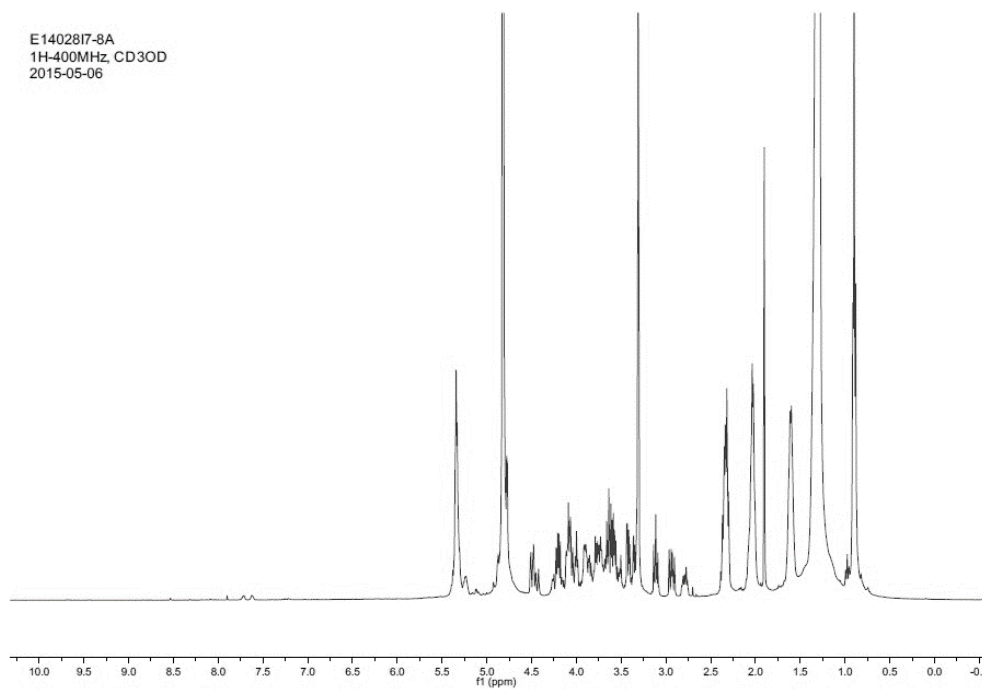


Figure 3 – ¹H NMR spectral data for E1402817 8A in CD₃OD (recorded at 400 MHz).

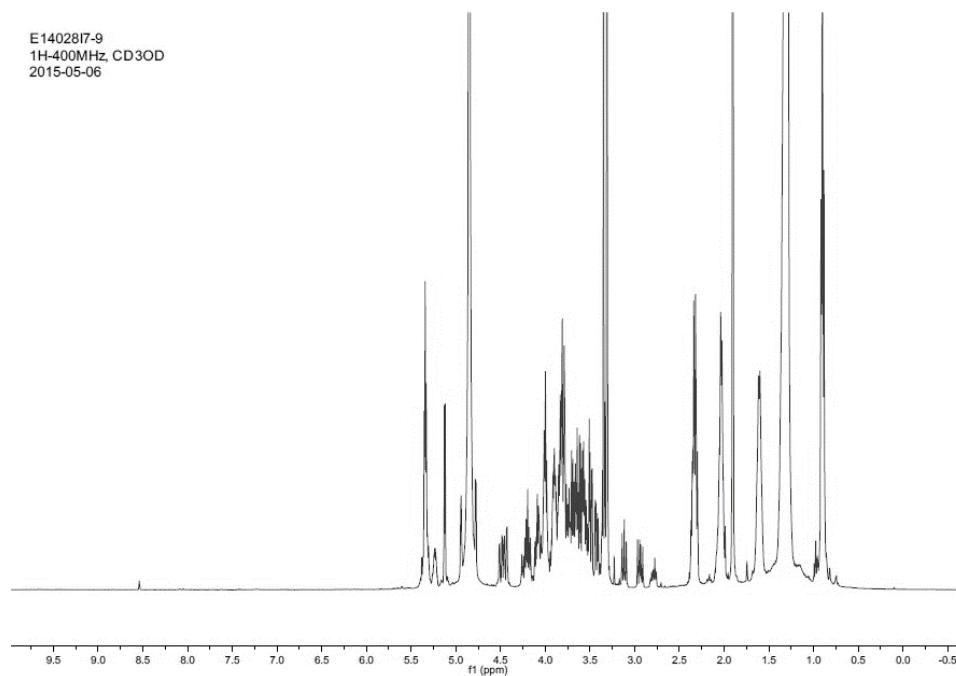


Figure 4 – ^1H NMR spectral data for E1402817 9 in CD_3OD (recorded at 400 MHz).

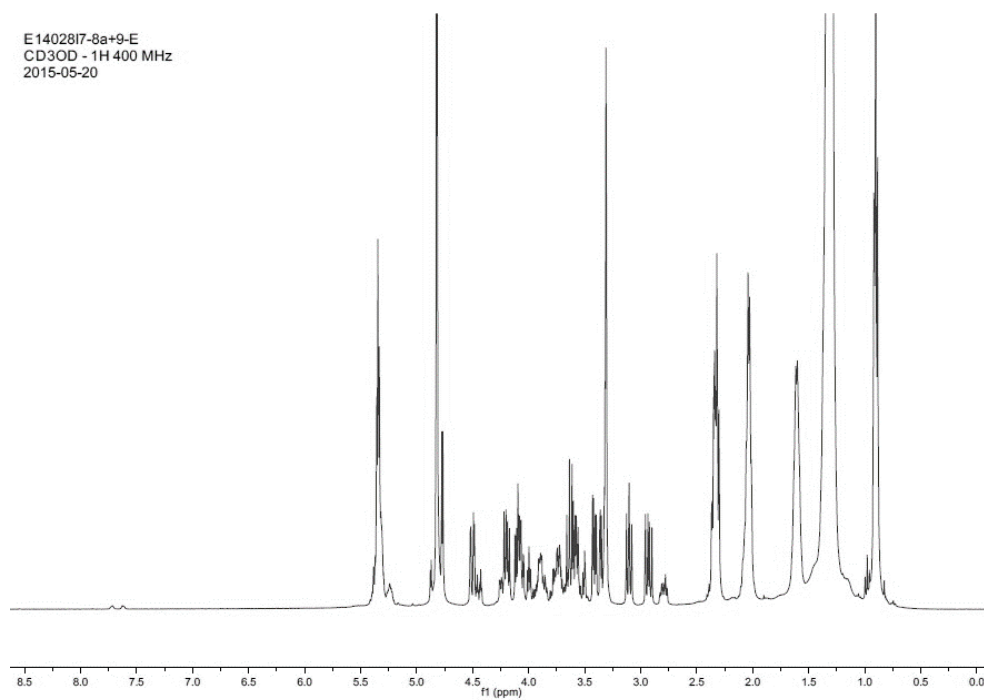


Figure 5 – ^1H NMR spectral data for E1402817 8A+9 E in CD_3OD (recorded at 400 MHz).

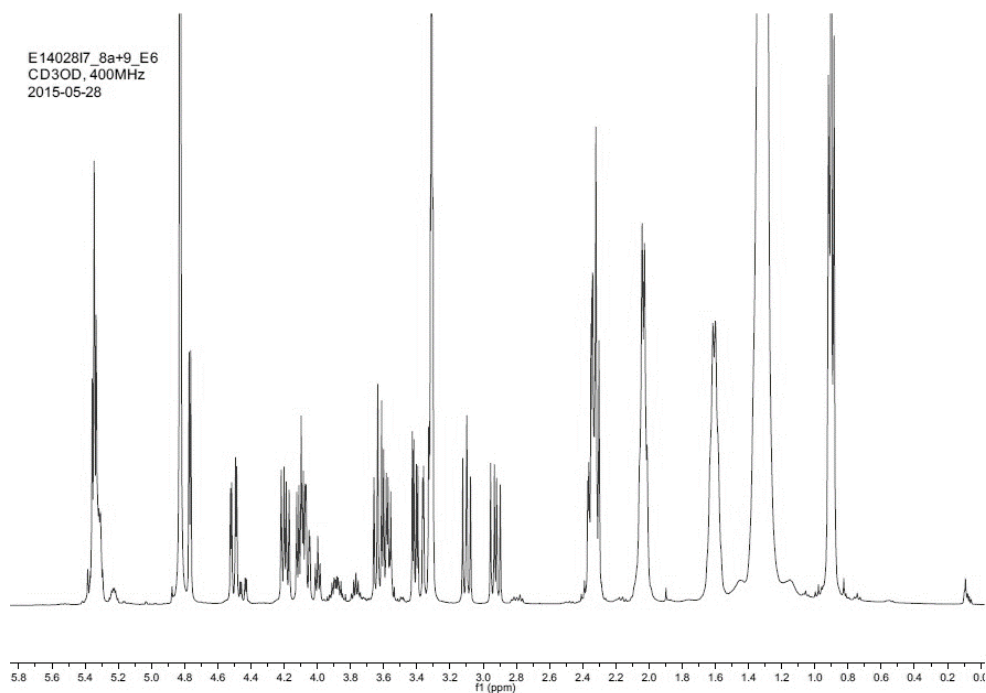


Figure 6 – ^1H NMR spectral data for E1402817 8A+9 E6 in CD_3OD (recorded at 400 MHz).

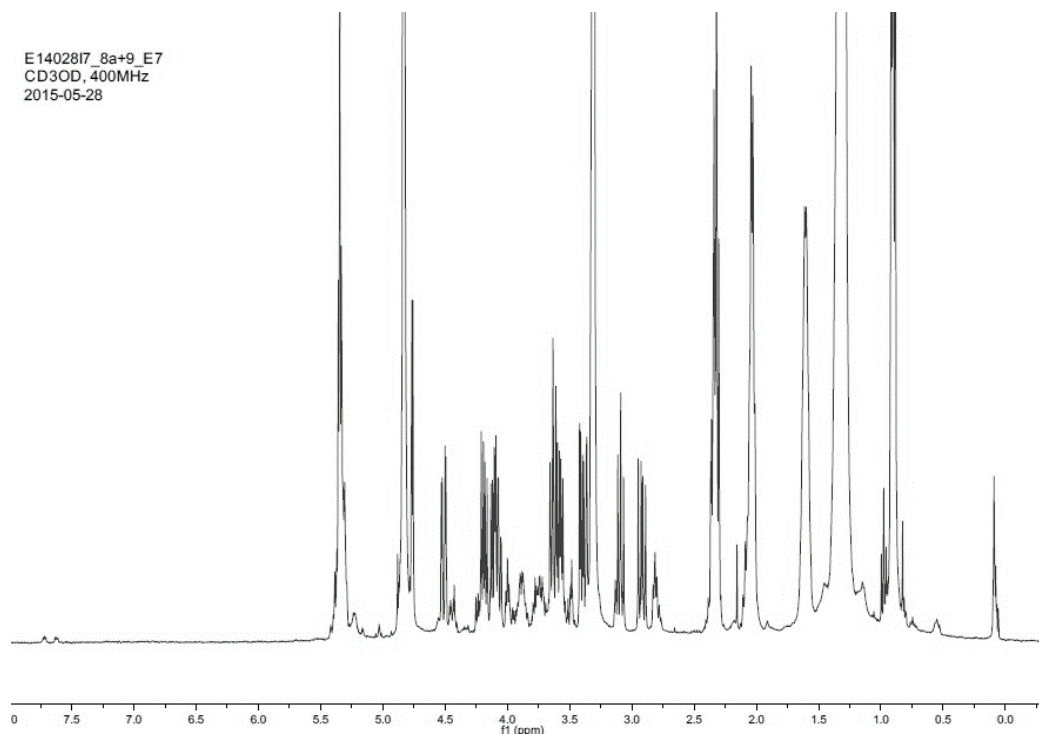


Figure 7 – ^1H NMR spectral data for E1402817 8A+9 E7 in CD_3OD (recorded at 400 MHz).

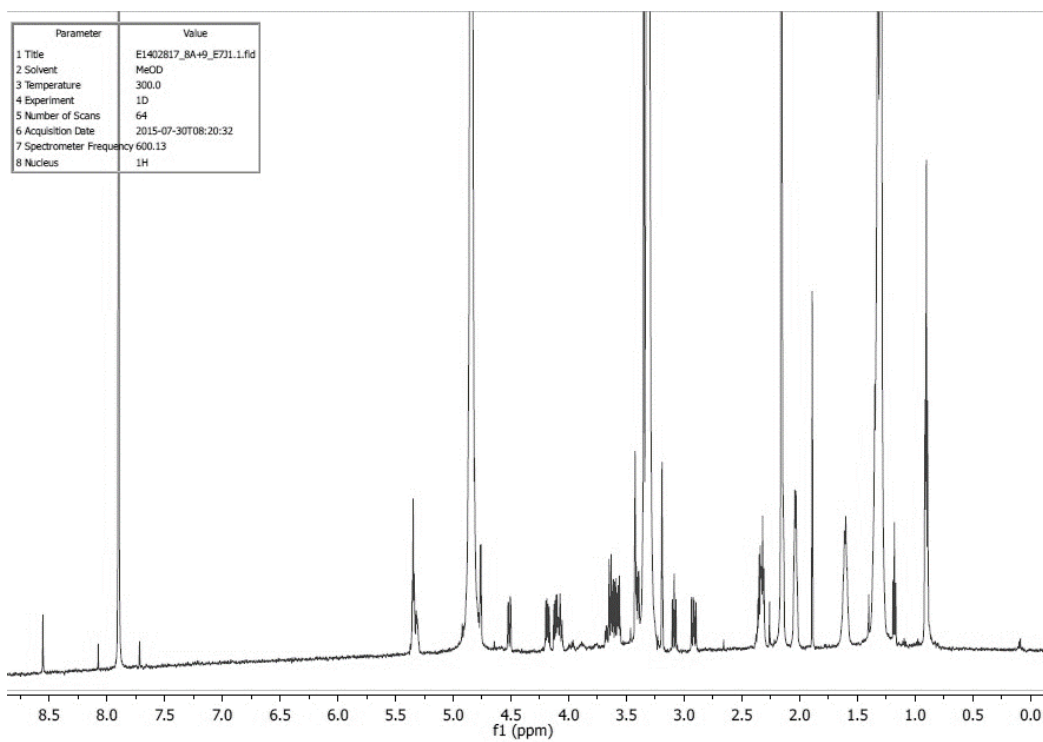


Figure 8 – ^1H NMR spectral data for E1402817 8A+9 E7 J1 in CD_3OD (recorded at 600 MHz).

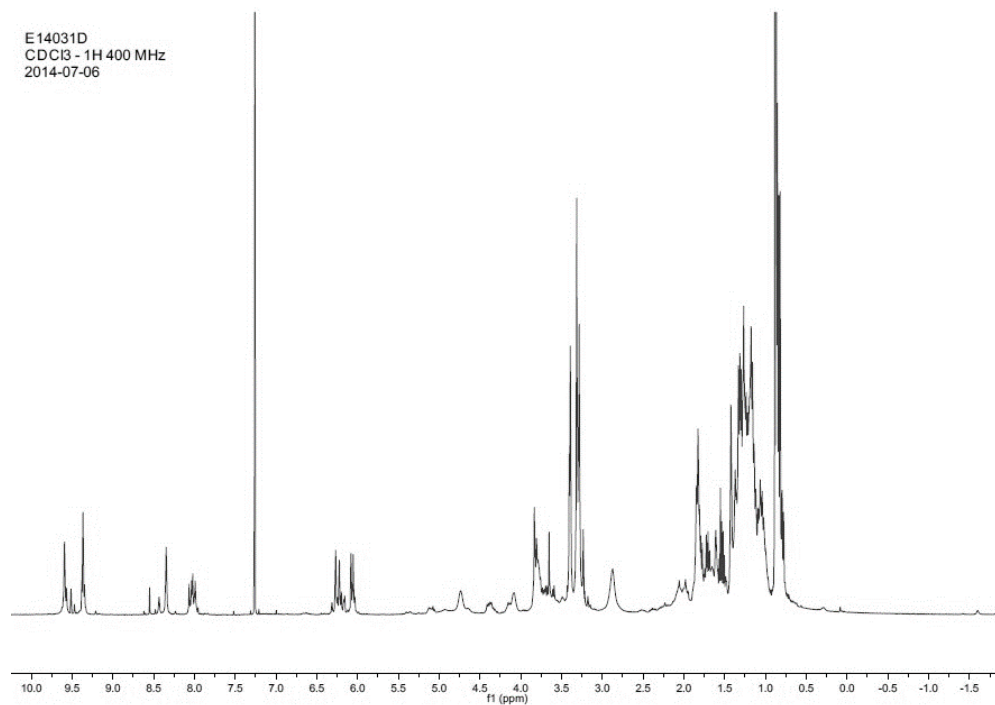


Figure 9 – ^1H NMR spectral data for E14031D in CDCl_3 (recorded at 400 MHz).

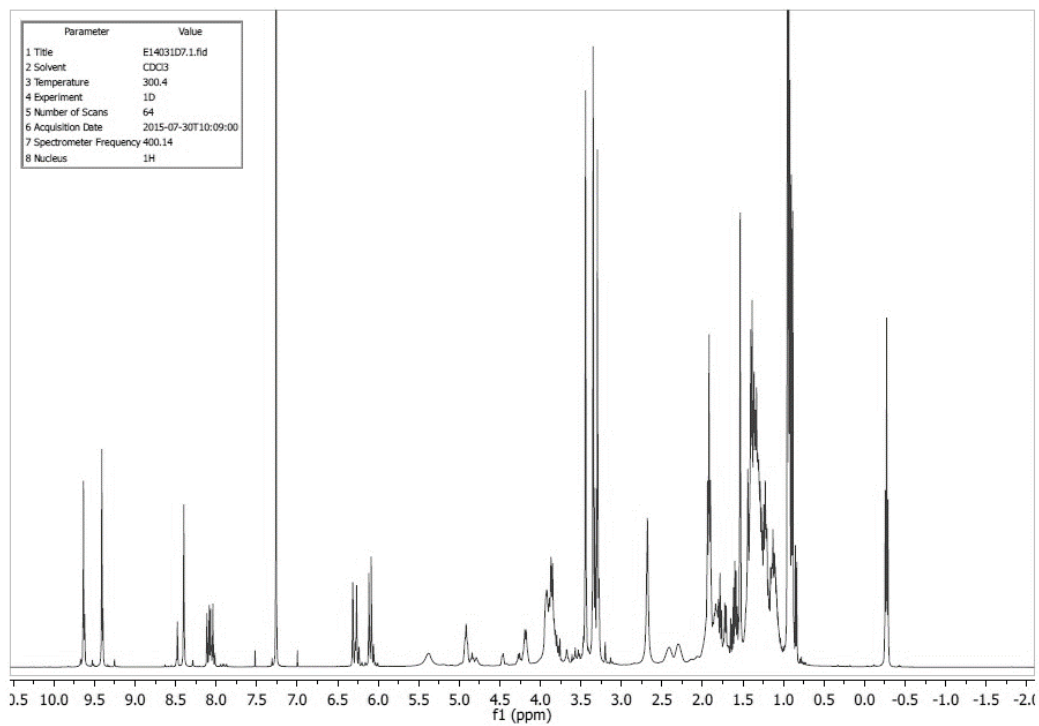


Figure 10 – ^1H NMR spectral data for E14031D7 in CDCl_3 (recorded at 400 MHz).

Appendix II - Abstract for the review paper "Obesity: the metabolic disease, advances on drug discovery and natural product research"

Castro, M., Preto, M., Vasconcelos, V. and Urbatzka, R. (submitted) "Obesity: the metabolic disease, advances on drug discovery and natural product research", *Current Topics in Medicinal Chemistry*.

Abstract: Obesity is a global health threat. OECD reported that more than half (52%) of the adult population in the European Union is overweight or obese. Obesity and obesity -related co-morbidities have deep negative effects on morbidity, mortality, professional and personal quality of life. Health-care costs represent a negative impact of this disease, with an associated economic cost of 100 billion US\$ per year in the United States. The most prescribed drugs for obesity treatment worldwide are Orlistat, and Phentermine/Topiramate extended release, while the major prescribed drug for the same disease in the US are Exenatide and Dapaglifozin. The so far developed drugs, targeting weight loss, have a long history of malignant secondary effects. There is still a lack of efficient and safe drugs to treat obesity and related metabolic complications since in many cases cure cannot be reached by bariatric surgery or healthy lifestyle habits. Terrestrial and aquatic organisms are a promising source of valuable, bioactive compounds, often with low risks for human health. Some of the natural compounds or organisms have been used for centuries by humans as traditional medicine foods. In this review, we give insights into the adipose tissue function and development, and the progress in traditional anti-obesity pharmacotherapy. A major focus is to highlight the state of the art of natural compounds with anti-obesity properties and their potential as candidates for drug development; an overview is given about natural compounds derived from different marine animal sources, cyanobacteria, marine phytoplankton, fungi or plants.

Appendix III – Oral communication "*In vitro* screening assay using the murine pre-adipocyte cell line 3T3-L1 to study anti-obesogenic activities of chemical compounds" at the IJUP - Encontro de Investigação Jovem da Universidade do Porto, 13-15th of May, 2015, Oporto, Portugal.




Abstract: Obesity is a global health threat with several etiologies. Standard obesity treatment may not be enough to treat obese people that represent more than half of the European Union population. The 3T3-L1 cell line has been widely used for the study of bioactive natural compounds research, including research of anti-obesity properties of several natural compounds as phloratannins from the brown algae *Ecklonia stolonifera* or meridianins from the tunicate *Aplidium meridianum*. Cyanobacteria, known as blue-green algae and producer of cyanotoxins, have shown high content in secondary metabolites with relevant activity. We are currently exploring the chemical richness of these prokaryotes by testing cyanobacterial strains regarding their anti-obesogenic activity in (pre)adipocyte cells. Various cyanobacterial strains were grown and their extracts were produced through simple vacuum filtration of their lyophilized mass suspended in a mixture of Dichloromethane and Methanol (2:1). These extracts were then fractioned using vacuum liquid chromatography. Bioactivity of the fractions was tested in the proliferation assay of preadipocyte cells. Proliferation can be assessed by the Sulforhodamine B (SRB) staining and the incorporation of Bromodeoxyuridine (BrdU) into the DNA. Furthermore, the 3-(4,5-dimethylthiazol-2-yl)-2,5-diphenyltetrazolium bromide assay (MTT bioassay) delivers information about the cellular viability and metabolic activity, through the reduction of MTT to formazan by mitochondrial activity.

The most polar fraction (eluted with 100% MeOH) of the cyanobacterial strain *Planktothrix planctonica* has shown the strongest effect on cell proliferation (above 50% compared with the solvent control). The same was verified for the MTT assay, where the activity of mitochondrial enzymes was increased. After consequent sub-fractionation, purified fractions were obtained and the most polar fraction (fraction 7) showed once again pro-proliferative activity through SRB and MTT assay. Further column chromatography will allow us to purify the single compound responsible for this activity and enable us to elucidate its chemical structure.

Appendix IV - Poster communication "In vitro screening assay using the murine pre-adipocyte cell line 3T3-L1 to study anti-obesogenic activities of chemical compounds" at the ICAAE - International Conference on Alternatives to Animal Experimentation, 8 and 9th of May, 2015, Lisbon, Portugal (Appendix II).

In vitro screening assay using the murine pre-adipocyte cell line 3T3-L1 to study anti-obesogenic or obesogenic activities of chemical compounds.

Castro, M., Preto, M., Vasconcelos, V., Urbatzka, R.

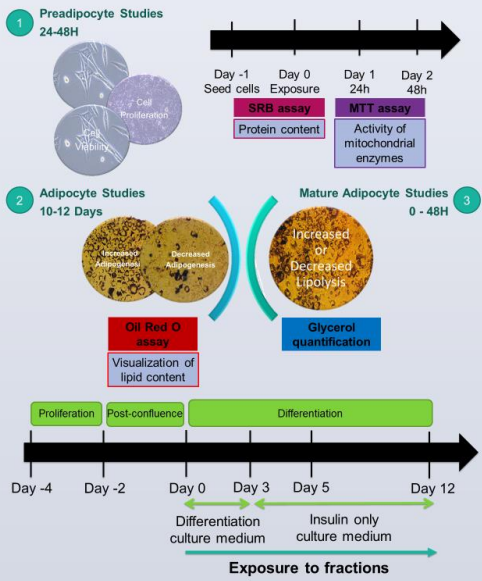
Introduction

Portugal has the third highest frequency of obese women in Western Europe. Some environmental compounds have been suspected to stimulate obesity, as phthalates, bisphenol A and alkylphenols. Other compounds can effectively prevent or treat it.

Model System

3T3-L1 cells offer an interesting model system to study obesogenic or anti-obesogenic activities of compounds. The following analysis can be performed:

- 1) Proliferation of pre-adipocytes
- 2) Adipogenesis/differentiation
- 3) Lipolysis of mature adipocytes




Focus of our Work: Cyanobacterial Compounds

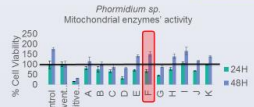

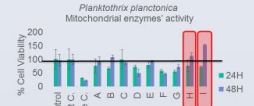
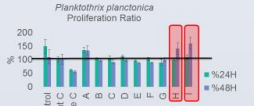

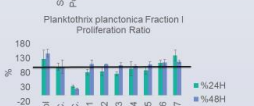
The Laboratory of Ecotoxicology, Genomics and Evolution (LEGE) at CIIMAR has a unique collection of cyanobacteria isolated from water samples and solid materials from the Portuguese coast and freshwater systems over the years. Cyanobacteria are 3,5 billion years old photosynthetic prokaryotes that have shown to be an important source of beneficial natural products.

Results

Strain	Biomass / g	Extract / g	Yield / %	Fractions	Total mass / mg	Yield / %
<i>Phormidium</i> sp.	16.7670	1.7445	10.40	A-K	2303.9	133.3
<i>Planktothrix planctonica</i>	18.6200	3.0227	16.23	A-I	2693.7	91.4
<i>Synechocystis</i> sp.	24.6338	4.4792	18.18	A-L	3644.5	81.4
<i>Oscillatoria limnetica</i>	13.4345	3.5292	26.27	A-J	2945.2	84.8
<i>Aphanizomenon</i> sp.	28.7120	4.426	15.42	A-J	3060.2	80.6
<i>Limnothrix</i> sp.	17.1140	2.2267	13.01	A-J	1016.3	55.5



Effects of Cyanobacterial Fractions on Pre-adipocyte Proliferation

Conclusions and Future Work

- ✓ Using the 3T3-L1 cell line a grand variety of studies can be performed in the adipose tissue. This murine pre-adipocyte cell line allows us to extrapolate results to human systems, since adipose tissue regulation is preserved in higher mammals. Further studies should confirm results in human adipocytes.
- ✓ The polar fraction I (100% Methanol) of *Planktothrix planctonica* has shown promising results, significantly increasing cell proliferation and viability.
- ✓ Following the successful isolation of compounds, we aim to elucidate the chemical structures of new and single compounds with anti-obesogenic activity.

Acknowledgements

This work was partially funded by the Project MARBIOTECH (reference NORTE-07-0124-FEDER-000047) within the SR&TD Integrated Program MARVALOR - Building research and innovation capacity for improved management and valorization of marine resources, supported by the Programa Operacional Regional do Norte (ON.2 – O Novo Norte) and by the European Regional Development Fund and also by NOVOMAR (reference 0687-NOVOMAR-1-P), supported by the European Regional Development Fund.

